An Energy Management System for Isolated Microgrids Considering Uncertainty

by

Daniel Olivares

A thesis
presented to the University of Waterloo
in fulfillment of the
thesis requirement for the degree of
Doctor of Philosophy
in
Electrical and Computer Engineering

Waterloo, Ontario, Canada, 2014

I hereby declare that I am the sole author of this thesis. This is a true copy of the thesis, including any required final revisions, as accepted by my examiners.

I understand that my thesis may be made electronically available to the public.

Abstract

The deployment of Renewable Energy (RE)-based generation has experienced a sustained global growth in the recent decades, driven by many countries' interest in reducing greenhouse gas emissions and dependence on fossil fuel for electricity generation. This trend is also observed in remote off-grid systems (isolated microgrids), where local communities, in an attempt to reduce fossil fuel dependency and associated economic and environmental costs, and to increase availability of electricity, are favouring the installation of RE-based generation. This practice has posed several challenges to the operation of such systems, due to the intermittent and hard-to-predict nature of RE sources. In particular, this thesis addresses the problem of reliable and economic dispatch of isolated microgrids, also known as the energy management problem, considering the uncertain nature of those RE sources, as well as loads.

Isolated microgrids feature characteristics similar to those of distribution systems, in terms of unbalanced power flows, significant voltage drops and high power losses. For this reason, detailed three-phase mathematical models of the microgrid system and components are presented here, in order to account for the impact of unbalanced system conditions on the optimal operation of the microgrid. Also, simplified three-phase models of Distributed Energy Resources (DERs) are developed to reduce the level of complexity in small units that have limited impact on the optimal operation of the system, thus reducing the number of equations and variables of the problem. The proposed mathematical models are then used to formulate a novel energy management problem for isolated microgrids, as a deterministic, multi-period, Mixed-Integer Nonlinear Programming (MINLP) problem. The multi-period formulation allows for a proper management of energy storage resources and multi-period constraints associated with the commitment decisions of DERs.

In order to obtain solutions of the energy management problem in reasonable computational times for real-time, realistic applications, and to address the uncertainty issues, the proposed MINLP formulation is decomposed into a Mixed-Integer Linear Programming (MILP) problem, and a Nonlinear programming (NLP) problem, in the context of a Model Predictive Control (MPC) approach. The MILP formulation determines the unit commitment decisions of DERs using a simplified model of the network, whereas the NLP formulation calculates the detailed three-phase dispatch of the units, knowing the commitment status. A feedback signal is generated by the NLP if additional units are required to correct reactive power problems in the microgrid, triggering a new calculation MINLP problem. The proposed decomposition and calculation routines are used to design a new deterministic Energy Management System (EMS) based on the MPC approach to handle uncertainties; hence, the proposed deterministic EMS is able to handle multi-period con-

straints, and account for the impact of future system conditions in the current operation of the microgrid. In the proposed methodology, uncertainty associated with the load and RE-based generation is indirectly considered in the EMS by continuously updating the optimal dispatch solution (with a given time-step), based on the most updated information available from suitable forecasting systems.

For a more direct modelling of uncertainty in the problem formulation, the MILP part of the energy management problem is re-formulated as a two-stage Stochastic Programming (SP) problem. The proposed novel SP formulation considers that uncertainty can be properly modelled using a finite set of scenarios, which are generated using both a statistical ensembles scenario generation technique and historical data. Using the proposed SP formulation of the MILP problem, the deterministic EMS design is adjusted to produce a novel stochastic EMS.

The proposed EMS design is tested in a large, realistic, medium-voltage isolated microgrid test system. For the deterministic case, the results demonstrate the important connection between the microgrid's imbalance, reactive power requirements and optimal dispatch, justifying the need for detailed three-phase models for EMS applications in isolated microgrids. For the stochastic studies, the results show the advantages of using a stochastic MILP formulation to account for uncertainties associated with RE sources, and optimally accommodate system reserves. The computational times in all simulated cases show the feasibility of applying the proposed techniques to real-time, autonomous dispatch of isolated microgrids with variable RE sources.

Acknowledgements

I will always be grateful to my supervisors Claudio Cañizares and Mehrdad Kazerani for their continuous guidance, support and encouragement during the course of my studies. I feel truly privileged to have worked with such high calibre persons.

Thanks to the members of my committee for their valuable comments, feedback and recommendations: Professors Kankar Bhattacharya, Ehab El-Saadany and David Fuller from the University of Waterloo, and Professor Hugh Rudnick for the Pontificia Universidad Católica de Chile.

I would also like to thank the friendship and help from my colleagues at the EMSOL Lab: Amir, Mohammad, Sumit, Isha, Nafeesa, Juan Carlos, Ehsan, Badr, Omar, Abdullah, Behnam, Victor, Indrajit, and Mostafa. Thanks to my friends Felipe, Mauricio, Jose, and Mehrdad for sharing those funny and refreshing conversations during the daily coffee breaks, and special thanks my dear friends Mariano and Adarsh, for building such a nice atmosphere in our office and sharing so many important moments and conversations just about everything during our time in Waterloo.

Thanks to my friends from Waterloo for making these 4 years in Canada such a wonderful experience: Aleli, Pancho, Angeles, Tomas, Sandra, Gonzalo, Claudia, Rodrigo, Rita, Leandro, Amparo, Nestor, Isabel, Hector, Mary, Xiomara, Fernando, Natalia, German, Alejandro, Francisco, Neelmoy, Massimo, Jutta, Samm, and Jock.

My deepest gratitude to my beloved parents Ricardo and Reyne, for being always there for me with love, understanding and words of encouragement, and thanks to Cecilia and Andrés, for being such great friends, and caring sister and brother. To them I owe who I am.

Thanks to my beloved wife Soledad, for standing beside me all this time with unfailing love and support, and to our daughter Dominga for being a new source of inspiration. This work is one of the results of a family endeavour we started about 5 years ago, and this achievement is as much theirs as mine.

Finally, I would like to thank CONICYT, Natural Resources Canada and the University of Waterloo for awarding the scholarships and providing the financial support that made this research possible.

Dedication

To Soledad and Dominga.

Table of Contents

List of Tables

List of Figures

List of Acronyms

AI : Artificial Intelligence

ACO : Ant Colony Optimization

ANN : Artificial Neural Network

BESS : Battery Energy Storage System

CAES : Compressed Air Energy Storage

CDF : Cumulative Distribution Function

CI : Connection Interface

DER : Distributed Energy Resource

DG : Distributed Generation

DSM : Demand Side Management

ELD : Economic Load Dispatch

EMS : Energy Management System

ESS : Energy Storage System

GA : Genetic Algorithms

GHG : Greenhouse gas

HHV : Higher Heating Value

LC : Local Controller

MAS : Multi-agent System

MGCC : Microgrid Central Controller

MILP : Mixed-Integer Linear Programming

MINLP : Mixed-Integer Nonlinear Programming

MPC : Model Predictive Control

NLP : Nonlinear Programming

OPF : Optimal Power Flow

PC : Point of Connection

PCC : Point of Common Coupling

PSO : Particle Swarm Optimization

PV : Photovoltaic

RE : Renewable Energy

RHC : Receding Horizon Control

SCIG : Squirrel-Cage Induction Generator

SG : Synchronous Generator

SMES : Superconducting Magnetic Energy Storage

SoC : State-of-charge

SP : Stochastic Programming

SUC : Stochastic Unit Commitment

UC : Unit Commitment

VSC : Voltage-Source Converter

VSI : Voltage-Source Inverter

Nomenclature

Parameters

Δt_{k_t}	Absolute time between step k_t and step $k_t + 1$ [hrs]
$\eta_{g_b}^{in}$	Battery-ESS charge efficiency [%]
$\eta_{g_b}^{out}$	Battery-ESS discharge efficiency [%]
$\eta_{g_{el}}$	Electrolizer efficiency [%]
$\eta_{g_{fc}}$	Fuel cell efficiency [%]
π_ω	Probability of scenario ω
A, B, C, D	Three phase ABCD parameter matrices
A_1, A_2^t, A_3, B_2	Recourse matrices in SUC
a_g	Quadratic term factor of cost function of generating units [\$/kWh^2]
b_g	Linear term factor of cost function of generating units [\$/kWh]
c_g	Constant term of cost function of generating units [\$]
$C_{sdn,g}$	Shut-down cost of generating units [\$]
$C_{sup,g}$	Start-up cost of generating units [\$]
d_c, d_s	Costs of Power curtailment and load shedding [\$/kWh]
H_{NLP}	Multi-period OPF look-ahead window [hr]
H_{SUC}	SUC look-ahead window [hr]

HHV	Hydrogen Higher Heating Value [kWh/Nm^3]
I_n^{max}	Maximum neutral current [A]
K_{emer}	Cost of emergency start-up and shut-down decisions [$]
K_{loss}	Constant active power losses of connection interface [kW]
$K_{Q^{aux}}$	Cost of auxiliary reactive power generation [$/kVAr]
l_c	Hydrogen compressor load, in per-unit of electrolizer load [p.u.]
M_{dn}	Minimum down-time of generating units [hr]
M_{up}	Minimum up-time of generating units [hr]
$P_{p,L}$	Active power of loads per phase [kW]
$Q_{p,L}$	Reactive power of loads per phase [kVAr]
R_{dn}	Maximum ramp-down rate of generating units [kW/hr]
r_{loss}	Series resistance of connection interface [Ohm]
R_{sv}	Reserve requirement [%]
R_{up}	Maximum ramp-up rate of generating units [kW/hr]
t_{k_t}	Absolute time at time-step k_t
T_{NLP}	Multi-period OPF time step [hr]
T_{SUC}	SUC time step [hr]
U	3-by-3 identity matrix
V_n^{nom}	Nominal line voltage at node n [kV]
x''_d, x''_q	Unsaturated direct- and quadrature-axis subtransient reactances of synchronous generator [Ohm]
x_d	Direct-axis synchronous reactance of synchronous generator [Ohm]
x_{gnd}	Grounding reactance of synchronous generator [Ohm]

x_{pos}, x_{pos}, x_0	Positive, negative and zero sequence reactances of synchronous generator [Ohm]
$Z_{p,L}$	Load impedance per phase [Ohm]
Z_{pos}, Z_{neg}, Z_0	Positive, negative and zero sequence impedances of synchronous generator [Ohm]
a_1	Parameters relevant to first-stage restrictions on Stochastic Unit Commitment (SUC)
$b_{2,t}, b_3$	Parameters relevant to second-stage restrictions on SP
$\mathbf{0}$	3-by-3 zero matrix
$\mathbf{A}$	3-by-3 sequence conversion matrix

Indices

g	Index for generating units
g^*	Index for simplified generators
g_b	Index for battery-Energy Storage Systems (ESSs)
g_i	Index for induction generators
g_n	Index for generating units connected to node n
g_s	Index for synchronous generators
g_{el}	Index for electrolyzers
g_{fc}	Index for fuel cells
g_{inv}	Index for inverter-interfaced generators
g_{rw}	Index for RE-based generators
H_{tank}	Index for hydrogen tanks
k_t	Index for time-steps of UC and multi-period OPF

L	Index for loads, $L = 1,...NL$
l	Index for series elements, l=1,...Nl
L_n	Index for loads connected to node n
p	Index for phases, p = a, b, c
r	Index for receiving-end
r_n	Index for receiving-ends connected to node n
s	Index for sending-end
s_n	Index for sending-ends connected to node n
t	Index for time-steps of SUC

Variables

$\overline{E}$	Vector of steady-state internal voltage phasors of synchronous generators [kV]
$\overline{I}$	Vector of three-phase line current phasors [A]
$\overline{V}$	Vector of three-phase line voltage phasors [kV]
$\widehat{P}_t$	Vector of power generation for all DER units at time t [kW]
$\widehat{w}_t$, $\widehat{u}_t$, $\widehat{v}_t$	Vectors of UC decision variables for all DER units at time t
$\widetilde{P}^{\omega}_{g_{rw}}$	Vector of RE power generation in scenario ω [kW]
E^p	Internal line voltage phasor of synchronous generator [kV]
I^{pp}	Phase current phasor [A]
I^p	Line current phasor [A]
$P^{in}_{g_b}$	Battery–ESS input power [kW]
$P^{out}_{g_b}$	Battery–ESS output power [kW]
P_{loss}	Total active power losses of connection interface [kW]

$P_{p,g}$	Active power of generating units per phase [kW]
$P_{shed,t}$, $P_{curt,t}$	Load shedding and power curtailment at time t [kW]
P_{source}	Total active power produced by the generating unit [kW]
Q_g^{aux}	Auxiliary reactive power generation [kVAr]
$Q_{p,g}$	Reactive power of generating units per phase [kVAr]
r'_r, x'_r	Rotor resistance and reactance of SCIG referred to stator [Ohm]
r_s, x_s	Stator resistance and reactance of SCIG [Ohm]
SOC_{g_b}	State of charge of battery-ESS [kWh]
$SOC_{H_{tank}}$	State of charge of an hydrogen tank [Nm^3]
u_g^{emer}	Emergency start-up binary decision variable
u_g	Start-up binary decision variable
v_g^{emer}	Emergency shut-down binary decision variable
V^{pp}	Line-to-line voltage phasor [kV]
V^p	Line voltage phasor [kV]
V_{rt}^p	Rotor line voltage phasor of SCIG referred to stator [kV]
V_{st}^p	Stator line voltage phasor of SCIG [kV]
v_g	Shut-down binary decision variable
w_g	Unit-commitment binary decision variable
x_m	Magnetizing reactance of SCIG [Ohm]
z_1, z_2	First and second stage variables on the Stochastic Programming (SP) problem

Chapter 1

Introduction

1.1 Research Motivation

The problem of reliable integration of intermittent energy sources into the power systems has gained great importance over the last few decades, motivated by the rapidly-increasing penetration of RE sources like wind and solar-Photovoltaic (PV). This trend is expected to persist for the next decades as several countries, in an attempt to reduce their greenhouse gas emissions, have developed ambitious plans to increase the levels of penetration of renewable generation. To serve this purpose, different incentive policies have been developed, including feed-in tariffs, renewable portfolio standards, tradable green certificates, investment tax credits and capital subsidies [1].

The use of modified feed-in tariff programs that cover off-grid systems (e.g., remote communities without connection to the main grid) has also been proposed in order to encourage the installation of RE technologies in remote areas to help increase availability of electricity, and reduce fossil fuel dependency, and its associated economical and environmental costs [2, 3]. The latter takes more relevance when considering that, according to estimates from the International Energy Agency, 1.3 billion people worldwide have no access to electricity from the existing electric grids, but can potentially be electrified with off-grid stand-alone systems that incorporate local RE sources [4]. In this context, microgrids provide a general framework to address the various technical and economical issues that arise from the integration of RE sources in the form of distributed generation in isolated networks [5].

A microgrid can be defined as a cluster of loads, Distributed Generation (DG) units and ESSs operated in coordination to achieve common local goals [5]. Microgrids are capable

of operating in grid-connected and stand-alone modes; however, a special case is identified when microgrids operate permanently in stand-alone mode, known as isolated microgrids (i.e., off-grid systems). From the technical viewpoint, the integration of RE sources in isolated microgrids presents more significant challenges due to their low inertia, limited number of controllable assets, and critical demand-supply balance [6]. The most relevant challenges in the operation of isolated microgrids include:

- *Bidirectional power flows*: Since distribution feeders were initially designed for unidirectional power flow, integration of DG units at low voltage levels that may cause reverse power flows can lead to complications in protection coordination, undesirable power flow patterns, fault current distribution, and voltage control.

- *Stability issues*: Local oscillations or other stability problems may emerge from the interaction of the control systems of DG units, requiring a thorough stability analysis classically performed only at a transmission system level.

- *Low inertia*: Unlike bulk power systems where high number of synchronous generators ensures a relatively large inertia, microgrids might show a low-inertia characteristic, especially if there is a significant share of power electronic-interfaced DG units. Although such an interface can enhance the system dynamic performance, the low inertia in the system can lead to severe frequency deviations in stand-alone operation if a proper control mechanism is not properly implemented.

- *Uncertainty*: The economical and reliable operation of microgrids requires a certain level of coordination among different DERs. This coordination becomes more challenging in isolated microgrids, where the critical demand-supply balance and presence of ESSs require solving a strongly coupled problem over an extended horizon, taking into account the uncertainty of parameters such as load profile and weather forecast. This uncertainty is more significant than those in bulk power systems, due to the reduced number of loads, and highly correlated and proportionally large variations of available energy resources.

The reliable integration of RE sources in isolated microgrids will only be possible if the aforementioned challenges are successfully overcome, since these negatively affect the grid operation if not properly addressed. For example, an inadequate handling of uncertainty in RE generation may result in frequent deficits of energy supply, which may lead to expensive load shedding measures or the need for more expensive generation, which may impact negatively the perception of RE sources as a viable alternative for use in isolated microgrids. In this context, this thesis concentrates on the issues of scheduling and dispatch of isolated

microgrids in the presence of intermittent energy sources by designing an adequate EMS for isolated microgrids. In the proposed EMS, the energy management problem is formulated as a mathematical program to be solved with suitable optimization algorithms. Unique traits of this research are the use of stochastic programming formulations of the energy management problem to account for uncertainties associated with RE sources, the use of a highly-detailed three-phase model of the microgrid to account for the effect of system imbalance, and the implementation and testing of an EMS for real-time, autonomous, practical applications in real microgrids.

1.2 Literature Review

The problem of energy management in microgrids consists of finding the optimal (or near optimal) UC and dispatch of the available DERs so that certain selected objectives are achieved. In particular, this problem gains more relevance with the presence of highly-variable energy sources, where the update rate of the unit dispatch command should be high enough to follow the sudden changes of load and non-dispatchable generators, and uncertainty needs to be taken into account. Hence, in order to allow seamless deployment of intermittent energy sources in stand-alone systems, proper EMSs and controls must be designed to ensure reliable, secure and economical operation of isolated microgrids.

In general, to determine the dispatch and UC of the microgrid, three main options can be identified: Real-time optimization, expert systems, and decentralized hierarchical control [7]. With regard to the EMS architecture, two main approaches can be identified: Centralized and Decentralized architectures. With these aspects in mind, an overview of the state-of-the-art research on EMSs for isolated microgrids is presented next.

1.2.1 Centralized EMS Approach

A centralized EMS architecture consists of a central controller provided with the relevant information of every DER unit and load within the microgrid, and the network itself (e.g., cost functions, technical characteristics/limitations, network parameters and modes of operation), as well as the information from forecasting systems (e.g., local load, wind speed, solar irradiance) in order to determine an appropriate UC and dispatch of the resources according to the selected objectives. The central controller can make decisions using either on-line calculations of the optimal (or near optimal) operation, or pre-built and continuously-updated databases with information of suitable operating conditions,

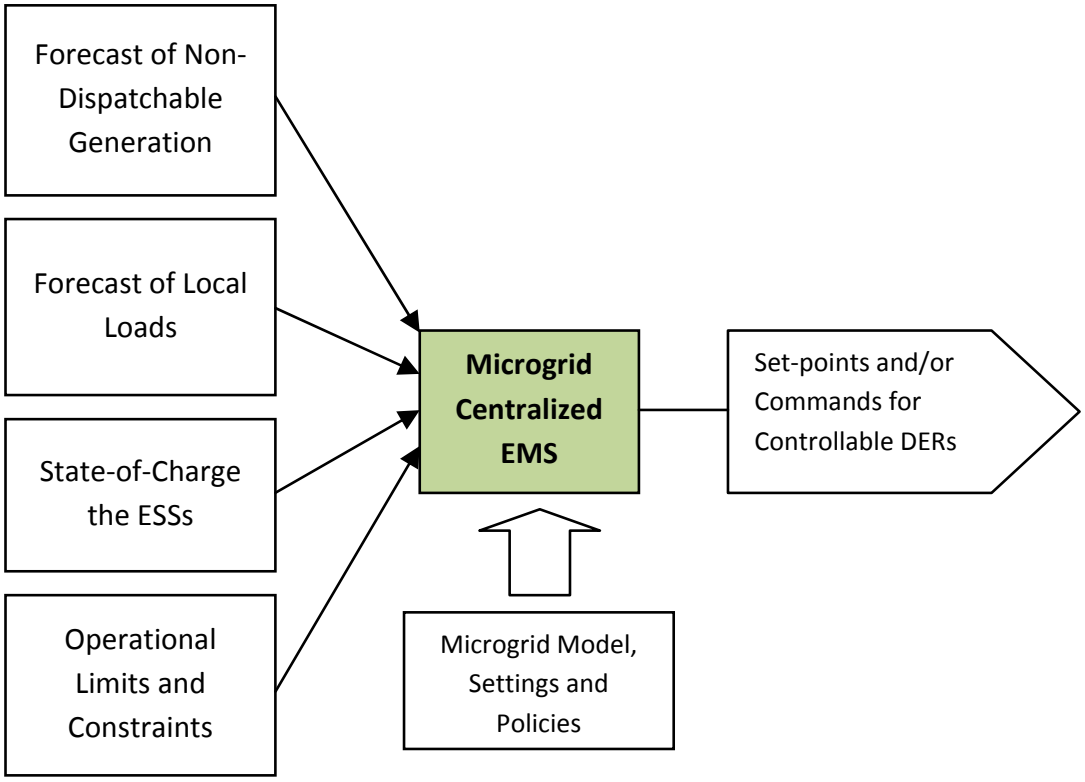

Fig. 1.1: Centralized EMS approach for isolated microgrids.

from off-line calculations or other heuristic approaches. A practical application of this approach is demonstrated in [8], and the general structure of a centralized EMS is shown in Fig. 1.1, where the input variables/parameters may include: Forecasted power output of the non-dispatchable generators for a pre-defined look-ahead window, forecasted local load for a pre-defined look-ahead window, State-of-charge (SoC) of the ESSs, operational limits of dispatchable generators and ESSs, and security and reliability constraints of the microgrid.

Output variables of the secondary controller are the reference values of the primary control system (e.g., output power and/or terminal voltage) for each dispatchable DER unit, together with decision variables for controlling loads for load shifting or shedding.

In small microgrids with a low number of generation scenarios, the offline calculation of

the optimal operation for all the possible scenarios may be the best alternative in terms of cost and systems performance. In the approach presented in [9], all possible operation states are analysed off-line and the optimal dispatch of the system for each scenario is calculated and stored in a look-up table to be accessed in real-time operation. Although this approach produces an instantaneous response of the system when the conditions change, the number of possible scenarios can become an issue if changes in the topology of distribution system are considered (faults or reconfiguration), or if time-coupling is considered in the operation of the microgrid. In particular, the presence of ESS in the microgrid would introduce time dependence in the calculation of the optimal dispatch, and a new dimension to the look-up table, since the state-of-charge of an ESS at a given time-step will depend on the state-of-charge and dispatch at the previous step; therefore, the optimal dispatch is not solely determined by a particular demand scenario. A similar approach is presented in [10], where a feed-forward Artificial Neural Network (ANN) with one hidden layer is trained with results of the OPF for several feasible scenarios of the microgrid. One of the advantages of this approach is that it allows a fast response of the centralized EMS even for scenarios not included in the training set, although optimality, or even feasibility, are not guaranteed in those cases. An on-line calculation of the OPF is performed with certain frequency to evaluate the quality of the solutions provided by the ANN, and decide if a new training with additional scenarios is needed. However, the use of significant ESS capacity is not considered in this case, and its optimal management would require a multi-period OPF calculation, which will greatly increase the number of scenarios to be considered in the ANN training.

An alternative approach to the ones proposed in [9,10] is to obtain a new solution of the optimal energy management problem for each operating condition on-line; however, in this case, special attention needs to be given to the problem formulation, so that solutions can be obtained in suitable computational times. In particular, the objective function may include cost functions of second or higher order polynomial equations with some start-up/shut-down decisions, as it is the case in [11]. Also, some complex constraints are needed to model the operational limitations of some DG units and ESSs or to represent controllable loads and commitment decisions. Furthermore, considering network constraints (load flow) adds another degree of complexity to the microgrid optimal energy management problem due to their non-linearity, as it is the case in [12]. In particular, the authors in [12] present a multi-period Nonlinear Programming (NLP) formulation of the energy management problem using a detailed, unbalanced, OPF model. Although the proposed model is designed for grid-connected microgrids, the authors recognize the importance of detailed network and device models on the energy management problem. The presented model is highly detailed in terms of system modelling; however, it does not include UC decision variables and

measures of uncertainty, which would greatly increase the complexity of the formulation.

Detailed formulations of the microgrid optimal energy management problem that include UC decisions fall into the category of Mixed-Integer Nonlinear Programming (MINLP) problems. In order to handle and solve such complex problem formulations, heuristic optimization techniques have been applied, including Genetic Algorithms (GA) [13, 14], Particle Swarm Optimization (PSO) [15], and Ant Colony Optimization (ACO) [16]. However, MINLP formulations are impractical for dispatch applications, due to the lack of reliable Mixed-Integer Linear Programming (MILP) solvers that are able to obtain "good" solutions in reduced computational times. Also, simplified formulations that concentrate exclusively on the active power dispatch have also been used in [11, 17–19], where power flow equations have been replaced by a single demand-supply balance equation. While such simplified approaches lead to linear or mixed-integer linear formulations that can be readily solved with commercial MILP solvers, important operational constraints related to voltage limits and reactive power flow are neglected.

To address the aforementioned system modelling issues, the authors in [20] present a two-stage energy management process where the scheduling of units is performed in a first stage neglecting the power flow equations and using a multi-period formulation, whereas the final dispatch is refined by a second stage that includes balanced power flow equations in the calculations, but uses only a single-step formulation. A cost function for ESSs, which penalizes deviations from the dispatch determined by the first stage, is also included in the second-stage problem. This sophisticated approach addresses several issues relevant for EMSs in isolated microgrids; however, system imbalance is not considered, and uncertainties associated with the forecasting system are not accounted for directly in the problem formulation, requiring an arbitrary spinning reserve equation.

The minimization of total operating cost is the most commonly pursued objective in EMSs for isolated microgrids; however, some approaches have also incorporated the reduction of Greenhouse gas (GHG) emissions as an additional objective for the microgrid operation. In this case, the energy management problem is formulated as a multi-objective optimization problem and solved with different techniques [21]. Pareto optimal solutions are investigated in [15] and [16] by using PSO and ACO techniques, respectively, while a weighted objective function that combines different individual objective functions, together with heuristic optimization techniques, are used in [17, 22–24]. Nevertheless, there is no clear criteria defined to establish the weight of each individual objective function in the dispatch problem; therefore, the optimal solutions produced by these algorithms are highly arbitrary.

In the most typical case of centralized EMS, the information about cost functions

and operating limits of DGs is transferred to the microgrids central controller in order to determine the appropriate system operation. However, it is possible to get a more active participation of generators and customers by allowing them to bid their power production and consumption, respectively, instead of simply communicating its cost functions and availability [25]. Although this alternative allows different players to have participation in the decision making, different players may need additional information and analysis skills in order to determine appropriate bids, if a multi-period operation planning is required.

ESS Considerations

The deployment of ESSs can have an important effect on the optimal operation of microgrids. In addition to balancing the demand-supply equation when power shortage or surplus are encountered, ESSs can be used to maintain dispatchable DG units operating at their maximum efficiencies, and can prevent or reduce the use of expensive energy sources during peak hours, also allowing the microgrid to defer investment on new capacity. After the UC decisions have been made in a previous stage, the dispatch of units in a microgrid is typically a single-step problem, in the sense that the microgrids state will depend exclusively on the demand and available power from non-dispatchable generators at that particular moment (snapshot problem), and the previous states will have no influence. However, in the presence of a long-term ESS, this is not the case, since future operating conditions will have an impact on the present operation of the ESSs.

The authors in [24] propose a multi-objective single-step formulation, where ESS dispatch is managed by incorporating a penalty term in the objective function that discourages the use of stored energy. This way, the proposed formulation prevents the use of all the stored energy at once; however, it is not able to properly handle the effect of future demand conditions in the present operation of the ESSs. To address this issue, multi-period formulations of the dispatch problem have been proposed in the literature to appropriately accommodate the storage resources in time [26–31].

In [26], a day-ahead Economic Load Dispatch (ELD) is performed for a microgrid with intermittent DGs and an ESS; the programmed dispatch is then adjusted every 15 minutes to ensure that the voltages are kept within acceptable limits, trying to maintain the dispatch of units as close to the predetermined values as possible . A more detailed formulation is presented in [27] for a microgrid with wind turbines and a hydrogen-based ESS, where the ELD is performed over several time steps, but only the results obtained for the next time step are actually implemented in the microgrid, and then the ELD is re-calculated for the following stages using an MPC technique. In [28], the benefits from an optimal management of the ESS via multi-period optimization are estimated to be

a reduction of 5% in the operation cost, although this result strongly depends on the particular size and efficiency of the considered ESS, and the cost characteristics of the microgrid generators. The importance of adequate ESS modeling for real-time microgrid's power generation optimization applications is highlighted in [32]; it is shown that several practical complexities such as start-up conditions, impact of environmental conditions, command delays, measurement errors, and standby losses could result in the violation of storage-related constraints, and consequently, could render the microgrid optimization problems infeasible.

Uncertainty Considerations

Uncertainty in the load and generation profiles has been mainly addressed indirectly in the dispatch problem by using the MPC approach, which is an optimization-based control strategy where an optimization problem is formulated and solved at each discrete time-step. MPC strategies are quite appealing for energy management of isolated microgrids, since they allow for the implementation of control actions that anticipate future events such as variations in power outputs from non-dispatchable DER units and instantaneous demand [11, 27].

In MPC, at each time-step, the solution to the optimal control problem is solved over a certain pre-defined horizon using the current state of the system as the initial state. The optimization calculates a control sequence for the whole horizon such that the selected objectives are minimized, but only the control action for the next time step is implemented. A particular application of the MPC approach in a centralized EMSs is presented in [11], where the dispatch of the microgrid is calculated every hour considering an optimization horizon of 48 hours, in order to capture complete load and generation profile patterns; however, the slow update-rate of the dispatch and simplified network models are weaknesses of the proposed approach.

Despite its advantages, an MPC approach might not be enough to ensure the reliable operation of isolated microgrids due to the critical demand-supply balance, and a more detailed modelling of the uncertainty might be necessary. Techniques such as robust optimization, stochastic optimization, and chance constrained optimization have been applied to UC in bulk power grids [33–36]. These techniques in combination with the traditional MPC approach offer advantages regarding the direct incorporation of uncertainty in the optimization models, which might help to achieve a more reliable operation of isolated microgrids.

1.2.2 Decentralized EMS Approach

A decentralized EMS intends to solve the energy management problem of a microgrid while providing the highest possible autonomy for different DERs and loads. Although this approach can still use a hierarchical structure for data exchange, decisions on the control variables are made locally. The autonomy of isolated microgrids is achieved using a hierarchical structure with at least 2 levels: Microgrid Central Controller (MGCC) and LCs [25] (a third level is considered in the case of grid-connected microgrids or inter-connected microgrids). The MGCC coordinates the aggregated operation of the DERs and loads within the microgrid, and is responsible for their reliable and economical operation, as well as interaction with the main grid. The LCs control DER units within the microgrid, or an aggregation of them, interacting with higher level controllers and trying to achieve local and global objectives. In a decentralized architecture, an LC can communicate with the MGCC and other LCs in order to share knowledge, request/offer a service, communicate expectations, and exchange any other information relevant to the operation of the microgrid.

Given its characteristics, decentralized EMSs have been primarily addressed in the literature by using the MAS framework. A MAS can be briefly described as a system composed of multiple intelligent agents, provided with local information, that interact with each other in order to achieve multiple global and local objectives. As can be expected, the connectivity of the agents, the functionalities and responsibilities assigned to each agent, and the characteristics of the information that agents can share, play an important role in the performance of the system. Agents are entities that act on the environment and have communication capability, some level of autonomy based on their own goals, and a limited knowledge of the environment (e.g., terminal measurements) [37]. Although communication between agents play an important role in the coordination of DERs, a large part of control is based on their autonomy and is performed locally.

An EMS based on the MAS concept for microgrids is proposed in [38], as an alternative for coordinated operation of microgrids in a competitive market environment and with multiple generator owners. The relevant microgrid players are grouped and represented by different agents that interact in a market environment in order to determine the operation of the microgrid. In this way, consumers, generators, and ESSs participate in the market by sending buying and selling bids to the MGCC based on their particular needs, availability, cost functions, technical limitations, expectations and forecasts. The MGCC is responsible for the settlement of the microgrid market by matching buying and selling bids maximizing the social welfare, while ensuring the feasibility of the resulting dispatch. A similar MAS approach is also proposed in [39], where power flow calculations are performed to verify

that the dispatch obtained in the market complies with technical standards and other operational constraints.

In [40], additional agents assigned to different tasks such as load shifting and load curtailment, to allow demand side management and real power mismatches produced in the real-time operation of the microgrid, are shared by the DG units in proportion to their available unused capacity. In order to keep the design flexible, an external relational database containing the scheduling procedures is considered, and a short-term battery-ESS is also considered to balance fast changes in demand, with no participation in the market.

An EMS using a so-called gossip-based technique, which can be considered as a special case of MAS, is proposed in [41]. According to the gossip-based control, different units exchange information regarding their operation, such as mismatches between programmed and actual power outputs, and marginal costs. To return the frequency and voltages to its original values after a system disturbance, DG units exchange the mismatches between their programmed and actual active and reactive power outputs, and calculate the average mismatch for the whole microgrid. The average mismatch is then added to the droop controllers' references to counteract the initial shift. Several strong assumptions must be made for the proposed approach to work properly, such as all droop controllers having the same droop constants, and voltage control within the microgrid being carried out from distant locations without considerable performance degradation. Optimality of the operation is obtained by progressively averaging random pairs of DG units, converging to a unique marginal cost.

Managing multi-period operation scheduling becomes a more challenging issue in decentralized control schemes, since not all the necessary information regarding systems state, data forecast and cost functions is available to all the agents. A MAS-based architecture is proposed in [42] that includes additional agents that may enable a multi-period operation scheduling of the microgrid. Service agents provide forecasting information and database services to the LCs to allow a better management of the energy resources over a more extended operating horizon; however, special protocols and procedures to handle the information to achieve this desired feature are yet to be studied.

The architecture of a decentralized EMS with service agents and the internal structure of an LC are shown in Figs. 1.2 and 1.3, respectively. A similar architecture is proposed in [43], which considers only generation-side bids and a sequential negotiation process; starting with the DG with lower full load average cost (FLAC), the active power mismatch for the next period of operation is negotiated with each DG in the microgrid until it is balanced.

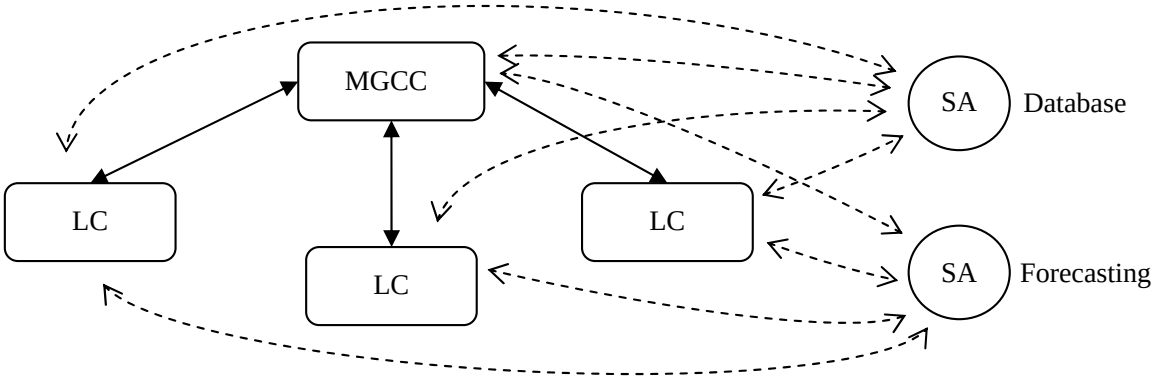

Fig. 1.2: MAS-based architecture with service agents.

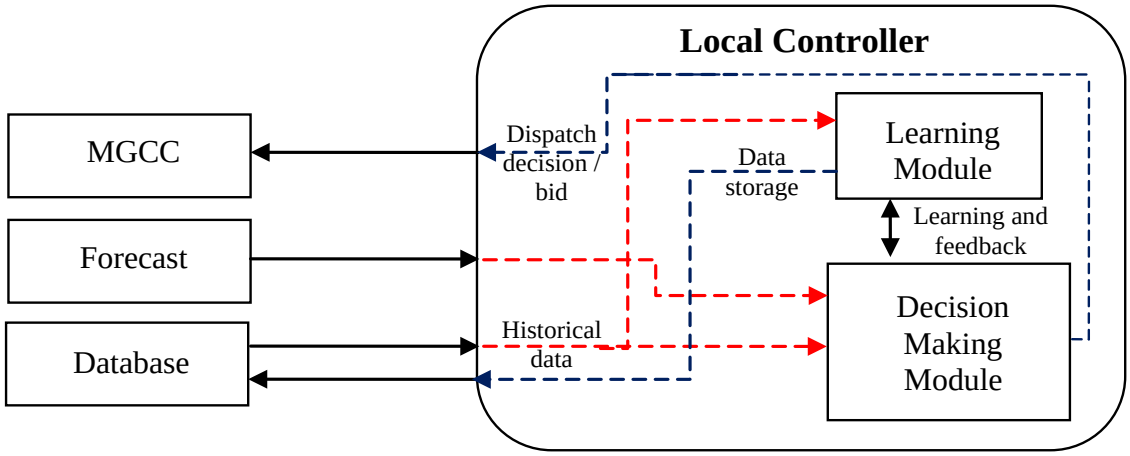

Fig. 1.3: Internal structure of an LC.

1.2.3 Discussion

Research on microgrid EMSs over the last 10 years has shown significant progress and yielded important outcomes. Different levels of detail on components modeling, network representation, and different EMS architectures and functionalities have been proposed; however, many issues still remain unresolved or insufficiently discussed. Particularly, a unified approach that incorporates highly detailed models of the microgrid and its components, and provides appropriate representation of time-coupling characteristics and uncertainty has not yet been developed.

A clear distinction between centralized and decentralized EMS approaches can be identified. Centralized approaches allow high levels of coordination in the operation of DERs, which are dispatched as a result of an optimization problem, at the cost of reduced autonomy of DERs. On the other hand, decentralized methodologies allow higher levels of autonomy in the operation of each DER, which is a disadvantage in microgrids that require strong cooperation between different DERs. The latter is the case of isolated microgrids, where the small number of generators and critical demand-supply balance demands high levels of coordination in order to operate the system in a secure and reliable way. In this context, the centralized method is more suitable for isolated microgrid applications [44], and hence the EMS techniques proposed in this thesis are based on this approach.

1.3 Objectives

Based on the state-of-the-art on EMSs for isolated microgrids discussed above, the main objectives pursued in this thesis are the following:

1. Propose detailed mathematical models for the microgrid system and components that are able to properly represent the effects of power flow patterns, voltage limits, and system imbalance for energy management applications in isolated microgrids.

2. Propose a deterministic formulation of the optimal energy management problem of isolated microgrids that employs detailed mathematical models in order to determine the optimal operation of DERs in time, given available forecasts for load and RE generation.

3. Propose a centralized EMS architecture that employs the formulation of the optimal energy management problem to obtain economical dispatch solutions that can be implemented in the real-time operation of actual isolated microgrids.

4. Investigate the impact of representing unbalanced system conditions on the optimal dispatch of isolated microgrids, using the proposed EMS design.

5. Apply a stochastic optimization approach to the proposed formulation of the optimal energy management problem, in order to account for the uncertainty associated with the external forecasting systems directly in the problem formulation.

6. Investigate the effects of considering uncertainty on the optimal dispatch of isolated microgrids, under different system conditions and EMS design parameters.

1.4 Thesis Outline

The rest of this thesis is structured as follows: Chapter 2 presents a background review of the main concepts, models and tools used in this thesis. It describes the microgrid concept in detail, existing models for the analysis of distribution systems, and the MPC approach. The formulation of the OPF and UC problems is also discussed, followed by a brief review of SP models.

Chapter 3 describes the proposed detailed mathematical models of the microgrid system and components. The models include three-phase representations of the distribution network, DGs units, ESSs, and loads, together with mathematical expressions that describe various operational constraints. Finally, the optimal energy management problem is presented as an MINLP problem.

Chapter 4 presents a novel deterministic, centralized EMS approach for isolated microgrids. First, a decomposition of the energy management problem into separate UC and OPF problems is discussed, which allows the problem to be solved in computational times suitable for real-time applications. Then, an MPC-based architecture of the EMS is presented, followed by a discussion on the EMS implementation. Finally, simulation results are presented, including a discussion on the effect of unbalanced system modelling.

Chapter 5 describes a novel stochastic, centralized EMS approach for isolated microgrids. In this chapter, a reformulation of the UC using stochastic programming is presented, and the implications of this reformulation on the EMS architecture and implementation are discussed. The chapter also includes simulation results for the proposed stochastic EMS and a discussion on the effects of uncertainty on the optimal dispatch of the microgrid, under different EMS parameters and system configurations.

Chapter 6 summarizes the main contents and contributions of this thesis, and suggests directions for future research work. Finally, Appendices A and B present detailed data

of the test system used for simulations, and the characteristics of the external forecasting system, respectively.

Chapter 2

Background Review

This chapter provides a general overview of the concepts, models, tools and techniques used in the development of the research presented in this thesis.

2.1 AC Microgrids

The concept of microgrid is introduced in the technical literature as a solution for the reliable integration of DERs, including ESSs, and controllable loads [45,46]. Such microgrid would be perceived by the main grid as a single element responding to appropriate control signals.

2.1.1 Microgrid Definitions

A detailed definition of microgrids is still under discussion in technical forums; however, in general, a microgrid can be described as a cluster of loads, DG units and ESSs operated in coordination to reliably supply electricity, connected to the host power system at the distribution level at a single point of connection or Point of Common Coupling (PCC). Microgrids with no connection to a host power system are referred to as isolated microgrids. This is the case of remote sites (e.g., remote communities or remote industrial sites) where an interconnection with the main grid is not feasible due to either technical and/or economic constraints; therefore, isolated microgrids operate permanently in stand-alone mode.

In general, microgrids can have any arbitrary configuration, as illustrated in Fig. 2.1. In cases where a strong coupling between the operation of different energy carrier systems

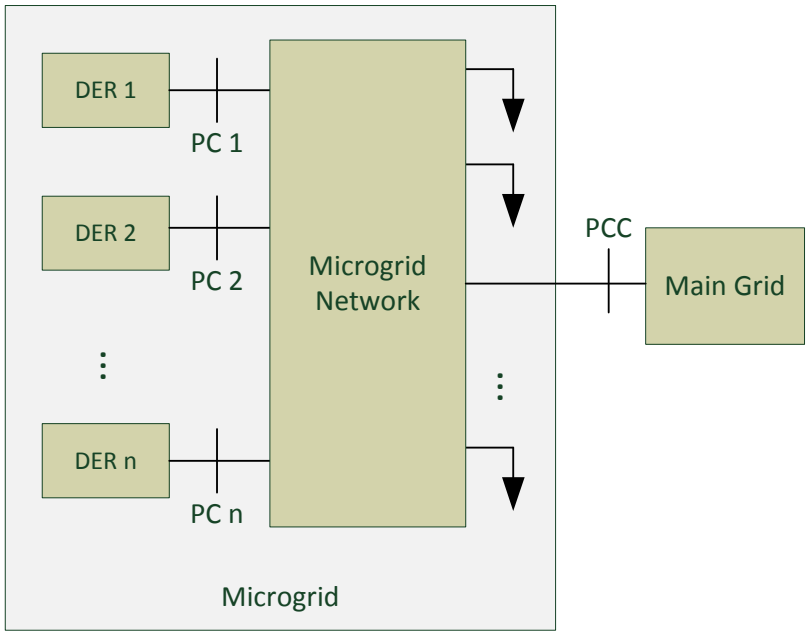

Fig. 2.1: Schematic diagram of a generic multiple-DER microgrid.

(heating, hot water, etc.) exists, microgrids can integrate and operate all these energy carriers in coordination. Being a concept still under development, different deployments and research projects on microgrids around the world present different perspectives and give emphasis to different aspects of the concept. These include microgrids of Bella Coola and Hydro-Quebec in Canada [5, 8], Consortium for Electric Reliability Technology Solutions (CERTS) in the United States [47], Microgrids and More Microgrids in Europe [48], Huatacondo in Chile [11], and New Energy and Industrial Technology Development Organization (NEDO) in Japan [5].

A microgrid is capable of operating in grid-connected and stand-alone modes, and handling the transitions between these two modes [49,50]. In the grid-connected mode, the power deficit can be supplied by the main grid, and excess power generated in the microgrid can be traded with the main grid and can provide ancillary services. The islanded mode of operation represents a more critical case, where the real and reactive power generated within the microgrid must be in balance with the demand of local loads.

2.1.2 Control and Protection Requirements

Microgrids, and integration of DER units in general, introduce a number of operational challenges that need to be addressed in the design of control and protection systems, in order to ensure that the present levels of reliability are not significantly affected and the potential benefits of DG are fully harnessed. The microgrid's control system must be able to ensure the reliable and economical operation of the microgrid, while overcoming the aforementioned challenges. In particular, desirable features of the control system include:

- *Output control*: Output voltages and currents of the various DER units must track their reference values and ensure oscillations are properly damped.
- *Power balance*: DER units in the microgrid must be able to accommodate sudden active power imbalances, either excess or shortage, keeping frequency and voltage deviations within acceptable ranges.
- *Demand Side Management (DSM)*: Where applicable, proper DSM mechanisms must be designed in order to incorporate the ability to control a portion of the load. Additionally, for the electrification of remote communities with abundant local renewable resources, the active participation of the local community may be beneficial in order to design cost-effective DSM strategies that enhance load-frequency control [51, 52].
- *Economic dispatch*: An appropriate dispatch of DER units participating in the operation of a microgrid can significantly reduce the operating costs, or increase the profit. Reliability considerations must also be taken into account in the dispatch of units, especially in stand-alone operation.
- *Transition between modes of operation*: A desirable feature of microgrids is the ability to work in both grid-connected and stand-alone modes of operation, including a smooth transition between them.

In the microgrid environment, characterized by frequent and multiple changes in topology, robustness and adaptiveness of controllers are desirable traits. Availability of measurements, communication, and high-speed computational facilities are additional challenges for all of the above requirements; for this reason, an attempt should be made in order to reduce the need for high-speed communications and computation in critical tasks.

Given the different time constants involved in the control tasks, ranging from fast dynamics in the output controls to slower dynamics in the economic dispatch, microgrids

feature a hierarchical control structure. Complexity and sophistication of the solutions for the control requirements of the microgrid will be very much dependent on whether it is designed to primarily operate in stand-alone or grid-connected mode. While in grid-connected mode of operation emphasis is put on the interaction with the main grid, reliability issues are more significant in stand-alone mode of operation. A description of controlled variables used in microgrid control and different types of DER units is presented next.

Controlled Variables

The main variables used to control the operation of a microgrid are voltage, frequency, and active and reactive powers. In the grid-connected mode of operation, the frequency of the microgrid and the voltage at the PCC are dominantly determined by the host grid. The main role of the microgrid control in this case is to accommodate the active and reactive powers generated by the DER units to supply the load demand. Reactive power injection by a DER unit can be used for power factor correction, reactive power supply, or voltage control at the corresponding Point of Connection (PC).

In stand-alone mode of operation, the microgrid operates as an independent entity. This mode of operation is significantly more challenging than the grid connected mode, because the critical demand-supply equilibrium requires the implementation of accurate load sharing mechanisms to balance sudden active power mismatches. Voltages and frequency of the microgrid are no longer supported by a host grid, and thus they must be controlled by different DER units. LCs ensure power balance in the microgrid utilizing local measurements, while power sharing can be determined either by properly calibrating these LCs, or by a central controller that communicates appropriate set points to DER units and controllable loads. The main objective of such a mechanism is to ensure that all units contribute to supplying the load in a pre-specified manner. A minute mismatch in the amplitude, phase angle or frequency of the output voltage of any unit in the group can lead to a relatively high circulating current. One possible approach is to have one inverter operate as a master unit that regulates the voltage of the microgrid [53], whereas the same or different unit can set the system frequency. The remaining DER units, in this case, are operated in PQ-mode [54].

Types of DER Units

The DER units present in a particular microgrid are very problem-specific and depend on a variety of factors, including whether the microgrid is designed to operate in grid-connected

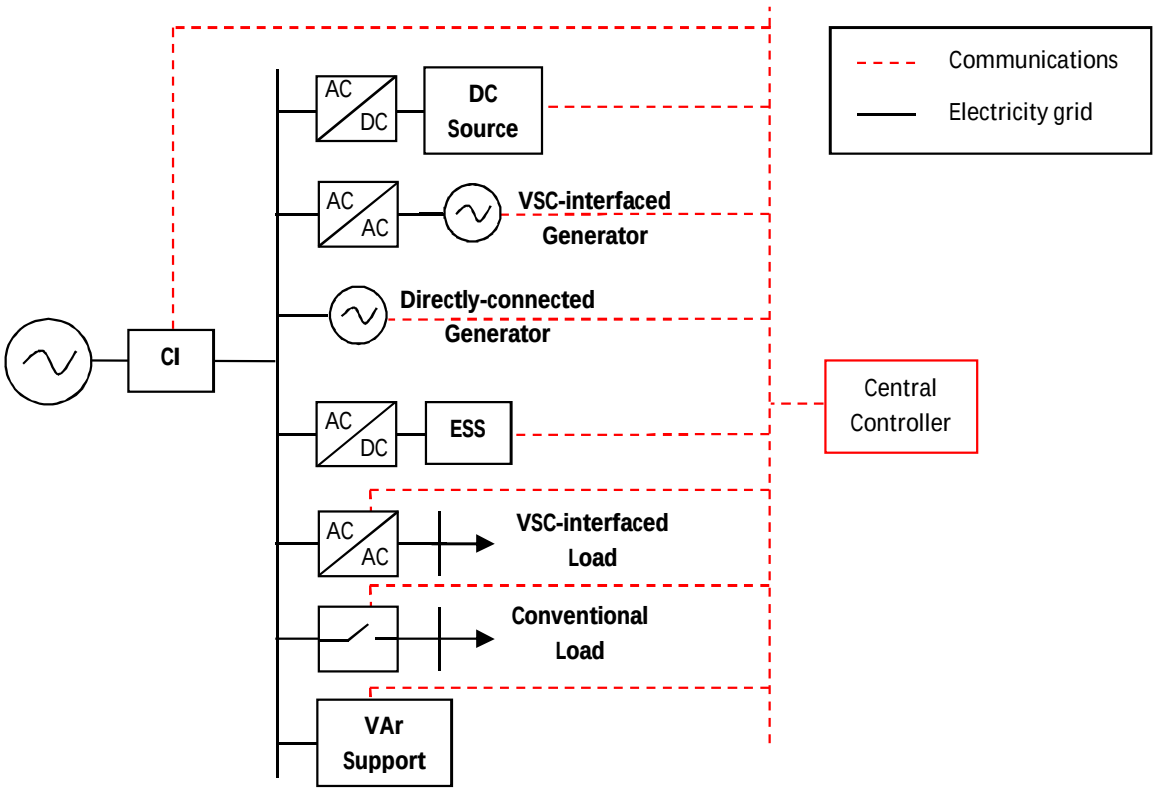

Fig. 2.2: Microgrid general components.

or stand-alone mode, the different generation technologies deployed, and the topology of the system [55]. In general, the components that can be found in a microgrid are illustrated in Fig. 2.2.

Microgrids are characterized by a single point of connection with the host grid. The Connection Interface (CI) at the PCC can be realized using electro-mechanical circuit breakers, solid state switches or even back-to-back converters. The connection of DC-type energy sources such as PV panels, fuel cells and energy storage technologies (batteries and ultracapacitors) requires the use of a DC-to-AC power converter interface. While some conventional generators can be connected directly to the microgrid and operate at 50/60 Hz, variable-speed generators such as wind turbines using synchronous machines, and high-speed microturbines require the use of AC-to-AC power converters to match the constant frequency and voltage of the microgrid. Wind turbines can also be less flexible

induction generators directly connected to the system, or more flexible doubly-fed induction generator. Loads within the microgrid can be controlled using either a conventional circuit breaker, or a more sophisticated AC-to-AC power electronic interface to allow more flexible control. Reactive power support can be provided by capacitor banks, SVCs or STATCOMs.

DER units can also be categorized based on their dispatchability. Dispatchable units (e.g., diesel generators) can be fully controlled; however, nondispatchable units cannot, and are typically operated to extract the maximum possible power. DER units based on renewable energy sources (e.g., wind turbines or photovoltaic units) are generally intermittent and their output is not fully controllable.

ESSs play a very important role in microgrids, because while renewable energy resources are the microgrids main drivers of the microgrid technology, their generation cannot provide firm capacity if not accompanied by ESSs, and thus has to be duplicated by other means of generation. Hence, ESSs can be combined with other nondispatchable DER units such as wind and solar energy to turn them into dispatchable units. In order to fully utilize the potential of ESSs in microgrids, appropriate control and management strategies are necessary (e.g., peak shaving, seasonal storage, frequency regulation, voltage support and reliability enhancement) [32]. Different ESS technologies include: Battery Energy Storage System (BESS), Compressed Air Energy Storage (CAES) systems, flywheels, thermal energy storage, pumped hydro and Superconducting Magnetic Energy Storage (SMES) [56], with each technology having different advantages and disadvantages depending on the intended application. An extensive list of applications for energy storage in transmission, distribution, and generation is presented in [57].

2.1.3 Control Hierarchy in a Microgrid

Microgrids feature a hierarchical control structure consisting of three control levels: primary, secondary, and tertiary [58–61], as depicted in Fig. 2.3. These control levels differ in their speed of response, the time frame in which they operate, and their infrastructure requirements (e.g., communication and computation requirements). Tertiary control level typically operates in the order of several minutes, providing signals to secondary level controls at microgrids and other subsystems that form the full grid. Secondary controls, on the other hand, coordinate internal primary controls within the microgrids and subsystems in the span of a few minutes. Finally, primary controls are designed to operate independently and react in predefined ways instantaneously to local events.

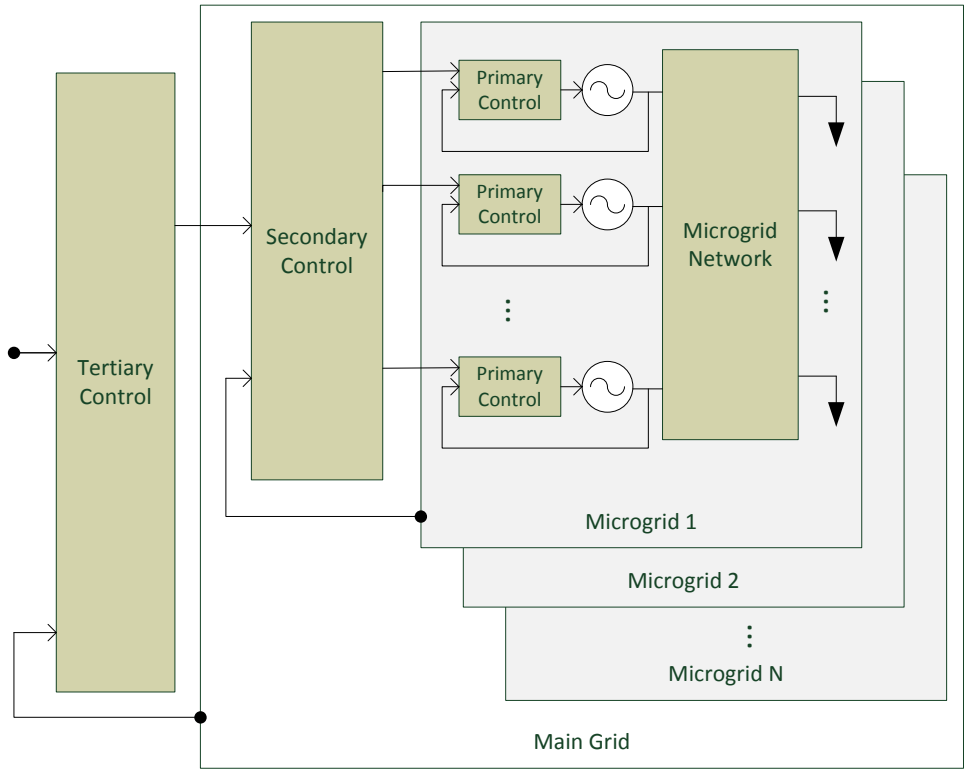

Fig. 2.3: Hierarchical control levels: primary control, secondary control, and tertiary control.

Primary Control

Primary control, also known as local control or internal control, is the first level in the control hierarchy, featuring the fastest response. This control is based exclusively on local measurements and does not rely on external communications. Given their speed requirements and reliance on local measurements, islanding detection, output control, and power sharing control are included in this category [49, 50, 62].

In synchronous generators, output control and power sharing is performed by the voltage regulator, governor, and the inertia of the machine itself. On the other hand, Voltage-Source Inverter (VSI)-interfaced units require a specially designed control to simulate the inertia characteristic of synchronous generators and provide appropriate frequency regulation. For this purpose, VSI controllers are composed of two stages: DG power sharing controller and inverter output controller. Power sharing controllers are responsible for the adequate share of active and reactive power mismatches in the microgrid, whereas inverter output controllers should control and regulate the output voltages and currents [49, 50, 53, 63, 64]. Inverter output control typically consists of an outer loop for voltage control and an inner loop for current regulation, in a nested configuration. Power sharing is performed by using active power-frequency and reactive power-voltage droop controllers that emulate the droop characteristics of synchronous generators [65], although several variations of this configuration have also been proposed.

Secondary Control

Secondary control, also referred to as the microgrid EMS, is responsible for the reliable, secure and economical operation of microgrids in either grid-connected or stand-alone mode. This task becomes particularly challenging in isolated microgrids with the presence of highly-variable energy sources, where the update rate of the unit dispatch command should be high enough to keep up with the changes of the load and non-dispatchable generator profiles. The objective of the EMS consists of finding the optimal (or near optimal) UC and dispatch of the available DER units, so that certain selected objectives are achieved by providing set points for real and reactive power of DERs [66].

With respect to the EMS architecture, two main approaches can be identified: centralized and decentralized architectures. In a centralized approach, a central controller is responsible for economic optimization of the microgrid, as well as maintaining reliable, secure, and safe operation of the grid [67]. In a typical decentralized approach, the optimal operation is sought through the implementation of market-like techniques, where

the individual DER units are controlled by local agents that exchange information with a coordinating agent to determine a market settlement [38].

Secondary control is the highest hierarchical level in microgrids operating in stand-alone mode, and operates on a slower time frame as compared to the primary control in order to decouple their operation, reduce the communication bandwidth, and allow enough time to perform complex calculations.

Tertiary Control

Tertiary control is the highest level of control, and sets long-term and typically "optimal" set points depending on the requirements of the host power system. This tertiary control is responsible for coordinating the operation of multiple microgrids interacting with one another in the system, and communicating needs or requirements from the host grid (voltage support, frequency regulation, etc.). For example, the overall reactive power management of a grid that contains several microgrids could be accomplished by properly coordinating, through a tertiary control approach, the reactive power injection of generators and microgrids at the PCC, based on a centralized loss minimization approach for the entire grid.

2.2 Distribution System Modelling

The integration of DG units at a distribution system level has brought attention to the issue of developing accurate models and tools for the analysis of distribution systems. Such models cannot be directly extended from existing transmission system models, as many assumptions typically made for transmission levels do not hold valid in distribution systems (e.g., balanced loading conditions, equal phase impedances, and negligible line resistances). This section presents a brief description of the models for distribution system elements discussed in [68,69], which are used throughout this thesis. The models use phasor representations of physical quantities, and are based on the assumption that neutral wires are grounded at multiple points, and hence the voltage of the neutral wire is zero throughout the distribution system.

2.2.1 Transmission Lines

In a transmission line segment, phase voltages and currents at each end can be related using 3-by-3 series-impedance and shunt-admittance matrices, which are calculated directly from

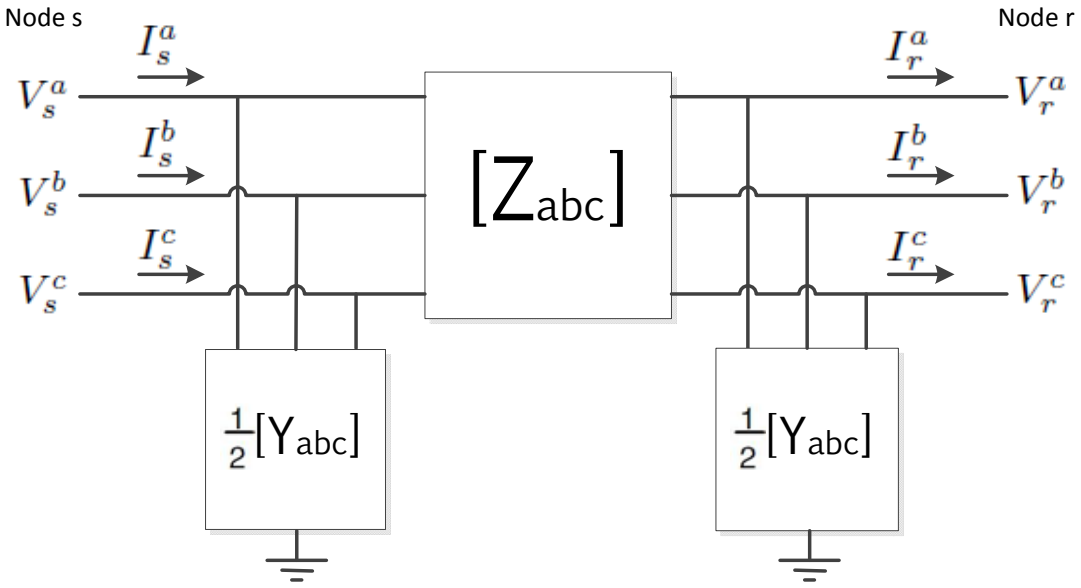

Fig. 2.4: Transmission line segment model.

the type of conductor and geometry of the poles. Thus, for the four-wire grounded-neutral line segment shown in Fig. 2.4, line voltages and currents at each end of the line can be related as follows:

$$\begin{bmatrix} V_s^a \\ V_s^b \\ V_s^c \\ I_s^a \\ I_s^b \\ I_s^c \end{bmatrix} = \begin{bmatrix} & \\ \text{A} & \text{B} \\ & \\ & \\ \text{C} & \text{D} \\ & \end{bmatrix} \begin{bmatrix} V_r^a \\ V_r^b \\ V_r^c \\ I_r^a \\ I_r^b \\ I_r^c \end{bmatrix} \tag{2.1}$$

where A, B, C and D are 3-by-3 matrices calculated from the series impedance matrix Z_{abc} and shunt admittance matrix Y_{abc} of the line, as follows:

$$A = U + \frac{1}{2} Z_{abc} Y_{abc} \tag{2.2}$$

$$B = Z_{abc} \tag{2.3}$$

$$C = Y_{abc} + \frac{1}{4} Y_{abc} Z_{abc} Y_{abc} \tag{2.4}$$

$$D = U + \frac{1}{2} Z_{abc} Y_{abc} \tag{2.5}$$

In (2.2) to (2.5), U is a 3-by-3 identity matrix. It is important to note that this general model also allows the representation of single-phase and two-phase feeders, where the differences will be reflected only on the entries of the impedance and admittance matrices of the line.

2.2.2 Transformers

Three-phase transformers are series elements connecting two nodes, where phasor voltages and currents at the source-side (s) are linear functions of phasor voltages and currents at the load-side (r), and vice versa. Thus, similar to transmission lines, phasor quantities on each side of the transformer can be related as follows:

$$\begin{bmatrix} V_s^a \\ V_s^b \\ V_s^c \\ I_s^a \\ I_s^b \\ I_s^c \end{bmatrix} = \begin{bmatrix} & & \\ A_t & & B_t \\ & & \\ & & \\ C_t & & D_t \\ & & \end{bmatrix} \begin{bmatrix} V_r^a \\ V_r^b \\ V_r^c \\ I_r^a \\ I_r^b \\ I_r^c \end{bmatrix} \tag{2.6}$$

where A_t, B_t, C_t and D_t are 3-by-3 matrices that depend on the transformer parameters, taps (considered fixed here), and winding connections [69]; voltages V^a, V^b and V^c represent line-to-ground voltages per-phase in the case of grounded wye transformer connections, and line-to-neutral voltages for ungrounded wye connections. For delta connections, the voltages represent equivalent line-to-neutral voltages, which can be converted to line-to-line voltages as follows:

$$\begin{bmatrix} V^{ab} \\ V^{bc} \\ V^{ca} \end{bmatrix} = \begin{bmatrix} 1 & -1 & 0 \\ 0 & 1 & -1 \\ -1 & 0 & 1 \end{bmatrix} \begin{bmatrix} V^{a} \\ V^{b} \\ V^{c} \end{bmatrix} \tag{2.7}$$

Finally, phasors I^a, I^b and I^c represent line currents, regardless of how winding are connected in the transformer.

2.2.3 Loads

Loads in distribution systems can be modelled as constant-power, constant-impedance, constant-current, or a combination of them. Regarding their connection, they can be either wye- or delta-connected, and can feature an arbitrary level of unbalance. For consistency with the models of other elements in distribution networks, load voltages and currents are expressed here in terms of line-to-neutral voltages and line currents. In the case of delta-connected loads, line-to-line and line-to-neutral voltages can be related using (2.7); similarly, phase currents in delta connection and line currents can be related as follows:

$$\begin{bmatrix} I^{a} \\ I^{b} \\ I^{c} \end{bmatrix} = \begin{bmatrix} 1 & 0 & -1 \\ -1 & 1 & 0 \\ 0 & -1 & 1 \end{bmatrix} \begin{bmatrix} I^{ab} \\ I^{bc} \\ I^{ca} \end{bmatrix} \tag{2.8}$$

Based on (2.7) and (2.8), the load equations can be expressed in a per-phase basis using line currents and line-to-neutral voltages, regardless of the type of connection of the load.

2.3 Model Predictive Control

MPC, also known as Receding Horizon Control (RHC), is an optimization-based control strategy in which a finite-horizon open-loop optimal control problem is formulated and solved at each time-step [70]. System states at future time-steps are calculated as a function of the control variables and initial system conditions, using a dynamic model of the system. The optimization calculates a control sequence for the whole finite horizon such that a selected objective function is minimized, but only the control action for the next time

step is implemented; this process repeats itself every time-step. Specifically, consider a discrete-time, time-invariant dynamic model of the system as follows:

$$x_{t+1} = F(x_t, u_t) \tag{2.9}$$

subject to the constraints:

$$x_t \in \mathbb{X}, u_t \in \mathbb{U} \tag{2.10}$$

where x_t is the vector of state variables and u_t the vector of control variables at time t. Based on these model and constraints, a finite-horizon optimal control problem can be formulated at time t as follows:

$$\mathcal{U}(x_t) = \begin{cases} \min\limits_{u_t|_t \dots u_{t+T}|_t} & \sum\limits_{\hat{t}=t}^{t+T} J_{\hat{t}}(x_{\hat{t}}|_t, u_{\hat{t}}|_t) \\ \text{s.t.} & x_t|_t = x_t \\ & x_{\hat{t}+1}|_t = F(x_{\hat{t}}|_t, u_{\hat{t}}|_t) \\ & x_{\hat{t}}|_t \in \mathbb{X} \\ & u_{\hat{t}}|_t \in \mathbb{U} \end{cases} \tag{2.11}$$

where x_t is the current state of the system, and $x_{\hat{t}}|_t$ is the vector of state variables at time $\hat{t}$, based on the known state of the system at time t, predicted based on the system model; similarly, $u_{\hat{t}}|_t$ is the vector of control variables at time $\hat{t}$ based on the known state of the system at time t. Function $J_{\hat{t}}(x_{\hat{t}}|_t, u_{\hat{t}}|_t)$ is the objective of the optimal control problem at time $\hat{t}$, which can be any measure of the control performance.

The solution of the optimal control problem $\mathcal{U}(x_t)$ in (2.11) will produce a set of optimal control actions $\{u_t^*|_t \dots u_{t+T}^*|_t\}$, given the initial state x_t. Only the first control action $u_t^*|_t$ will be applied to the system, and the problem will be solved again at $t+1$ to obtain a new set of solutions based on the state $x_{t+1}|_{t+1}$ [71,72]. The procedure is illustrated in Fig. 2.5.

In order to obtain the best possible results from the optimization problem, there is an incentive for using larger optimization horizons T; however, the resulting optimization problem may be too big to be solved in reasonable computational times. Furthermore, the accuracy and resolution of the prediction model typically decrease with larger horizons due to the increase in number and depth of uncertainties, which limits the quality of the obtained solutions.

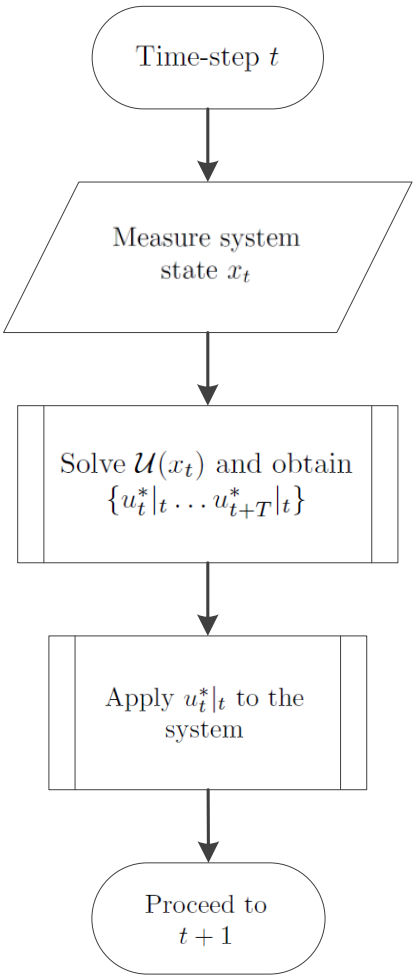

Fig. 2.5: MPC approach.

MPC strategies are quite appealing for energy management of microgrids, since they allow for the implementation of control actions that anticipate future events such as variations in power outputs from non-dispatchable DGs and instantaneous demand.

2.4 Optimal Power Flow and Unit Commitment

OPF and UC are important tools in the operation of power systems, and correspond to subproblems that determine the overall economical steady-state operation of power systems. Each problem focuses on different aspects of the operation, with the OPF solving the instantaneous economical dispatch of available units, and the UC solving the economical scheduling of generating units. Hence, in general, the OPF corresponds to an instantaneous "snapshot" problem, and the UC corresponds to a multi-period problem.

2.4.1 OPF Formulation

The OPF problem was first formulated during the sixties as an extension of the conventional ELD of power systems [73]. Unlike the ELD problem, the OPF includes a detailed modeling of the electricity network, allowing the incorporation of additional technical constraints such as thermal limits of transmission lines and limits on voltages and phase angles. In general, the OPF is formulated as a non-linear constrained optimization problem that determines the instantaneous optimal steady-state of the power system, according to a defined objective function, subject to specified operating and security requirements. The desired optimal steady-state of the system is achieved by adjusting the control variables, which typically include the active and reactive power outputs from generators, reactive power injection from reactive compensation equipment (SVC, STATCOM, etc.), load shedding commands, and transformer tap settings, to name a few. With regard to the objective function, several alternatives have been considered for the OPF problem, including:

- Minimization of total cost of operation.
- Minimization of the deviation from pre-specified settings.
- Minimization of active power losses.
- Minimization of cost of load curtailment.

- Minimization of cost of installation of new equipment (e.g., capacitors bank and reactors).
- Minimization of total greenhouse gasses emissions.

In its general form, the OPF problem can be formulated as follows:

$$\begin{aligned} \min_{u} \quad & J_{OPF}(x, u, \tilde{p}) \\ \text{s.t.} \quad & g(x, u, \tilde{p}) = 0 \\ & h(x, u, \tilde{p}) \leq 0 \end{aligned} \tag{2.12}$$

where $\tilde{p} \in \Re^l$ is a vector of parameters representing the system demand, equipment connection status, fuel prices, etc.; vector $u \in \Re^m$ represents the control variables (under control of the operator); and vector $x \in \Re^n$ represents the state variables, such as voltages, phase angles and frequency. The equality constraints represent the steady-state power balance of the system, or load flow equations, while the inequality constraints represent the operating limits, such as voltage and current limits.

The OPF formulation offers several advantages with respect to the conventional ELD method. These include allowing calculation of locational marginal costs through the formulation of bus-wise supply-demand balances; enabling representation of operational constraints associated with the transmission system; allowing improvements in the system performance by using different objective functions; and enabling incorporation of more control variables.

The original formulation of the OPF problem was modified in [74] by incorporating additional security constraints in $g(.)$ and/or $h(.)$, which in general correspond to the N-1 contingency criteria. This formulation, known as security-constrained OPF (SCOPF), ensures proper operation of the system under pre- and post-contingency conditions for a selected set of contingencies. Additional criteria have been implemented ever since, including voltage stability, transient stability and small-signal stability constraints [75].

The most commonly-used objective function in the operation of power systems is the minimization of the total cost of operation. Thus, based on a non-linear efficiency curve for the generators, the heat-rate function, and consequently its cost function, can be modelled as a monotonically increasing convex quadratic function [76]; therefore, the objective function for the OPF minimizing the total operating cost of N_g generators can be expressed as:

$$J_{OPF} = \sum_{g=1}^{N_g} \left(\alpha_g P_g^2 + \beta_g P_g + \gamma_g\right) \tag{2.13}$$

with α_g, β_g, and γ_g known constants.

Equality constraints corresponding to the power balance equations for a system of N_b nodes can be written in a polar form as:

$$P_i^{inj} = V_i \sum_{j=1}^{N_b} V_j \left[G_{i,j} cos(\theta_{i,j}) + B_{i,j} sin(\theta_{i,j})\right] \quad i = 1, \ldots, N_b \tag{2.14}$$

$$Q_i^{inj} = V_i \sum_{j=1}^{N_b} V_j \left[G_{i,j} sin(\theta_{i,j}) - B_{i,j} cos(\theta_{i,j})\right] \quad i = 1, \ldots, N_b \tag{2.15}$$

where $P_i^{inj} = P_i^{gen} - P_i^{load}$ is the difference of generation and load active powers injected to the system at node i; $Q_i^{inj} = Q_i^{gen} - Q_i^{load}$ is the net reactive power injected to the system at node i; $V\angle\theta_i$ is the complex voltage at node i, represented in terms of its magnitude and phase angle; $\theta_{i,j}$ is the phase angle between the voltages at nodes i and j; and $Y_{i,j} = G_{i,j} + jB_{i,j}$ is the ij^{th} element of the Y_{bus} (nodal admittance) matrix of the system, which can be a function of other control variables in the OPF problem, such as transformer tap settings, series compensation equipment, etc.

Security limits typically included in the OPF formulations are: voltage limits, bounds on phase angles, and limits on active and reactive power generation. Additional technical limits such as thermal limits on transmission lines, tap changer limits, and FACTS operation limits may also be included in the set of inequality constraints for a more detailed formulation.

Several optimization techniques have been applied to solving the OPF problem over the years. A review of the most important techniques reported in literature until 1993 is presented in [77] and [78], including non-linear programming, quadratic programming, Newton-based methods, linear programming, mixed-integer programming and interior point methods. A more recent review incorporates also optimization techniques based on Artificial Intelligence (AI) [79].

2.4.2 UC Formulation

The UC can be formulated as a multi-period mixed-integer optimization problem as follows:

$$\begin{aligned} \min_{u} \quad & \sum_{t=1}^{T} J_{UC}(x_t, u_t, \tilde{p}_t) + G(w_t) \\ \text{s.t.} \quad & g(x_t, u_t, w_t, \tilde{p}_t) = 0 \quad \forall t \\ & h(x_t, u_t, w_t, \tilde{p}_t) \leq 0 \quad \forall t \end{aligned} \tag{2.16}$$

where $\tilde{p} \in \Re^l$ is a vector of parameters representing the system demand, fuel prices, minimum up-times and minimum down-times of generators, ramping limits, etc.; vector $u \in \Re^m$ represents the continuous control variables (e.g., active power dispatch); vector $x \in \Re^n$ represents the state variables, such as voltages and phase angles; and $w \in \{0, 1\}$ represents the binary control variables associated with start-up and shut-down operations of the generation units.

The objective function in (2.16) is separated in two parts, where the fist term $J_{UC}(.)$ represents, in a traditional formulation, the fuel costs of generators, and the second term $G(.)$ represents the costs associated with start-up and shut-down operations of generators, together with the fixed operational costs when a generation unit is committed. Equality constraints include the steady-state power balance of the system, or load flow equations, and logic constraints associated with the binary decision variables. Inequality constraints represent the operating limits of the units, including output power limits, ramping rate limits, and minimum up- and minimum down-times.

A classical approach is to formulate the UC as an MILP problem. In this case, power balance equations are simply represented by an active power demand-supply balance of the system; voltages and currents throughout the system are not modelled in this approximation. In this case, the problem can be solved using highly efficient commercial grade MILP solvers, such as CPLEX.

In cases where scheduling of units is significantly constrained by the network conditions, a network model is required; for example, UC formulations may include DC-power flow models to account for flow limits in the transmission lines. If a high level of detail is represented, the grid can be fully represented using equations (2.14) and (2.15), plus additional security constraints, which would result in an MINLP formulation.

Given the relevance of the UC in the operation of power systems, a wealth of solution techniques have been explored in the literature with the objective of obtaining adequate solutions in reasonable computational times [80]. The most relevant techniques include Dynamic Programming [81, 82], Branch-and-Bound [83, 84], Interior Point methods [85], Lagrangian Relaxation [86, 87] and AI-based techniques [88–90].

2.5 Stochastic Programming

The formulation of deterministic optimization problems assume that problem entries, other than the variables of the problem, are known fixed data. In most real-world problems this assumption does not hold true, as many parameters correspond to inexact measurements or statistical estimations (e.g., future power generation from RE sources). A general practice in these cases is to fix the parameters to their statistical mean or best estimate; however, depending on the problem structure, this practice may lead to very expensive or even infeasible solutions of the real problem if parameters deviate from the values assumed in the problem formulation. In order to avoid these problems, it is necessary to adopt optimization methodologies that account for these variations, and provide a certain level of "immunity" of the solutions against them. In this context, the SP approach provides an appealing framework for dealing with parametric uncertainty in optimization problems.

In SP, it is assumed that the probability distributions of the uncertain parameters are known, or can be estimated with reasonable accuracy. Hence, the SP problem is formulated so that the expected value of the objective function is optimized, subject to the feasibility of the solution for any realization of the uncertainty (with a certain confidence level) [91]. A particular, widely used, case of SP corresponds to the two-stage SP formulation. Two-stage SP considers a separation of decision variables into 2 subsets: first-stage and second-stage variables. First-stage variables need to be determined under uncertainty before the realization of a random process, while second-stage variables are obtained after the uncertainty has been revealed. In this way, the two-stage SP solution produces a unique set of first-stage decisions, and one set of second-stage decisions for each possible realization of the uncertainty. More specifically, consider the following deterministic optimization problem:

$$\begin{aligned} \min_{z} \quad & J(z, \overline{\xi}) \\ \text{s.t.} \quad & g(z, \overline{\xi}) = 0 \\ & h(z, \overline{\xi}) \leq 0 \end{aligned} \tag{2.17}$$

where $z \in \Re^N$ is the vector of decision (state and control) variables in the problem, and $\overline{\xi} \in \Re^l$ corresponds to the vector of expected values of uncertain parameters ξ. Assuming that z can be separated into first- and second-stage variables as $z = [z_1; z_2]^T$, with $z_1 \in \Re^p$ and $z_2 \in \Re^q$, and that the probability distribution of ξ is known or can be estimated with reasonable accuracy, the two-stage SP version of (2.17) can be formulated as follows:

$$\min_{z_1} \quad \mathbb{E}\left(\mathcal{J}(z_1, \xi)\right) \tag{2.18}$$

where:

$$\mathcal{J}(z_1, \xi) = \begin{cases} \min\limits_{z_2} & J(z_1, z_2, \xi) \\ \text{s.t.} & g(z_1, z_2, \xi) = 0 \\ & h(z_1, z_2, \xi) \leq 0 \end{cases} \tag{2.19}$$

In cases where the probability distribution can be properly estimated using a finite set of scenarios $\Xi = \{\xi_1, \xi_2, \ldots, \xi_K\}$, with corresponding probabilities $\Pi = \{\pi_1, \pi_2, \ldots, \pi_K\}$, a two-stage SP problem can be equivalently formulated as a large deterministic program [92], as follows:

$$\begin{aligned} \min_{z_1, z_{2,k}} \quad & \sum_k \pi_k J(z_1, z_{2,k}, \xi_k) \\ \text{s.t.} \quad & g(z_1, z_{2,k}, \xi_k) = 0 \qquad k = 1, \ldots, K \\ & h(z_1, z_{2,k}, \xi_k) \leq 0 \qquad k = 1, \ldots, K \end{aligned} \tag{2.20}$$

where $z_{2,k}$ represents the vector of second-stage variable for each realization of the uncertainty ξ_k. This is known as the deterministic equivalent of a stochastic problem [91], and allows the use of conventional commercial solvers for deterministic mathematical programs. In linear stochastic programs, the deterministic equivalents feature a particular L-shaped matrix structure, which facilitates the application of decomposition methods (e.g., benders decomposition).

2.6 Summary

This chapter reviewed various concepts and tools used throughout this thesis. The microgrid concept was introduced first, providing an overview of its control requirements and hierarchical control structure. The modelling of distribution systems was presented briefly, discussing the general models for lines, transformers and loads. The MPC technique was also introduced, including a discussion on implementation issues and the advantages of the method in microgrid control applications. The UC and OPF problems were then presented, together with some traditional problem formulations and solution methods. Finally, the SP approach was presented as an alternative to account for uncertainties in the formulation of optimization problems.

Chapter 3

A Three-phase Model of the Microgrid

Isolated microgrids are diesel-based radial distribution systems evolving to a more diversified energy supply, including intermittent renewable sources, energy storage, and other types of fuel. For this reason, these microgrids feature some of the same complexities of conventional distribution systems, including high power losses, significant voltage drops along the feeders, and considerable phase imbalance. Such complexities might have an impact on the optimality and feasibility of the dispatch strategies, and therefore, need to be properly accounted for in the design of the EMS.

This chapter presents a three-phase model of the microgrid. The proposed model uses rectangular coordinates for phasor representation, and power flow equations are presented using branch equations instead of the conventional formulation with nodal equations. This formulation has the advantage of using node voltages and branch currents as variables, which allows a more direct representation of current and voltage limits. For simplicity, the time-step index k_t has been omitted in equations that relate variables at a single time-step; such equations apply to all time steps.

3.1 Lines, Transformers and Loads

Due to similarities, series elements (e.g., transmission/distribution lines, transformers) in microgrids can be represented based on the same principles of distribution system modelling. In this context, each series element can be represented using a generalized three-phase ABCD parameter matrix, as illustrated in Fig. 3.1. Thus, as discussed in Chapter 2,

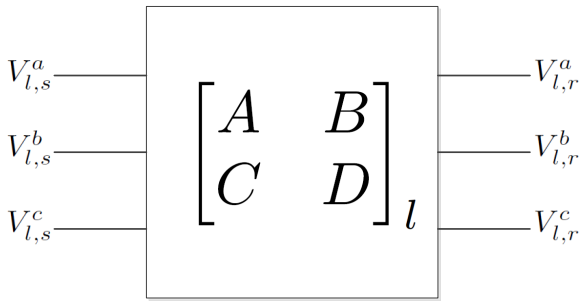

Fig. 3.1: Generic series element.

phasor voltages and currents at sending and receiving ends are related using the three-phase ABCD parameter matrix of the element as follows:

$$\begin{bmatrix} \overline{V}_{l,s} \\ \overline{I}_{l,s} \end{bmatrix} = \begin{bmatrix} A & B \\ C & D \end{bmatrix} \begin{bmatrix} \overline{V}_{l,r} \\ \overline{I}_{l,r} \end{bmatrix} \quad \forall l \tag{3.1}$$

As a convention, phasor voltages are expressed as line-to-ground quantities, and phasor currents as line quantities. The calculation of the ABCD matrices for transmission lines and transformers with different winding connections is described in [69].

Loads in a microgrid are modelled as a mix of constant-power and constant-impedance components per phase. The relations between load voltages and currents in constant-power loads and constant-impedance loads are given by (3.2) and (3.3), respectively:

$$V^p_L I^{p*}_L = P_{p,L} + jQ_{p,L} \quad \forall p, \forall L \tag{3.2}$$

$$V^p_L = Z_{p,L} I^p_L \quad \forall p, \forall L \tag{3.3}$$

In the case of delta-connected loads, equations (3.2) and (3.3) can be used to represent the relation between line-to-line voltages and phase currents. Then, the line-to-line voltages and phase currents can be related with line-to-neutral voltages and line currents using the following relations:

$$\begin{bmatrix} V^{ab} \\ V^{bc} \\ V^{ca} \end{bmatrix} = \begin{bmatrix} 1 & -1 & 0 \\ 0 & 1 & -1 \\ -1 & 0 & 1 \end{bmatrix} \begin{bmatrix} V^{a} \\ V^{b} \\ V^{c} \end{bmatrix} \tag{3.4}$$

$$\begin{bmatrix} I^{a} \\ I^{b} \\ I^{c} \end{bmatrix} = \begin{bmatrix} 1 & 0 & -1 \\ -1 & 1 & 0 \\ 0 & -1 & 1 \end{bmatrix} \begin{bmatrix} I^{ab} \\ I^{bc} \\ I^{ca} \end{bmatrix} \tag{3.5}$$

3.2 Generators

3.2.1 Directly-connected Synchronous Generators

Directly-connected synchronous generators are modelled as a special case of series element connecting internal machine voltages and terminal voltages, as illustrated in Fig. 3.2. Hence, internal and terminal machine voltages and currents can be related using an ABCD matrix as follows:

$$\begin{bmatrix} \overline{E}_{g_s} \\ \overline{I}_{g_s} \end{bmatrix} = \begin{bmatrix} A_{g_s} & B_{g_s} \\ C_{g_s} & D_{g_s} \end{bmatrix} \begin{bmatrix} \overline{V}_{g_s} \\ \overline{I}_{g_s} \end{bmatrix} \quad \forall g_s \tag{3.6}$$

This matrix for synchronous generators is calculated from the phase-impedance matrix of the machine as follows:

$$\begin{bmatrix} A_{g_s} & B_{g_s} \\ C_{g_s} & D_{g_s} \end{bmatrix} = \begin{bmatrix} U & Z_{g_s,abc} \\ \mathbf{0} & U \end{bmatrix} \quad \forall g_s \tag{3.7}$$

where the phase-impedance matrix of the machine can be estimated from the sequence-frame impedance values, using the sequence-to-phase transformation matrix, as follows:

$$Z_{g_s,abc} = \mathbf{A}\ Z_{seq,g_s}\ \mathbf{A}^{-1} \tag{3.8}$$

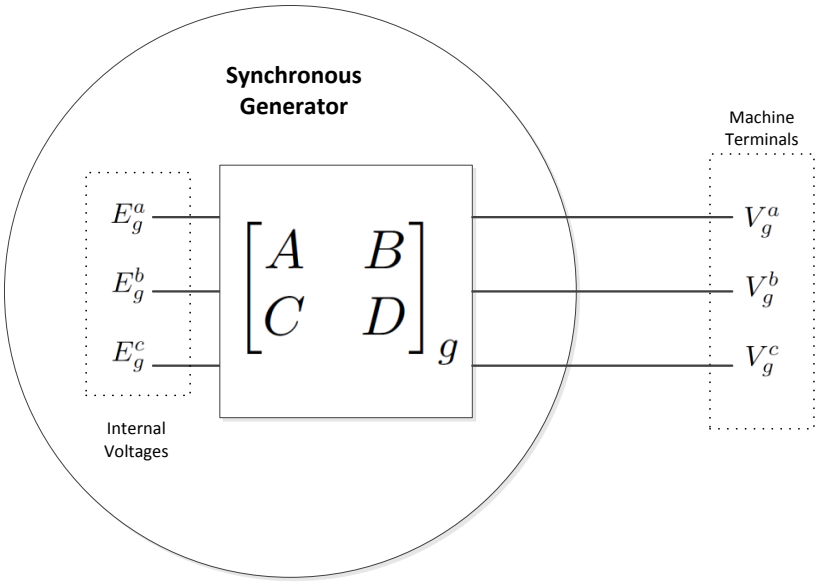

Fig. 3.2: Synchronous generator model.

where:

$$Z_{g_s,seq} = \begin{bmatrix} Z_{0,g_s} & 0 & 0 \\ 0 & Z_{pos,g_s} & 0 \\ 0 & 0 & Z_{neg,g_s} \end{bmatrix}$$

$$\mathbf{A} = \begin{bmatrix} 1 & 1 & 1 \\ 1 & a^2 & a \\ a & a & a^2 \end{bmatrix}$$

$$a = 1\angle 120^\circ$$

For simplicity, generator saliency and internal resistances are neglected in the model. Thus, the positive sequence reactance of the machine can be estimated as:

$$x_{pos,g_s} = x_{d,g_s}$$

Negative- and zero-sequence reactances of the synchronous generator can be obtained from the unsaturated direct- and quadrature-axis sub-trasient reactances, as follows [93]:

$$x_{neg,g_s} = \frac{x''_{d,g_s} + x''_{q,g_s}}{2}$$

$$x_{0,g_s} = \frac{x_{neg,g_s}}{4} + 3x_{gnd,g_s}$$

The internal synchronous machine voltage is produced by the rotor field winding rotating at homogeneous synchronous speed; therefore, in steady-state conditions, the internal machine voltage is of positive sequence. Such condition can be represented using the following equations:

$$E^a_{g_s} + E^b_{g_s} + E^c_{g_s} = 0 \quad \forall g_s \tag{3.9}$$

$$|E^a_{g_s}| = |E^b_{g_s}| = |E^c_{g_s}| \quad \forall g_s \tag{3.10}$$

It is important to note that equations (3.9) and (3.10) are also valid for negative sequence voltages; however, when used as constrains in an optimization problem, a reasonable starting point in the solution algorithm will ensure convergence to a pure positive sequence voltage.

3.2.2 Directly-connected SCIG

Directly-connected SCIGs are also modelled as a special case of series element, interfacing the machine terminals with the negative resistance representing the mechanical power input. Based on the sequence frame model of the induction machine [69], shown in Fig. 3.3, it is possible to relate sequence quantities of the machine's rotor and stator, for the positive and negative sequences, as follows:

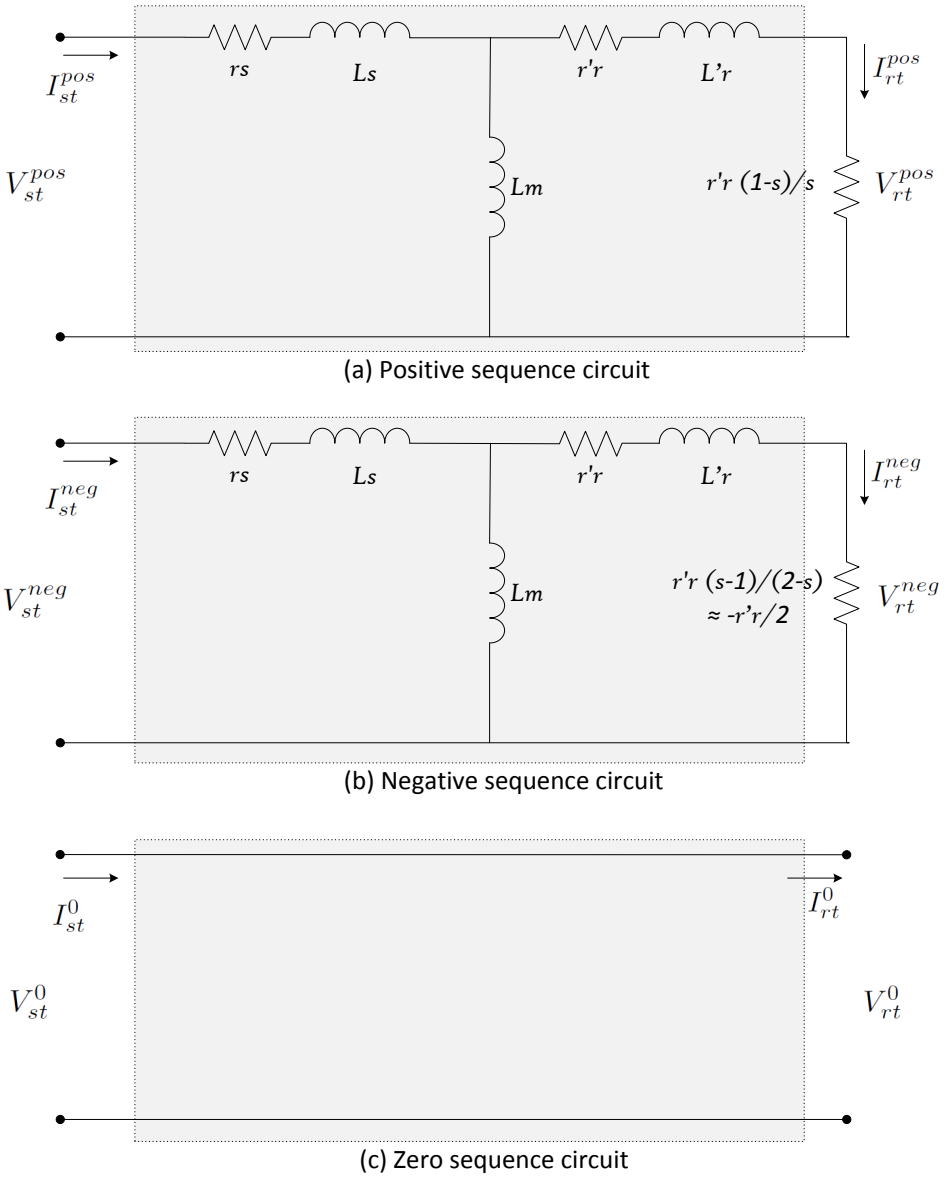

Fig. 3.3: Sequence-frame steady-state model of SCIGs.

$$\begin{bmatrix} V^x_{st,g_i} \\ I^x_{st,g_i} \end{bmatrix} = \begin{bmatrix} a_{seq} & b_{seq} \\ c_{seq} & d_{seq} \end{bmatrix} \begin{bmatrix} V^x_{rt,g_i} \\ I^x_{rt,g_i} \end{bmatrix} \quad \forall g_i \tag{3.11}$$

where $x \in \{pos, neg\}$, and:

$$\begin{bmatrix} a_{seq} & b_{seq} \\ c_{seq} & d_{seq} \end{bmatrix} = \begin{bmatrix} 1 + \dfrac{r_s + jx_s}{jx_m} & r_s + r'_r + j(x_s + x'_r) \\ & + \dfrac{(r_s + jx_s)(r'_r + jx'_r)}{jx_m} \\ \dfrac{1}{jx_m} & 1 + \dfrac{r'_r + jx'_r}{jx_m} \end{bmatrix} \tag{3.12}$$

Being a 3-wire element, the induction machine's zero sequence circuit is an open circuit; however, the series element model of the induction generator can be assumed to be a short circuit for zero sequence (see Fig. 3.3), which mathematically can be represented as follows:

$$\begin{bmatrix} V^0_{st,g_i} \\ I^0_{st,g_i} \end{bmatrix} = \begin{bmatrix} 1 & 0 \\ 0 & 1 \end{bmatrix} \begin{bmatrix} V^0_{rt,g_i} \\ I^0_{rt,g_i} \end{bmatrix} \quad \forall g_i \tag{3.13}$$

Hence, sequence quantities at stator terminals and rotor of the induction machine are related as follows:

$$\begin{bmatrix} \overline{V}^{seq}_{st,g_i} \\ \overline{I}^{seq}_{st,g_i} \end{bmatrix} = \begin{bmatrix} A_{seq} & B_{seq} \\ C_{seq} & D_{seq} \end{bmatrix} \begin{bmatrix} \overline{V}^{seq}_{rt,g_i} \\ \overline{I}^{seq}_{rt,g_i} \end{bmatrix} \quad \forall g_i \tag{3.14}$$

where the ABCD matrix of the induction generator, in the sequence frame, can be defined as follows:

$$A_{seq} = \begin{bmatrix} 1 & 0 & 0 \\ 0 & a_{seq} & 0 \\ 0 & 0 & a_{seq} \end{bmatrix} \qquad B_{seq} = \begin{bmatrix} 0 & 0 & 0 \\ 0 & b_{seq} & 0 \\ 0 & 0 & b_{seq} \end{bmatrix}$$
$$C_{seq} = \begin{bmatrix} 0 & 0 & 0 \\ 0 & c_{seq} & 0 \\ 0 & 0 & c_{seq} \end{bmatrix} \qquad D_{seq} = \begin{bmatrix} 1 & 0 & 0 \\ 0 & d_{seq} & 0 \\ 0 & 0 & d_{seq} \end{bmatrix} \tag{3.15}$$

Equation (3.15) can then be expressed in the natural abc frame, using the sequence-to-phase transformation matrix, as follows:

$$\begin{bmatrix} \overline{V}_{g_i} \\ \overline{I}_{g_i} \end{bmatrix} = \begin{bmatrix} \overline{V}_{st,g_i} \\ \overline{I}_{st,g_i} \end{bmatrix} = \begin{bmatrix} A_{g_i} & B_{g_i} \\ C_{g_i} & D_{g_i} \end{bmatrix} \begin{bmatrix} \overline{V}_{rt,g_i} \\ \overline{I}_{rt,g_i} \end{bmatrix} \quad \forall g_i \tag{3.16}$$

where:

$$\begin{bmatrix} A_{g_i} & B_{g_i} \\ C_{g_i} & D_{g_i} \end{bmatrix} = \begin{bmatrix} \mathbf{A} & \mathbf{0} \\ \mathbf{0} & \mathbf{A} \end{bmatrix} \begin{bmatrix} A_{seq} & B_{seq} \\ C_{seq} & D_{seq} \end{bmatrix} \begin{bmatrix} \mathbf{A}^{-1} & \mathbf{0} \\ \mathbf{0} & \mathbf{A}^{-1} \end{bmatrix} \tag{3.17}$$

Finally, the three-phase model of the induction generator is completed by the following equation, which describes the relation between voltages across and currents through the equivalent internal resistances of the machine:

$$\left[\overline{I}_{rt,g_i}\right] = \frac{1}{3}\left[\left(\frac{\delta}{r_r}\right)\widetilde{\mathbf{A}} - \left(\frac{2}{r_r}\right)\widetilde{\mathbf{A}}^T\right]\left[\overline{V}_{rt,g_i}\right] \quad \forall g_i \tag{3.18}$$

where:

$$\widetilde{\mathbf{A}} = \begin{bmatrix} 1 & a & a^2 \\ a^2 & 1 & a \\ a & a^2 & 1 \end{bmatrix}$$

$$\delta = \frac{s}{1-s}$$

Equation (3.18) assumes that the negative-sequence rotor resistance can be approximated as:

$$\frac{r_r(s-1)}{2-s} \approx \frac{-r_r}{2} \tag{3.19}$$

In steady-state conditions, the induction generator's slip is not expected to be higher than 1% [94]; hence, in such conditions, the approximation in (3.19) would produce a maximum error of approximately 0.5% in the value of the negative-sequence equivalent rotor resistance.

3.2.3 Inverter-interfaced Units

In principle, inverter-interfaced DERs can feature a more flexible operation as compared to synchronous and induction generators; however, such flexibility depends on the characteristics of the output control [95]. In this work, inverter-interfaced DERs are modelled as independent voltage sources per-phase, with current limits. In the case of 4-wire Voltage-Source Converters (VSCs), the following additional equation is required to limit the maximum neutral current:

$$|I^a_{g_{inv}} + I^b_{g_{inv}} + I^c_{g_{inv}}| \leq I^{max}_{n,g} \quad \forall g_{inv} \tag{3.20}$$

This neutral current limit is set to zero in the case of a 3-wire VSCs. A VSC featuring dq-voltage control will produce positive-sequence (balanced) output voltage, which can be modelled using equations (3.9) and (3.10). If the VSC is also capable of controlling negative-sequence components, such equations are not necessary and can be replaced by the following equation, which forces the zero-sequence voltage to zero:

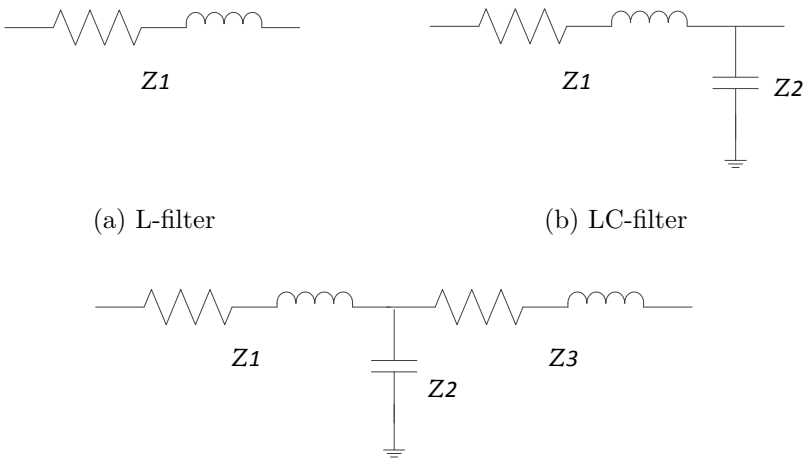

(a) L-filter

(b) LC-filter

(c) LCL-filter

Fig. 3.4: Conventional inverter output filters.

$$V^a_{g_{inv}} + V^b_{g_{inv}} + V^c_{g_{inv}} = 0 \quad \forall g_{inv} \tag{3.21}$$

Finally, if the VSC controls positive-sequence, negative-sequence, and zero-sequence independently, no additional equations are required, since in this case each phase can be considered an independent voltage source.

Output Filters

The connection of VSC-interfaced DERs with the grid typically takes place via a low-pass filter, in order to attenuate high-frequency harmonics produced by the switching process. Such low-pass filters also have an effect at fundamental frequency, and therefore they need to be properly modelled in the power flow equations.

The simplest low-pass filter topology corresponds to the first-order series inductor; however, more sophisticated alternative topologies can also be used. Figure 3.4 shows 3 typical low-pass filters used in VSC applications [95, 96].

Similar to transmission lines, low-pass filters can be modelled as additional series elements connecting VSCs with the grid, and relating three-phase voltage and current phasors at each end using the corresponding ABCD matrix. In the case of the LCL third-order low-pass filter, the ABCD matrix can be calculated as follows:

$$A_f = \begin{bmatrix} a_f & 0 & 0 \\ 0 & a_f & 0 \\ 0 & 0 & a_f \end{bmatrix} \qquad B_f = \begin{bmatrix} b_f & 0 & 0 \\ 0 & b_f & 0 \\ 0 & 0 & b_f \end{bmatrix}$$
$$C_f = \begin{bmatrix} c_f & 0 & 0 \\ 0 & c_f & 0 \\ 0 & 0 & c_f \end{bmatrix} \qquad D_f = \begin{bmatrix} d_f & 0 & 0 \\ 0 & d_f & 0 \\ 0 & 0 & d_f \end{bmatrix} \tag{3.22}$$

where:

$$\begin{bmatrix} a_f & b_f \\ c_f & d_f \end{bmatrix} = \begin{bmatrix} 1 + \dfrac{Z_1}{Z_2} & Z_1 + Z_3 + \dfrac{Z_1 Z_3}{Z_2} \\ \dfrac{1}{Z_2} & 1 + \dfrac{Z_3}{Z_2} \end{bmatrix} \tag{3.23}$$

3.2.4 Simplified Generator Models

In microgrids with several DERs of different types and sizes, it might not be necessary and/or desirable to model all units with the same level of detail. While a number of DERs will play an important role in the optimal steady-state of the microgrid, others might have little effect on the power flow patterns and operation cost. The latter is the case of small DG units in the order of tens of kW in microgrids with total installed capacity in the order of a few MW. Hence, in order to avoid unnecessarily increasing the number of equations and variables in the mathematical model, this section introduces simplified, three-phase generator models for small units in microgrids.

The simplified models consider equivalent DER units connected directly to the microgrid network without interface (low-pass filter and/or transformer), as illustrated in Fig. 3.5. Thus, DERs are modelled as independent voltage sources per phase, subject to additional constraints depending on the type of DER, and the characteristics of the connection interface.

If the DER is only able to control the positive-sequence output voltages, as it is the case with synchronous generators and some VSC-interfaced units, the positive-sequence voltage at the terminals of the equivalent DER is assumed to be controlled, but negative-

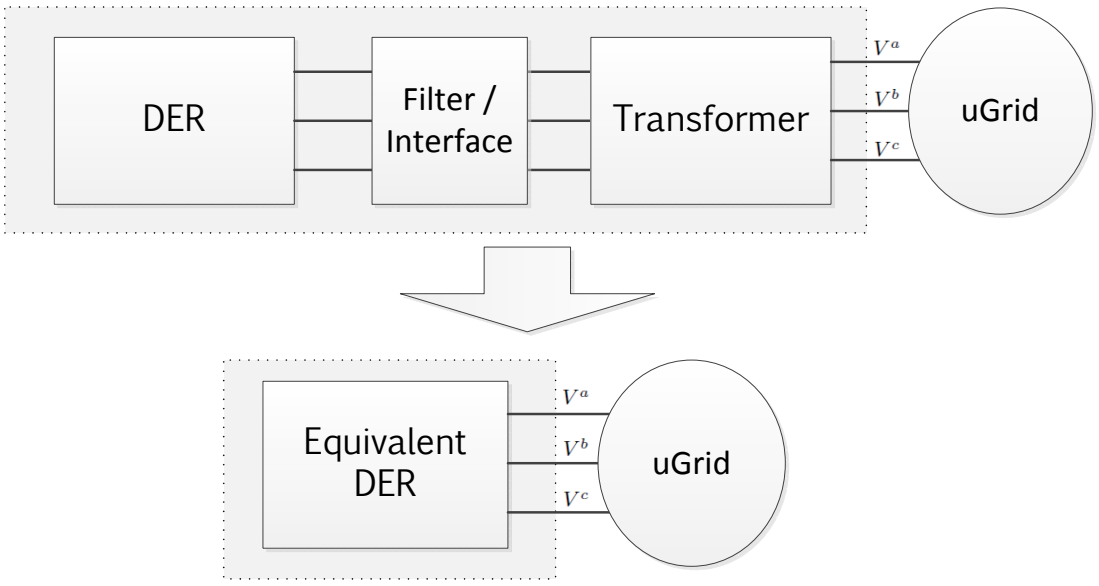

Fig. 3.5: Simplified three-phase DER model.

and zero-sequence components are determined by the conditions of the system and the sequence impedances of the interface. Mathematically, this can be represented as follows:

$$\begin{bmatrix} V_{g^*}^0 \\ V_{g^*}^{neg} \end{bmatrix} = - \begin{bmatrix} Z_{0,g^*} & 0 \\ 0 & Z_{neg,g^*} \end{bmatrix} \begin{bmatrix} I_{g^*}^0 \\ I_{g^*}^{neg} \end{bmatrix}$$
$$\implies \begin{bmatrix} 1 & 1 & 1 \\ 1 & a^2 & a \end{bmatrix} \begin{bmatrix} V_{g^*}^a \\ V_{g^*}^b \\ V_{g^*}^c \end{bmatrix} = \begin{bmatrix} Z_{0,g^*} & 0 \\ 0 & Z_{neg,g^*} \end{bmatrix} \begin{bmatrix} 1 & 1 & 1 \\ 1 & a^2 & a \end{bmatrix} \begin{bmatrix} I_{g^*}^a \\ I_{g^*}^b \\ I_{g^*}^c \end{bmatrix} \tag{3.24}$$

where the sequence impedances Z_{neg,g^*} and Z_{0,g^*} correspond to the interface (low-pass filter and/or transformer) negative- and zero-sequence impedances as seen from the microgrid; hence:

$$Z_{neg,g^*} = Z_{neg,trf} + Z_{neg,filter} \tag{3.25}$$

For Z_{0,g^*} , depending on the transformer winding connections, the following cases can be identified:

- For delta or ungrounded-wye connections on the microgrid's side, or ungrounded-wye on the DER's side: $Z_{0,g^*} = \infty$.
- For delta connection on the DER's side, and grounded-wye on the microgrid's side: $Z_{0,g^*} = Z_{0,trf} + Z_{0,trf-gnd}$.
- For grounded-wye at both sides: $Z_{0,g^*} = Z_{0,trf} + Z_{0,filter}$.

In cases where the DER unit also controls negative-sequence components, only the zero-sequence component in (3.24) is imposed. Finally, if the DER controls the three sequence components, equation (3.24) is not required.

3.3 Energy Storage

As discussed in Chapters 1 and 2, ESSs play an important role in the deployment of RE sources in microgrids, given their ability to re-shape daily load profiles by shifting power consumption in time. Therefore, appropriate steady-state models of ESSs are necessary for incorporation in the microgrid's energy management problem. In this work, two ESS technologies are modelled, namely, battery-ESS and fuel cell-electrolizer with hydrogen storage; however, the models developed can be easily extended to other types of ESS by simply adjusting efficiencies and conversion factors.

The evolution of the SoC of ESSs in time is modelled using an energy balance equation, which considers different charging and discharging efficiencies. In the case of battery-ESS, it is necessary to identify charging and discharging cycles separately in order to apply the corresponding efficiencies; hence, two positive variables, $P^{out}_{g_b}$ (discharge) and $P^{in}_{g_b}$ (charge), are introduced, as follows:

$$P_{g_b} = P^{out}_{g_b} - P^{in}_{g_b} \quad \forall g_b \tag{3.26}$$

Thus, using a simplified book-keeping model for the SoC [97], the battery-ESS balance constraints are the following:

$$SOC_{g_b,k_t+1} = SOC_{g_b,k_t} + \left(P^{in}_{g_b,k_t} \eta^{in}_{g_b} - \frac{P^{out}_{g_b,k_t}}{\eta^{out}_{g_b}} \right) \Delta t_{k_t} \quad \forall g_b, \forall k_t \tag{3.27}$$

where, at each time-step in the ESS operation, the SoC cannot be higher than its upper limit and lower than its lower limit:

$$SOC_{g_b,k_t} \leq SOC_{g_b}^{max} \quad \forall g_b, \forall k_t \tag{3.28}$$

$$SOC_{g_b,k_t} \geq SOC_{g_b}^{min} \quad \forall g_b, \forall k_t \tag{3.29}$$

Although the previous equations do not force only one of the variables $P_{g_b}^{out}$ or $P_{g_b}^{in}$ to be non-zero at a time, this will always be the case in an optimal solution of the energy management problem that minimizes cost. Thus, for example, if both P_{g_b,k_t}^{in} and P_{g_b,k_t}^{out} were different from zero, with $P_{g_b,k_t}^{in} > P_{g_b,k_t}^{out}$, there would exist another combination of $\overline{P_{g_b,k_t}^{in}}$ and $\overline{P_{g_b,k_t}^{out}}$ such that $\overline{P_{g_b,k_t}^{in}} - \overline{P_{g_b,k_t}^{out}} = P_{g_b,k_t}^{in} - P_{g_b,k_t}^{out}$, with $\overline{P_{g_b,k_t}^{out}} = 0$, that produces the same power input of the battery-ESS with lower ESS losses (cheaper operation).

Using a similar methodology, hydrogen storage SoC balance constraints depend on the power generated by fuel cells and absorbed by electrolizers connected to each hydrogen tank, as follows:

$$\begin{aligned} SOC_{H_{tank},k_t+1} &= SOC_{H_{tank},k_t} \\ &+ \left(\frac{1}{1+l_c} \frac{\sum_{g_{el} \to H_{tank}} P_{g_{el},k_t}^{H_{tank}} \eta_{g_{el}}}{HHV} - \frac{\sum_{g_{fc} \to H_{tank}} P_{g_{fc},k_t}^{H_{tank}}}{HHV \eta_{g_{fc}}} \right) \Delta t_{k_t} \quad \forall H_{tank}, \forall k_t \end{aligned} \tag{3.30}$$

$$SOC_{H_{tank},k_t} \leq SOC_{H_{tank}}^{max} \quad \forall H_{tank}, \forall k_t \tag{3.31}$$

$$SOC_{H_{tank},k_t} \geq SOC_{H_{tank}}^{min} \quad \forall H_{tank}, \forall k_t \tag{3.32}$$

where $P_{g_{el},k_t}^{H_{tank}}$ and $P_{g_{fc},k_t}^{H_{tank}}$ are the input power of the electrolizers connected to the hydrogen tank H_{tank} at time k_t, and the output power of the fuel-cells connected to H_{tank} at time k_t, respectively. Parameter l_c represents the load of the hydrogen compressor, estimated as a percentage of $P_{g_{el},k_t}^{H_{tank}}$. The equations assume that efficiencies of fuel cells and electrolizers are calculated based on the Higher Heating Value (HHV) of hydrogen [98].

3.4 Other Operational Constraints

In order to properly model the operation of the microgrid, the mathematical models of the microgrid elements are complemented by a set of constraints to represent the connection between elements and additional operational characteristics. Thus, Kirchhoff's current law at each node and phase of the microgrid are enforced using the following equations:

$$\sum_{l} I^{p}_{l,r_n} + \sum_{g} I^{p}_{g_n} = \sum_{l} I^{p}_{l,s_n} + \sum_{L} I^{p}_{L_n} \quad \forall p, \forall n \tag{3.33}$$

where I^{p}_{l,r_n} is the current injected by the receiving end of line l, which is connected to node n, through phase p; $I^{p}_{g_n}$ is the current injected to phase p of node n by generator g_n; I^{p}_{l,s_n} is the current absorbed from node n by the sending end of line l through phase p; and $I^{p}_{L_n}$ is the current absorbed by load L_n, through phase p at node n.

Voltages of elements connected to the same node are forced to be equal, for each phase, as follows:

$$V^{p}_{l,s_n} = V^{p}_{l,r_n} = V^{p}_{L_n} = V^{p}_{g_n} = V^{p}_{n} \quad \forall p, \forall n \tag{3.34}$$

The power generated by DERs at the point of connection with the microgrid, for each phase, is calculated from the terminal phasor currents and voltages, as follows:

$$P_{p,g} + jQ_{p,g} = V^{p}_{g} I^{p*}_{g} \quad \forall p, \forall g \tag{3.35}$$

The total power generated by directly-connected DERs is calculated as the sum of powers generated the three phases. However, in the case of inverter-interfaced DERs, an estimation of the VSC power losses need to be included in the calculation; this can be expressed mathematically as follows:

$$P_{source,g} = P_{loss,g} + \sum_{p} P_{p,g} \quad \forall p, \forall g \tag{3.36}$$

In this work, VSC power losses are modelled as a function of the output current, using the following quadratic term (resistive losses) plus a constant loss factor (when the VSC is connected):

$$P_{loss,g} = \begin{cases} 0 & \text{not-interfaced} \\ K_{loss,g} w_g + \sum_p |I_g^p|^2 r_{loss,g} & \text{VSC-interfaced} \end{cases} \tag{3.37}$$

where w_g represents the commitment status of unit g. The proposed estimation is not based on a physical model of the VSC operation, but it is rather a practical approximation of conventional efficiency curves provided by VSC manufacturers [99,100], which are presented as a function of the active power output. Thus, the efficiency curve is expressed as a function of the output currents, assuming a balanced operation, and rated power factor and terminal voltages, from which the parameters $K_{loss,g}$ and $r_{loss,g}$ can be readily calculated.

Each DER's output power is limited by its maximum and minimum permitted values when turned on, or forced to zero otherwise, using the following constraints:

$$P_{source,g} \leq P_g^{max} w_g \quad \forall g \tag{3.38}$$

$$P_{source,g} \geq P_g^{min} w_g \quad \forall g \tag{3.39}$$

Similarly, output currents for each phase are limited by their maximum values as follows:

$$I_g^p \leq I_g^{max} w_g \quad \forall g, \forall p \tag{3.40}$$

The maximum power outputs P_g^{max} of RE sources (i.e., wind and solar) correspond to their forecasted values, from available forecasting systems, as follows:

$$P_{g_{rw}}^{max} = \widetilde{P}_{g_{rw}} \quad \forall g_{rw} \tag{3.41}$$

The following logic constraints are necessary to properly represent unit commitment decisions at each time-step, and ensure that each DER unit is not turned-on and -off simultaneously.

$$u_{g,k_t} - v_{g,k_t} = w_{g,k_t} - w_{g,k_t-1} \quad \forall g, \forall k_t \tag{3.42}$$

$$u_{g,k_t} + v_{g,k_t} \leq 1 \quad \forall g, \forall k_t \tag{3.43}$$

where u_{g,k_t} and v_{g,k_t} correspond to the start-up and shut-down decisions for unit g at time-step k_t, respectively.

Minimum up-time and minimum down-time constraints of DER units are also considered using the following equations [101]:

$$\left[\sum_{\widehat{k_t}:\ t_{\widehat{k_t}}=t_{k_t}-M_{up,g}}^{k_t-1} w_{g,\widehat{k_t}}\Delta t_{\widehat{k_t}}\right] - M_{up,g}\, v_{g,k_t} \geq 0 \quad \forall g, \forall k_t \tag{3.44}$$

$$M_{dn,g}\,(1-u_{g,k_t}) - \left[\sum_{\widehat{k_t}:\ t_{\widehat{k_t}}=t_{k_t}-M_{dn,g}}^{k_t-1} w_{g,\widehat{k_t}}\Delta t_{\widehat{k_t}}\right] \geq 0 \quad \forall g, \forall k_t \tag{3.45}$$

These equations guarantee that, once turned-on, a particular unit g remains dispatched for at least $M_{up,g}$ hours. Similarly, if the unit is turned-off, it will remain off for no less than $M_{dn,g}$ hours. Ramping rate limits of DER units are enforced by the following constraints:

$$\begin{aligned} P_{source,g,k_t+1} - P_{source,g,k_t} - u_{g,k_t+1}P_g^{max} \\ \leq R_{up,g}\Delta t_{kt} \quad \forall g, \forall k_t \end{aligned} \tag{3.46}$$

$$\begin{aligned} P_{source,g,k_t} - P_{source,g,k_t+1} - v_{g,k_t+1}P_g^{max} \\ \leq R_{dn,g}\Delta t_{kt} \quad \forall g, \forall k_t \end{aligned} \tag{3.47}$$

The following reserve constraint ensures that enough generation is committed at each time-step to compensate for sudden load/generation variations and/or account for contingencies:

$$\sum_{g_d} w_{g_d}\left[P_{g_d}^{max} - P_{g_d}\right] = R_{sv}\sum_{g} P_g \tag{3.48}$$

The microgrid's multi-period operation cost, typically used as the objective function of the energy management problem, considers both generators' heat-rates and costs associated

with start-up and shut-down operations. Thus, the total operation cost is calculated as follows:

$$J = \sum_{g,k_t} \left[\left(a_g P^2_{source,g,k_t} + b_g P_{source,g,k_t} + c_g w_{g,k_t} \right) \Delta t_{k_t} + C_{sup} u_{g,k_t} + C_{sdn} v_{g,k_t} \right] \tag{3.49}$$

where the operation of DER units driven by RE sources and ESSs are assumed to be zero cost. Hence, based on the proposed three-phase models, the energy management problem of a microgrid is formulated as the minimization of the total operation cost J defined in (3.49), subject to an applicable subset of the constraints (3.1)-(3.48). This formulation corresponds to an MINLP problem.

3.5 Summary

This chapter presented the following three-phase phasor models of the microgrid network and components, for use in the formulation of the microgrid's energy management problem:

- Transmission lines and transformers were modelled using three-phase ABCD matrices to relate voltages and currents at each end, and load models included constant-impedance and constant-power loads.
- Directly-connected generators (Synchronous Generator (SG) and SCIG) were presented as a special case of a series element connecting an internal (rotor) bus with the machine terminals; thus, equivalent three-phase ABCD matrices were derived for each case.
- Inverter-interfaced units were modelled as an independent voltage source per phase, subject to additional constraints depending on the VSC topology and control flexibility.
- Simplified generator models that group generators and connection interfaces (i.e., filters and trasformer) in a single element were also introduced, in order to reduce the number of variables and equations in the energy management problem.
- ESSs were modelled using book-keeping balance equations and SoC constraints.

- Additional operational constraints for individual elements, and the microgrid as a whole, were presented.

Finally, the energy management problem was defined using these three-phase models as an MINLP formulation.

Chapter 4

Deterministic EMS Approach

The formulation of the microgrid's energy management problem is an important part in the design of EMSs for isolated microgrids; however, it is also necessary to design appropriate calculation and implementation methodologies for the application of the optimal dispatch commands in the real-time operation of the system. In this context, this chapter discusses the design and architecture of the proposed EMS for isolated microgrids, which is based on the detailed mathematical models described in Chapter 3. Simulation results are also presented to demonstrate the performance of the EMS in a realistic MV microgrid test system, and to investigate the impact of unbalanced system conditions and modelling on the optimal dispatch of isolated microgrids.

As discussed in Chapter 1, centralized EMS approaches present various advantages over decentralized approaches for isolated microgrid applications, including higher levels of coordination in the operation and the ability to handle multi-period constraints; thus, the proposed EMS features a centralized architecture. Using this approach, all the relevant information from the microgrid is assumed to be gathered at a single point (central controller), which enables the calculation of dispatch commands by solving the energy management problem using conventional optimization techniques, as discussed in detail next.

4.1 Problem Decomposition

MINLP formulations are generally very hard to solve, and commercially available MINLP solvers are seldom able to find solutions in reasonable computational times, even for small-sized systems. In fact, for the microgrid test system described in Appendix B, the MINLP

formulation was tested in GAMS [102] using BARON, BONMIN, and KNITRO MINLP solvers, but none of them were able to converge to a solution after 3 hours of calculations. Meta-heuristic methods have also been used to optimize this type of models; however, if not properly customized for the specific problem, they also perform poorly in terms of computational times. Hence, an MINLP problem formulation is not suitable for microgrid EMS real-time applications, and hence alternative problem formulations are required. Thus, a decomposition of the original MINLP problem into an MILP and an NLP problem is proposed here, as shown in Fig. 4.1. With this approach, solutions can be obtained in real-time, allowing the implementation of optimal dispatch commands in the actual operation of the microgrid, with frequent updates using an MPC approach to adequately deal with forecasts errors.

The separation of UC and OPF problems is a common practice in the operation of bulk power systems. This separation is based on the fact that, in well-designed power systems, UC decisions are mainly influenced by the demand-supply balance of active power, with the effect of transmission constraints and reactive power requirements being modelled with approximated/simplified models, while the actual dispatch needs to account for detailed power flow constraints. Additionally, constraints in the UC and OPF problems respond to different dynamics, and therefore require different update rates and resolutions. Using a similar approach, a decomposition of the MINLP formulation into an MILP problem, representing the UC of the microgrid, and an NLP problem, representing a multi-period OPF, is proposed here in order to reduce solution times of the energy management problem and enable their implementation in the real-time operation of isolated microgrids.

The MILP (UC) problem uses a single-node model of the microgrid, where all the nonlinear power flow constraints are replaced by a single active-power demand-supply balance equation. Other than the power flow constraints, the only nonlinear equation in the system is the objective function (total cost of operation), which is incorporated in the MILP formulation using a piece-wise linear approximation, as follows:

$$J_{uc} = \sum_{g,k_t} \left[\sum_{h} \left(b_g^h P_{source,g,k_t}^h + c_g^h w_{g,k_t}^h \right) \Delta t_{k_t} + C_{sup} u_{g,k_t} + C_{sdn} v_{g,k_t} \right] \tag{4.1}$$

$$\sum_{h} w_{g,k_t}^h \leq 1 \quad \forall g, \forall k_t \tag{4.2}$$

$$w_{g,k_t} = \sum_{h} w_{g,k_t}^h \quad \forall g, \forall k_t \tag{4.3}$$

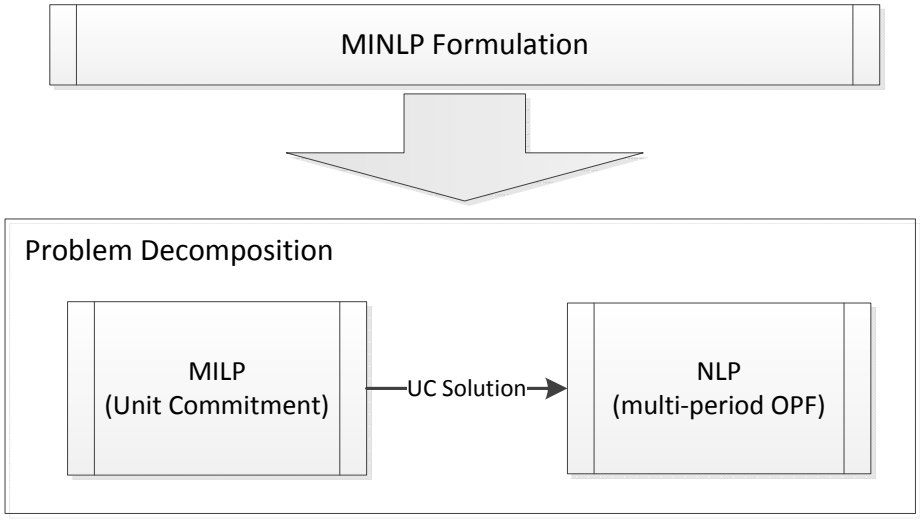

Fig. 4.1: MINLP problem decomposition.

$$P_{source,g,k_t} = \sum_h P^h_{source,g,k_t} \quad \forall g, \forall k_t \tag{4.4}$$

$$P_g^{min,h} w^h_{g,k_t} \leq P^h_{source,g,k_t} \leq P_g^{max,h} w^h_{g,k_t} \quad \forall g, \forall k_t \tag{4.5}$$

where h is the index for linear segments used to approximate the nonlinear cost function, $P_g^{min,h}$ and $P_g^{max,h}$ represent the power limits of the interval in which each linear approximation is defined, w^h_{g,k_t} are binary variables to identify which linear segment is active (interval commitment status), b_g^h and c_g^h are linear and constant cost terms of each linear interval, respectively. Depending on the sizes of diesel generators, a suitable linear approximation can be obtained using 1 or 2 linear segments, specially when considering the reduced operating range used to avoid carbon build-up [103]. The complete MILP formulation of the UC problem is provided in Appendix A. The NLP problem (multi-period OPF), on the other hand, includes all the nonlinear equations presented in Chapter 3, using the binary variable values obtained in the UC.

The UC and multi-period OPF problems are solved sequentially. Thus, the MILP problem solves for the UC decision variables (binary variables), at each time-step, for the entire optimization horizon. Once this binary variables have been fixed by the MILP

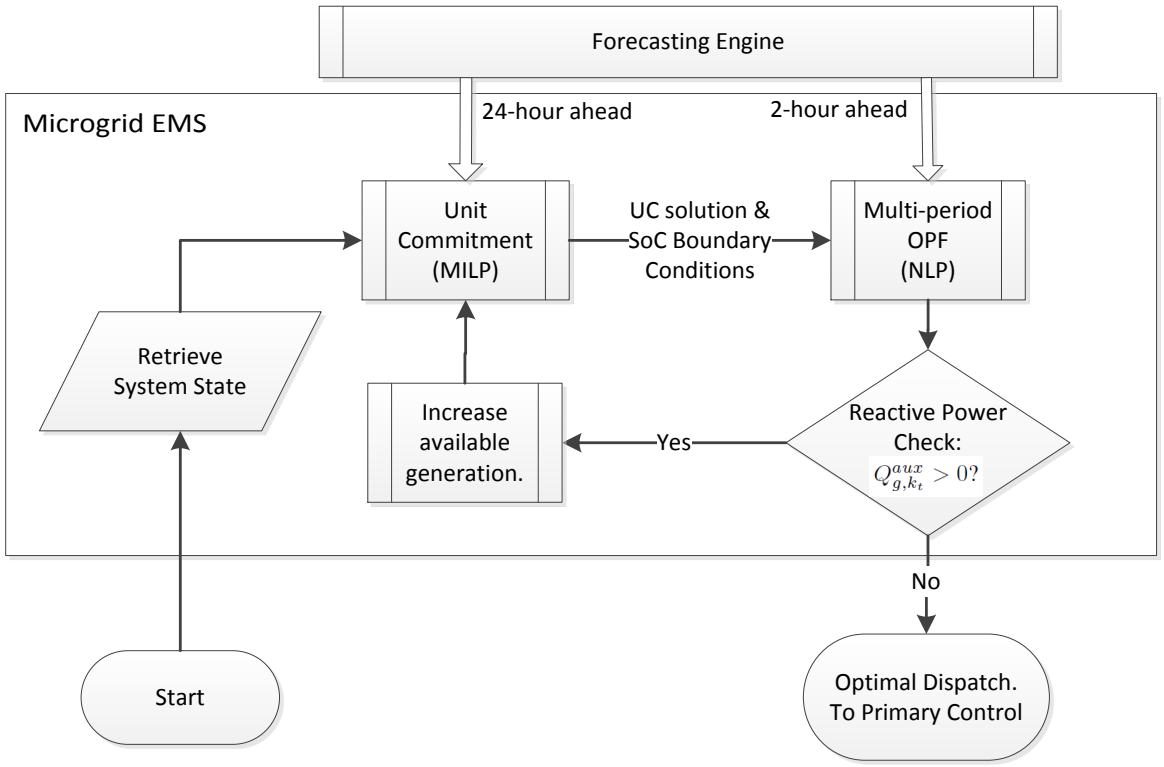

Fig. 4.2: EMS internal structure.

problem, the actual dispatch strategy is re-calculated with a higher level of detail using the NLP approximation. This refined dispatch is then used to determine the reference values for the primary level control system of the microgrid, as depicted in Fig. 4.2.

In heavily-loaded systems, it is possible that the solution of the unit commitment variables obtained by the MILP problem cannot be implemented in the microgrid because of insufficient reactive power resources. This condition would lead to the infeasibility of the NLP problem, and thus malfunctioning of the EMS. To correct this issue, an additional positive variable Q^{aux}_{g,k_t} is introduced in the model, which represents a positive, balanced, extra reactive power injection of generator g at instant k_t that is not subject to unit commitment constraints and is penalised strongly in the objective function. Therefore, the reactive injection of generator g is calculated as:

$$Q_{p,g,k_t} = \mathrm{Im}\{V^p_{g,k_t} {I^p_{g,k_t}}^*\} + Q^{aux}_{g,k_t} \quad \forall g, \forall p, \forall k_t \tag{4.6}$$

If after the NLP problem is solved, there exist a non-zero Q^{aux}_{g,k_t}, a feedback signal is sent to the MILP problem to increase the available generation at the corresponding time-steps. This mechanism repeats itself until all Q^{aux}_{g,k_t} in the NLP solution are negligible, yielding a feasible solution of the original multi-period OPF problem. This heuristic approach is able to correct reactive power deficits in the microgrid by committing additional dispatchable units; however, the proposed mechanism is expected to operate only a limited number of times, since frequent operations would yield higher operation costs that may justify investments in reactive power compensation.

It is possible that, after receiving the feedback signal from the NLP problem, the only possibility is to turn on a DG unit that has been recently turned off, which may render the MILP problem infeasible due of minimum down-time constraints. Although small fossil-fuel based generators are quite flexible in terms of turn-on and -off operations, it is desirable to limit these operations to reduce cost and frequency of maintenance; hence, minimum down-time and minimum up-time constraints are not necessarily technical limits of the devices, but rather desired operational conditions. In order to account for this condition and avoid infeasibility of the MILP problem, a high-cost emergency turn-on and turn-off operation is allowed by introducing auxiliary variables u^{emer}_{g,k_t} and v^{emer}_{g,k_t}. Therefore, the minimum up-time and minimum down-time constraints are modified as follows:

$$\left[\sum_{\widehat{k_t}:\ t_{\widehat{k_t}}=t_{k_t}-M_{up,g}}^{k_t-1} w_{g,\widehat{k_t}}\Delta t_{\widehat{k_t}}\right] - M_{up,g}\left(v_{g,k_t} - v^{emer}_{g,k_t}\right) \geq 0 \quad \forall g, \forall k_t \tag{4.7}$$

$$M_{dn,g}\left(1 - \left(u_{g,k_t} - u^{emer}_{g,k_t}\right)\right) - \left[\sum_{\widehat{k_t}:\ t_{\widehat{k_t}}=t_{k_t}-M_{dn,g}}^{k_t-1} w_{g,\widehat{k_t}}\Delta t_{\widehat{k_t}}\right] \geq 0 \quad \forall g, \forall k_t \tag{4.8}$$

The aforementioned considerations require a re-formulation of the total cost of operation, defined in equation (3.49), as follows:

$$\begin{aligned} z_{uc} = \sum_{g,k_t}\Bigg[\sum_h \left(b^h_g P^h_{source,g,k_t} + c^h_g w^h_{g,k_t}\right)\Delta t_{k_t} + C_{sup}u_{g,k_t} + C_{sdn}v_{g,k_t} \\ + K_{Q^{aux}}Q^{aux}_{g,k_t} + K_{emer}(u^{emer}_{g,k_t} + v^{emer}_{g,k_t})\Bigg] \end{aligned} \tag{4.9}$$

The weight factor $K_{Q^{aux}}$ must be high enough to guarantee that all reactive power resources from the available DGs are utilized first, and Q^{aux}_{g,k_t} is used only as the last resort. Similarly, a high value of K_{emer} guarantees that emergency turn-on and turn-off operations are only used to avoid infeasibility.

4.2 Model Predictive Control Approach

The optimal multi-period dispatch of the microgrid can be obtained by solving the energy management problem described in Chapter 2, where the results of this calculation are based on known, fixed problem parameters (e.g., future load and generation from RE sources). Based on this fact, for the dispatch commands to be meaningful, the actual values of the parameters must not deviate much from those assumed in the formulation of the energy management problem and, if that is not the case, a new calculation of the energy management problem with more accurate/updated estimations of the value of parameters is required. Hence, the solution of the energy management problem should be updated to optimally accommodate load and forecasts variations, without interfering with faster control mechanisms (primary control) [44]. These conditions require the EMS's update rate to be in the order of several seconds to few minutes. In this work, following an MPC approach, an update rate of 5 minutes is chosen, which is consistent with the fastest available wind/solar power forecasting systems and suitable for capturing typical load fluctuations [104]. That is, every 5 minutes the EMS action is triggered, and the decomposed energy management problem is solved. Hence, the EMS is provided with updated load and renewable generation forecasts every 5 minutes, and is assumed to have full autonomous control over the dispatch of every DG in the microgrid.

UC decision variables typically follow slower dynamics as compared to dispatch commands since, while optimal dispatch commands are expected to change with slight changes in the load, the optimal UC decisions respond to longer-term trends in load variations. Thus, it is not necessary to obtain a new solution for the MILP problem with the same frequency as in the NLP problem. However, the MILP problem is typically much easier and faster to solve, and therefore there is no significant improvement in solving this problem at a slower rate in terms of computational effort.

In order to capture slower load patterns that affect UC decisions, the MILP problem requires a longer optimization horizon as compared to the NLP problem. Furthermore, it is not computationally efficient to calculate unbalanced OPFs over extended horizons, considering that future dispatches are very likely to change as forecasts are updated. In this work, a horizon of 24 hours is used for the MILP problem, while a 2-hours horizon is

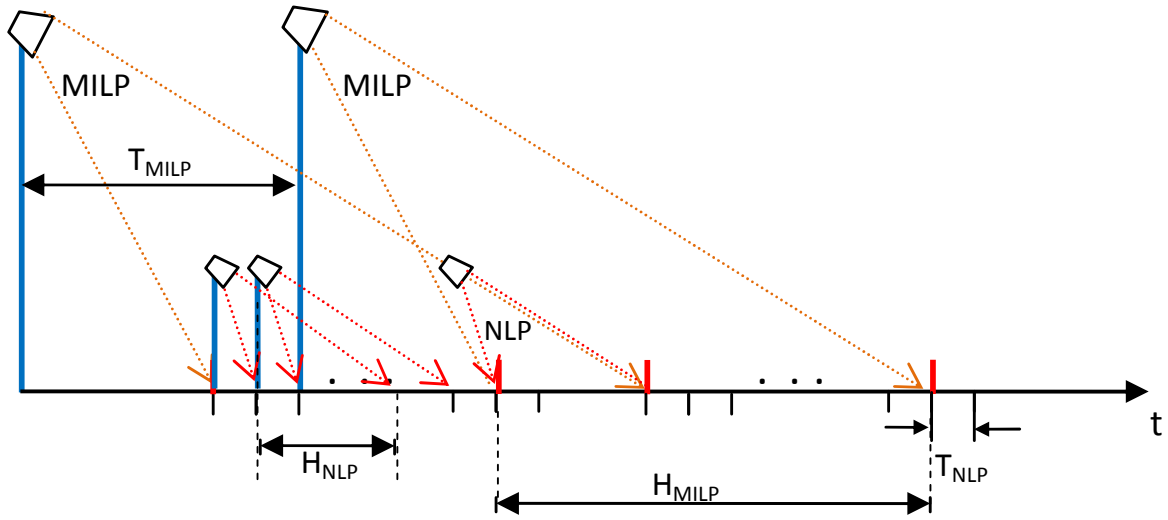

Fig. 4.3: EMS operation in time: Time-steps and horizons.

selected for the NLP problem. Thus, the MILP problem is able to capture daily load and renewable generation patterns, and provide boundary conditions for the SoC of ESSs in the NLP problem; this boundary condition is necessary to make sure that the stored energy is not depleted in the horizon of the NLP problem. The NLP problem then calculates detailed dispatch strategies, and is able to detect power flow problems in a shorter term, as illustrated in Fig. 4.2. Figure 4.3 illustrates the operation of the microgrid EMS in time, where the MILP problem is solved with time step T_{MILP} and a horizon H_{MILP}, whereas the NLP problem is solved with time step T_{NLP} and horizon H_{NLP}, with $T_{MILP} \geq T_{NLP}$ and $H_{MILP} \geq H_{NLP}$.

4.3 Implementation

The proposed EMS uses a moving horizon of 24 hours; however, it does not consider a homogeneous time resolution over this time span. While the first few minutes can be forecasted with high accuracy and resolution, resolution decreases as the forecasting horizon is extended; this characteristic responds to limitations of existing forecasting systems, as higher time resolutions are only meaningful for short-term forecast. This is also a desirable trait, as more detailed information is required for operation scenarios in the near future

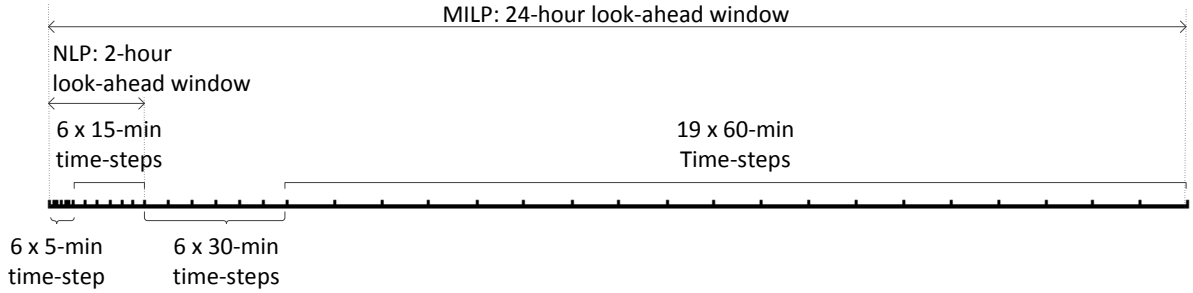

Fig. 4.4: EMS horizon variable time-steps.

(more certain scenarios) than for less certain scenarios in the far future. For this reason, 4 different time resolutions are used in the proposed EMS, as illustrated in Fig. 4.4. Hence, the multi-period OPF problem uses a 2-hour horizon in 12 time-steps, whereas the UC problem uses a 24-hour horizon in 37 time-steps.

4.4 Simulation Results

The performance of the EMS is tested for 24 hours of operation, with dispatch updates every 5 minutes. The model is coded in the high-level optimization modelling language GAMS [102], and MILP and NLP problems are solved using CPLEX [105] and COIN-IPOPT [106] solvers, respectively. Simulations are performed in the EMSOL6 server, which features an Intel Xeon CPU L7555 at 1.86 GHz (4 processors), and 64 GB of RAM, running on Windows Server 2008 R2 Enterprise 64-bit.

4.4.1 Test System and Study Cases

The designed centralized EMS for isolated microgrids is tested on a CIGRE medium voltage network presented in [107], which is based on the European MV distribution network benchmark. A single-line diagram of the 16-bus 12.47 kV test system is shown in Fig. 4.5, based on the diagram provided in [107]. In this modified test system, a connection to the main grid has been replaced by a bus with 3 diesel generator units, with a combined capacity of 4,700 kW. The system features a total installed capacity of 8,760 kW, considering battery-ESS, fuel-cells, and intermittent renewable energy sources. Nominal ratings of DGs are shown in Table 4.1, with typical values being assumed for technical parameters

and heat-rates of DGs [108, 109]. A detailed description of the test system and parameters is provided in Appendix B.

The loads have been divided into 2 categories: residential and commercial, with different daily load profiles. Residential loads are assumed to be composed of 80% constant-impedance load, and 20% constant-power load, whereas commercial loads are composed of 50% constant-impedance load and 50% constant-power load. Residential load, wind power and solar power forecasts were obtained from real data generated by forecasting systems used in a rural microgrid in Huatacondo, Chile [11]. Further characteristics of the forecasting system are provided in Appendix C. Nominal daily profiles for load and available power from RE sources are illustrated in Fig. 4.6, in per unit of the nominal load and rated capacity, respectively. The values $K_{Q^{aux}}$= US$1/kVAr and K_{emer}= US$300 were used for all the study cases.

Simplified models have been used to represent inverter-interfaced units of the test system, where battery-ESS units (Units 08 and 18) and the microturbine (Unit-21) are considered to be connected to the system through a wye-grounded to wye-grounded transformer, and are assumed to have full control (3 sequences) of the voltage on the microgrid's side of the transformer. The rest of the units are connected through a delta to wye-grounded transformer, and are assumed to only have control over positive and negative sequences.

Base Case: Unbalanced Conditions

Many medium-voltage networks operate under unbalanced conditions due to single-phase feeder connections, or uneven distribution of loads. For example, autonomous grids supplying remote communities in Northern Canada present seasonal phase imbalance due to different distribution of loads in summer and winter times. For this reason, loads in the test system have been considered unevenly distributed among the 3 phases, with phase-a feeding 30.1%, phase-b 35.7%, and phase-c a 34.2% of the total load. Single-phase feeders have been represented as lumped single-phase passive loads.

The loading of the system is controlled using the parameter λ, which multiplies the load at each node of the system. A value of $\lambda = 1.4$ is chosen as a base case, which produces a combined peak load of approximately 5 MW. Lower and upper voltage limits at all nodes of the microgrid are 0.93 p.u. and 1.07 p.u., respectively.

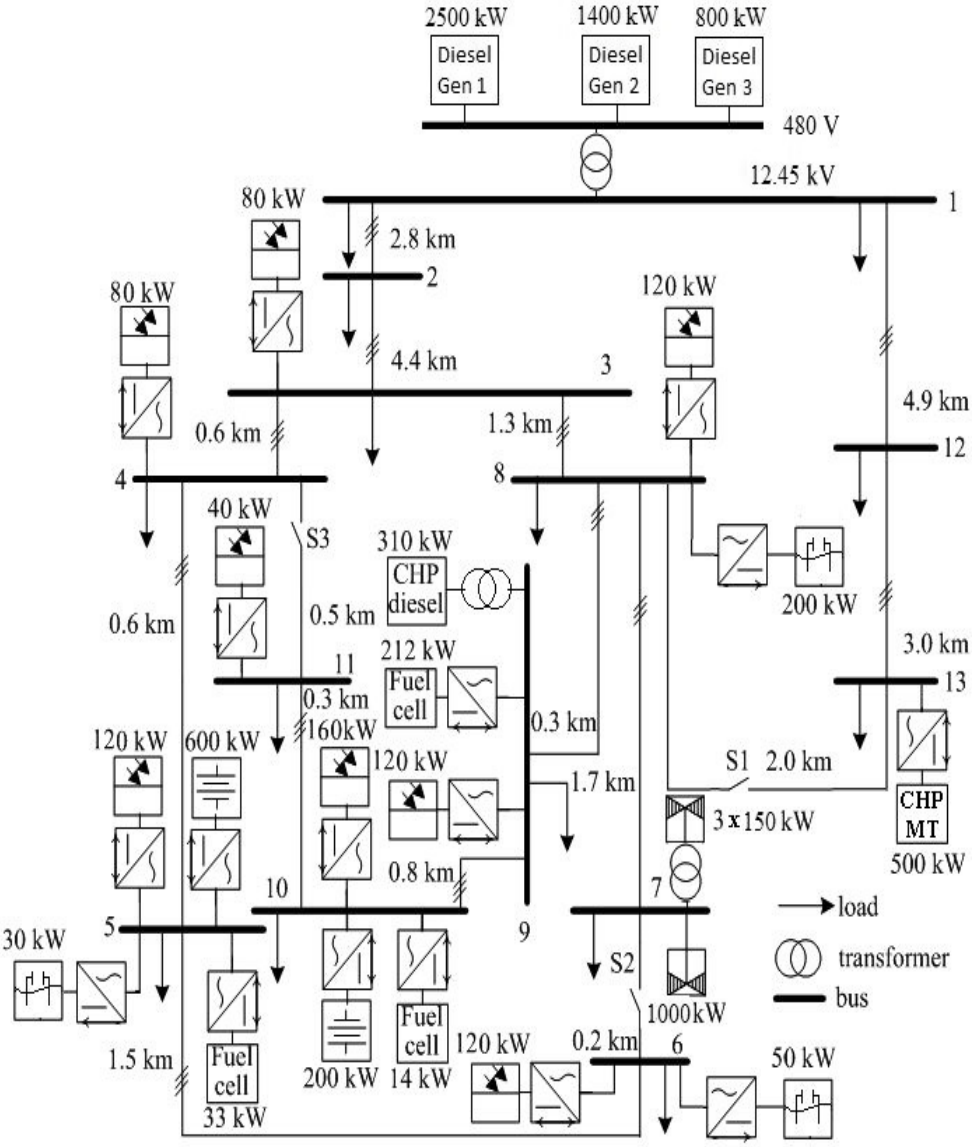

Fig. 4.5: Microgrid MV test system.

Table 4.1: Microgrid test system DERs ratings

No.	Node	DER type	$P_{max}\,[kW]$
1	14	Diesel Generator	800
2	15	CHP diesel	310
3	14	Diesel Generator	1400
4	14	Diesel Generator	2500
5	3	Photovoltaic	80
6	4	Photovoltaic	80
7	5	Photovoltaic	120
8	5	Battery	600
9	5	Residential fuel cell	33
10	5	Electrolyzer	30
11	6	Photovoltaic	120
12	6	Electrolyzer	50
13	8	Photovoltaic	120
14	8	Electrolyzer	200
15	9	Photovoltaic	120
16	9	CHP fuel cell	212
17	10	Photovoltaic	160
18	10	Battery	200
19	10	Residential fuel cell	14
20	11	Photovoltaic	40
21	13	CHP Microturbine	500
22	7	Wind turbine (inverter-interfaced)	1000
23	16	Wind turbine (SCIG)	150
24	16	Wind turbine (SCIG)	150
25	16	Wind turbine (SCIG)	150

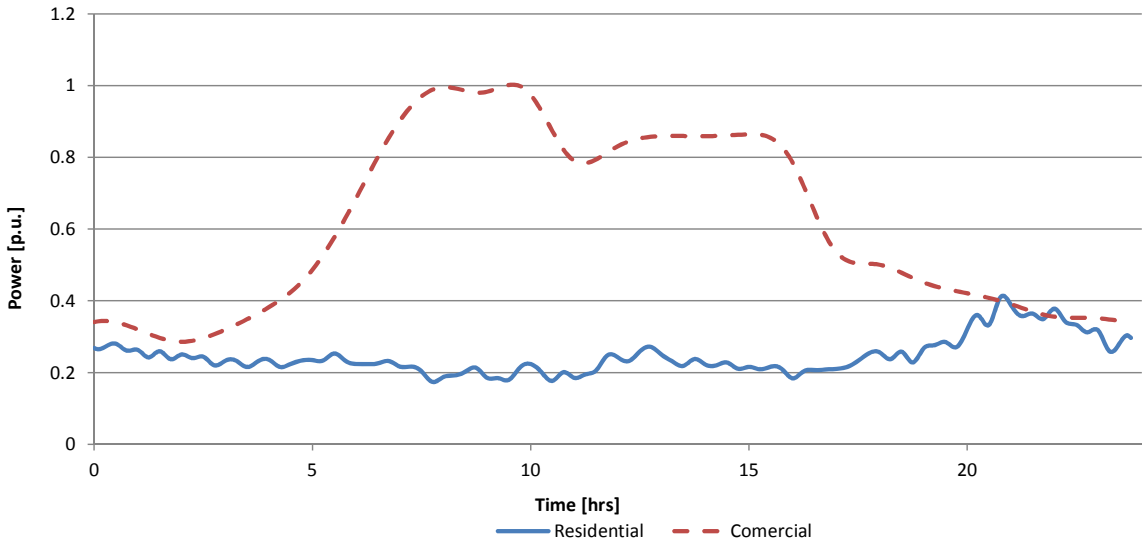

(a)

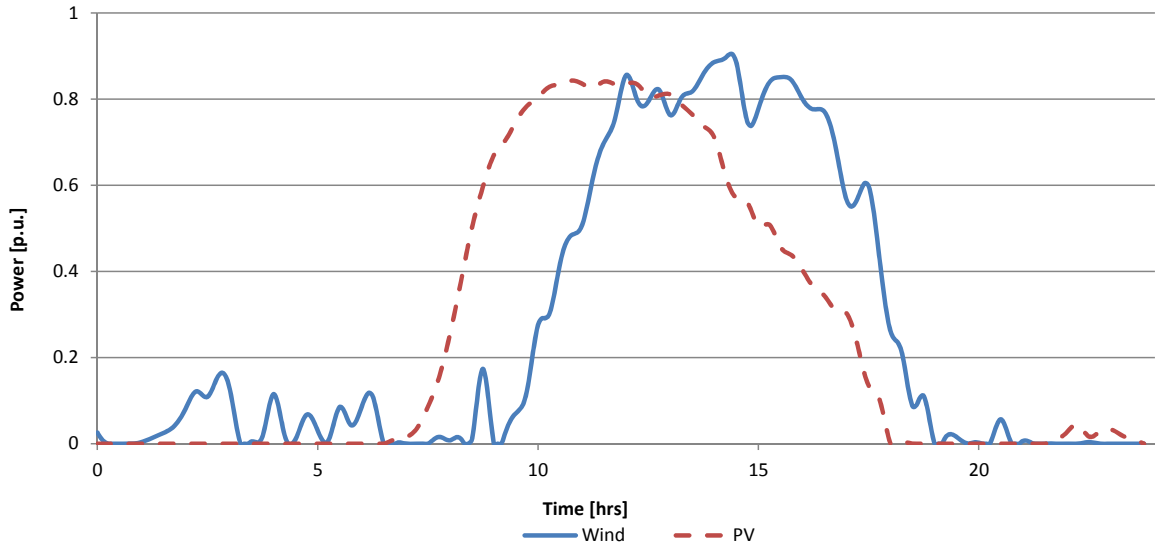

(b)

Fig. 4.6: Test system (a) load and (b) RE profiles.

Balanced Approximation

For comparison purposes, the optimal dispatch is calculated using a balanced microgrid model approximation. In the balanced microgrid approximation the loads are assumed to be evenly shared among the phases, and the rest of the parameters in the model remain unchanged with respect to the base case (unbalanced model). This approximation represents a less critical scenario in terms of system losses, voltage drops, and reactive power requirements as compared to the exact unbalanced network model. This can be illustrated in an extreme example where the same power is distributed evenly among the phases, versus the case where the load is concentrated in only one of the phases; in this case, it is clear that the unbalanced case will yield higher system losses (active and reactive power) and larger voltage drops.

4.4.2 System's steady-state optimal conditions

Results of the optimal dispatch obtained by the EMS with unbalanced modelling are shown in Fig. 4.7 using a stacked-area plot. The optimal dispatch of battery-ESSs has been plotted in a way to properly show charging and discharging cycles; hence, negative areas in the figure correspond to charging cycles of the batteries. Note that battery-ESS units charge during off-peak hours 0 to 4 with the power available from Unit-04 (diesel) and Unit-21 (microturbine), and discharge during peak-hours 5 to 10, thus reducing the use of the more expensive Unit-03 (diesel). A second charging cycle is observed between hours 11 and 15 due to a peak in wind-power generation. Given the low efficiency of fuel-cells and electrolizers, these units are not significantly used by the EMS in the daily dispatch shown in Fig. 4.7.

Reactive power dispatch of diesel generators is shown in Fig. 4.8. It can be observed, as expected, that reactive power requirements are higher during the peak-load, approximately between hours 6 and 15. System losses represent a 5.34% of the energy generated during the 24 hours, with a peak of 8.57% during peak load hours.

Microgrid's system imbalance is illustrated in Figs. 4.9, which shows the total power generation profile in each phase. The level of imbalance in the microgrid and the phase with the highest loading vary over the 24 hrs, which can be observed during peak-load hours (hours 6 to 8), where phase-a replaces phase-b as the most loaded in the system.

Finally, the voltage profiles of phase-a at bus-1, and generation buses 14, 15 and 16 are illustrated in Fig. 4.10. It is observed in the figure that voltages are raised during peak-

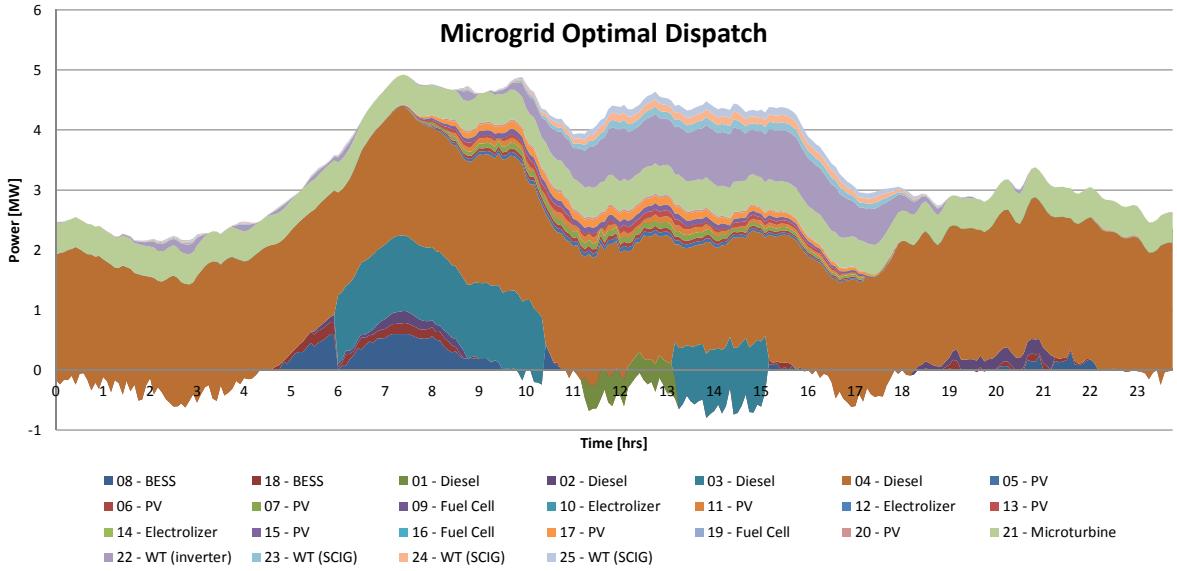

Fig. 4.7: Microgrid's Optimal Dispatch for Base Case.

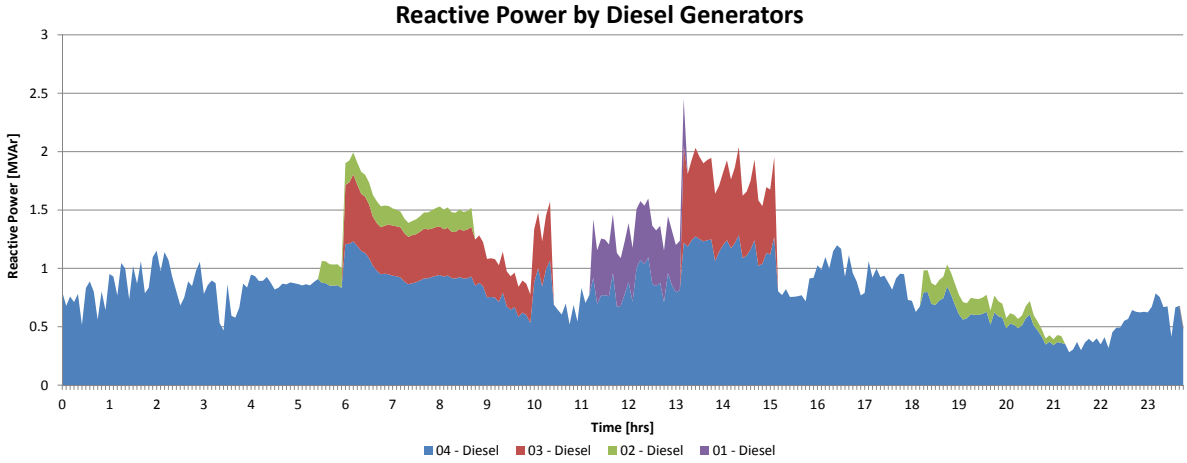

Fig. 4.8: Reactive power generation by diesel units for Base Case.

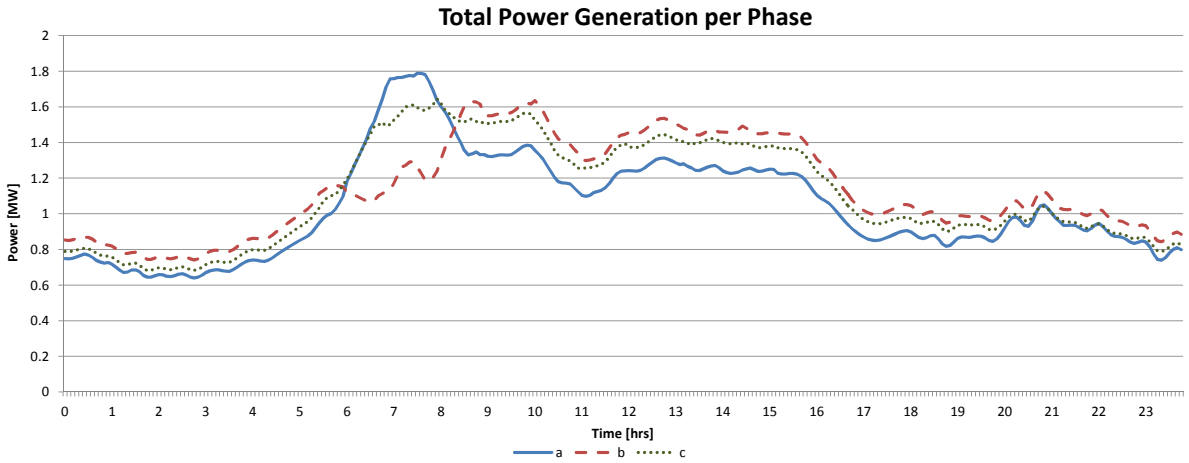

Fig. 4.9: Total power generation per-phase for Base Case.

hours (between hours 6 and 9) due to the increased reactive power generation to maintain the voltage levels in the microgrid within limits.

The total simulation time of the EMS for 24 hours of operation is 6,632s for 286 iterations, thus yielding an average computational time of approximately 23s per iteration, which is within the desired 5-minutes dispatch window, making it suitable for real-time applications.

4.4.3 Balanced versus Unbalanced Modelling

The use of a balanced system approximation has an impact on calculations of the optimal microgrid operation, as illustrated in Fig. 4.11. Note that the two cases have some similarities on the dispatch over the 24-hour window; however, differences can be found in the actual dispatch of the units, and more importantly, in the UC decisions. The differences can be appreciated more clearly in Fig. 4.12, where only the dispatch of diesel generators is shown. In particular, 3 time-windows of interest are identified in these figures:

- *Window A1*: The same units are committed in both cases for this window; however, significant differences in the dispatch commands can be observed for Unit-02 (diesel), Unit-08 and Unit-18 (battery-ESS). After Unit-03 (diesel) is turned-on around hour 6, battery-ESS units show a significantly higher dispatch in the balanced approximation as compared to the unbalanced model. This can be attributed

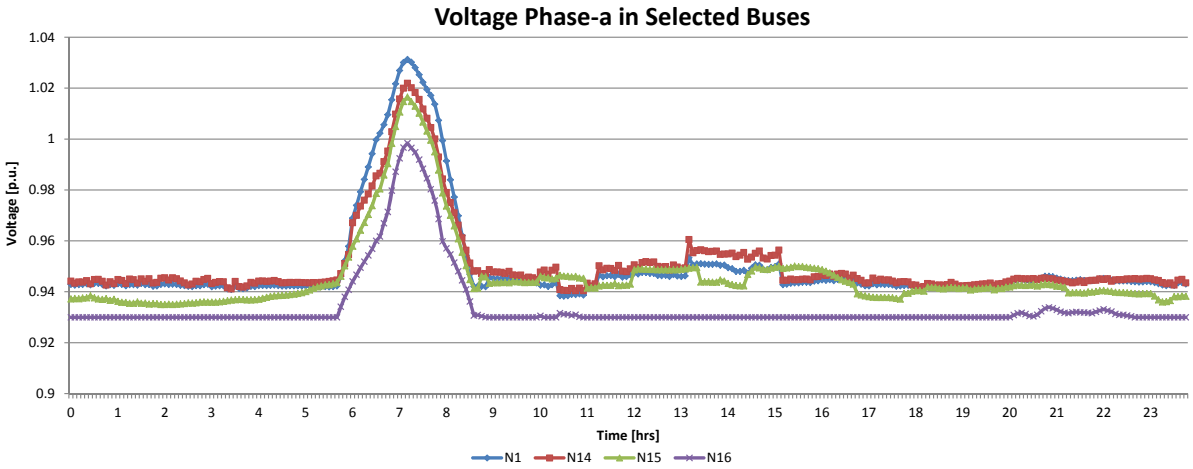

Fig. 4.10: Voltage level at selected buses in phase-a for Base Case.

to an underestimation of future load requirements in the balanced approximation, which translates into more power available for present use, and less reserves required for future operation.

- *Window A2*: After Unit-03 is turned-off (near hour 10), Unit-04 increases its dispatch to supply the load in both models; however, near hour 11, the unbalanced model detects reactive power problems that were overlooked by the balanced approximation, and requests a new unit to be committed in a new calculation of the MILP. Unit-03 cannot be turned back on immediately due to minimum down-time and minimum power output constraints, and instead, Unit-01 is turned-on to supply the deficit. After Unit-01 is turned-on, the UC MILP problem generates turn-off signals for this machine in the following time-steps, since this formulation does not consider reactive power; however, Unit-01 is prevented from turning-off by the OPF NLP solution. After 2 hours, Unit-01 can be turned-off and replaced by the more economical Unit-03.

- *Window A3*: Similar to Window A1, the same units are committed; however, differences can be observed in the dispatch of battery-ESS units around hour 17, and Unit-02 between hours 18 and 21.

It can be observed in Fig. 4.11 that there is an underestimation of the total load and reactive power requirements by the balanced approximation, which is more critical during

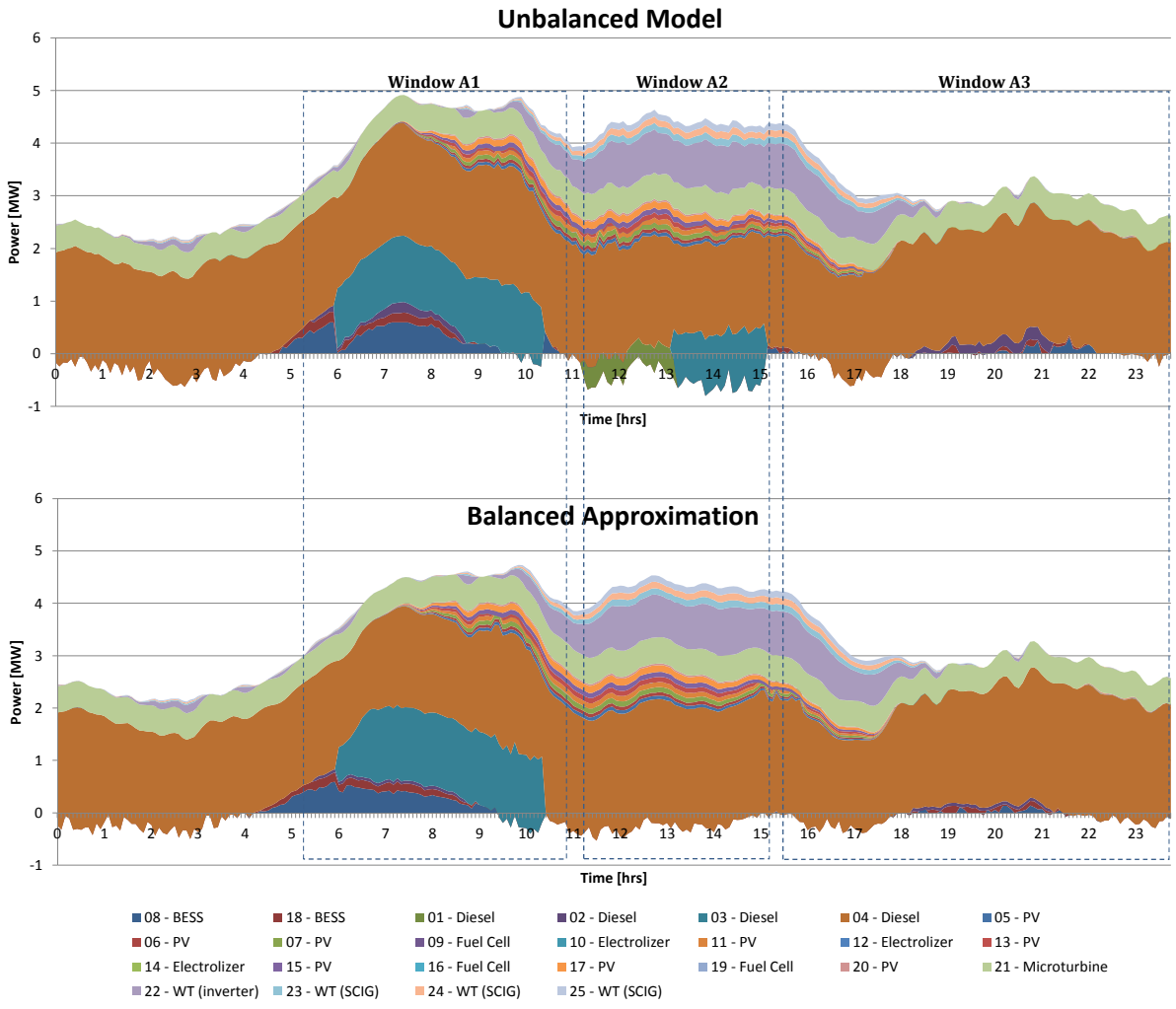

Fig. 4.11: Comparison of dispatch for unbalanced model and balanced approximation.

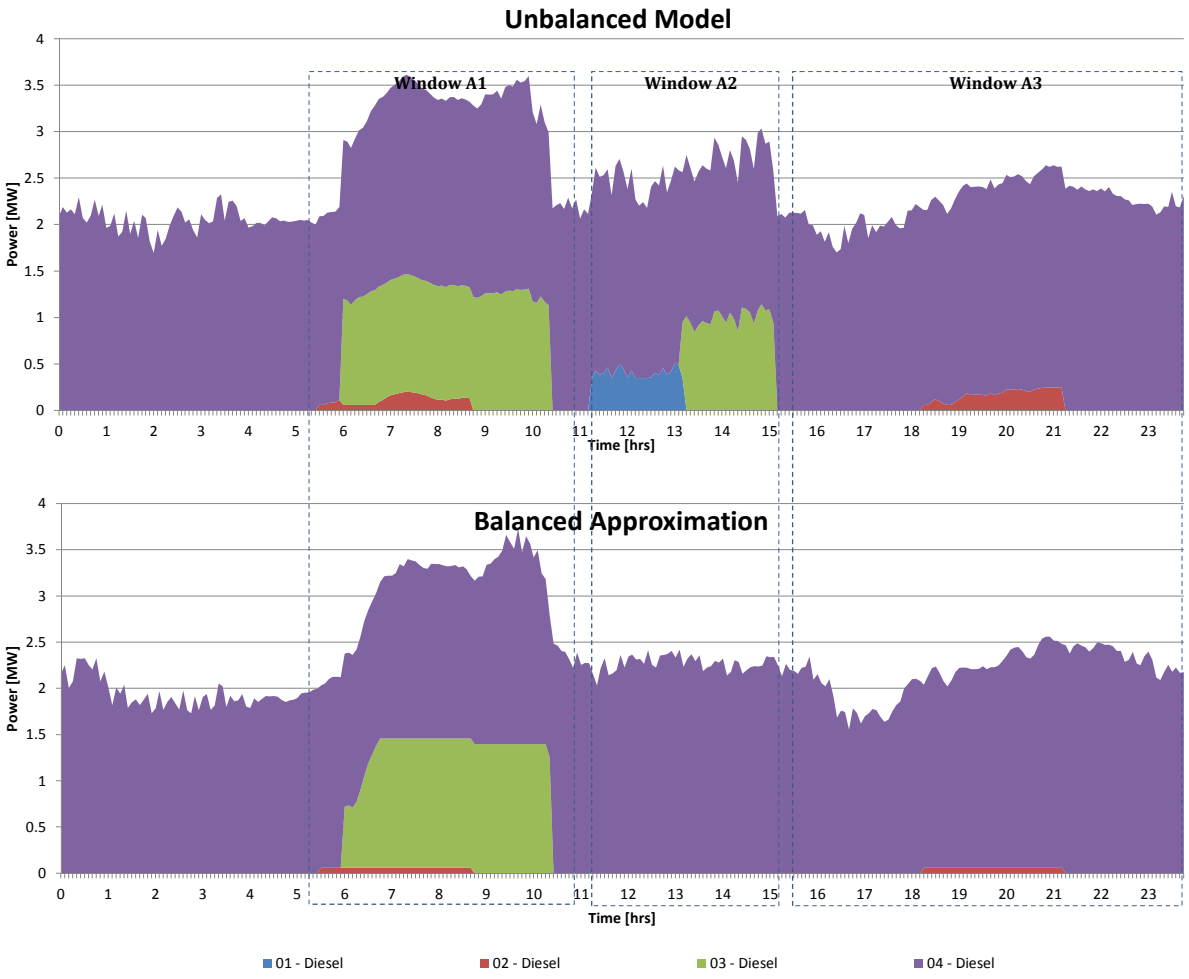

Fig. 4.12: Unbalanced model versus balanced approximation for diesel generators.

peak-load hours (between hours 6 and 16). Thus, differences in the dispatch commands obtained with balanced and unbalanced models are more significant in heavily-loaded systems, while it may go unnoticed in lightly-loaded microgrids. In this context, dispatch commands produced by EMSs based on balanced approximations of unbalanced microgrids may lead to under-estimation of the active and reactive power requirements, or infeasible dispatch solutions. The total load is underestimated by the balanced approximation in this case for 2 main reasons:

- The same load, supplied in an unbalanced configuration, will produce higher system losses as compared to a balanced configuration, as previously explained.
- The power absorbed by impedance loads is voltage-dependent; therefore, in an unbalanced network, higher voltages in one of the phases will lead to higher power.

Table 4.2 shows a summary of the simulation results. Note that a total of 35 warning feedback signals of reactive power deficits are generated in the detailed unbalanced model, while these problems are not detected by the balanced approximation. The new UC decisions obtained by the MILP, after receiving the warning feedback signals from the NLP, did not require emergency star-up or shut-down actions. Finally, observe that the peak load is under-estimated by 3.65% by the balanced approximation.

Table 4.2: Summary of Simulation Results ($\lambda = 1.4$)

	Unbalanced Model	Balanced Model
No. of iterations with $u^{emer}_{g,k_t} > 0$	0	0
No. of iterations with $v^{emer}_{g,k_t} > 0$	0	0
No. of iterations with $Q^{aux}_{g,k_t} > 0$	35	0
Peak load	4.92 MW	4.74 MW

A more critical case is presented in Figs. 4.13 and 4.14, where the loading parameter λ has been increased to 1.5. In this case, similar but more pronounced differences between the balanced approximation and the unbalanced model can be observed. Thus, UC decisions are different during longer periods of the operation (Windows B2 and B4), and more significant dispatch differences are observed in Windows B1 and B3. System losses in the unbalanced model show a modest increase with respect to the base case, reaching a 5.4% of the energy generated during the 24 hours, with a peak of 8.64% during peak load hours.

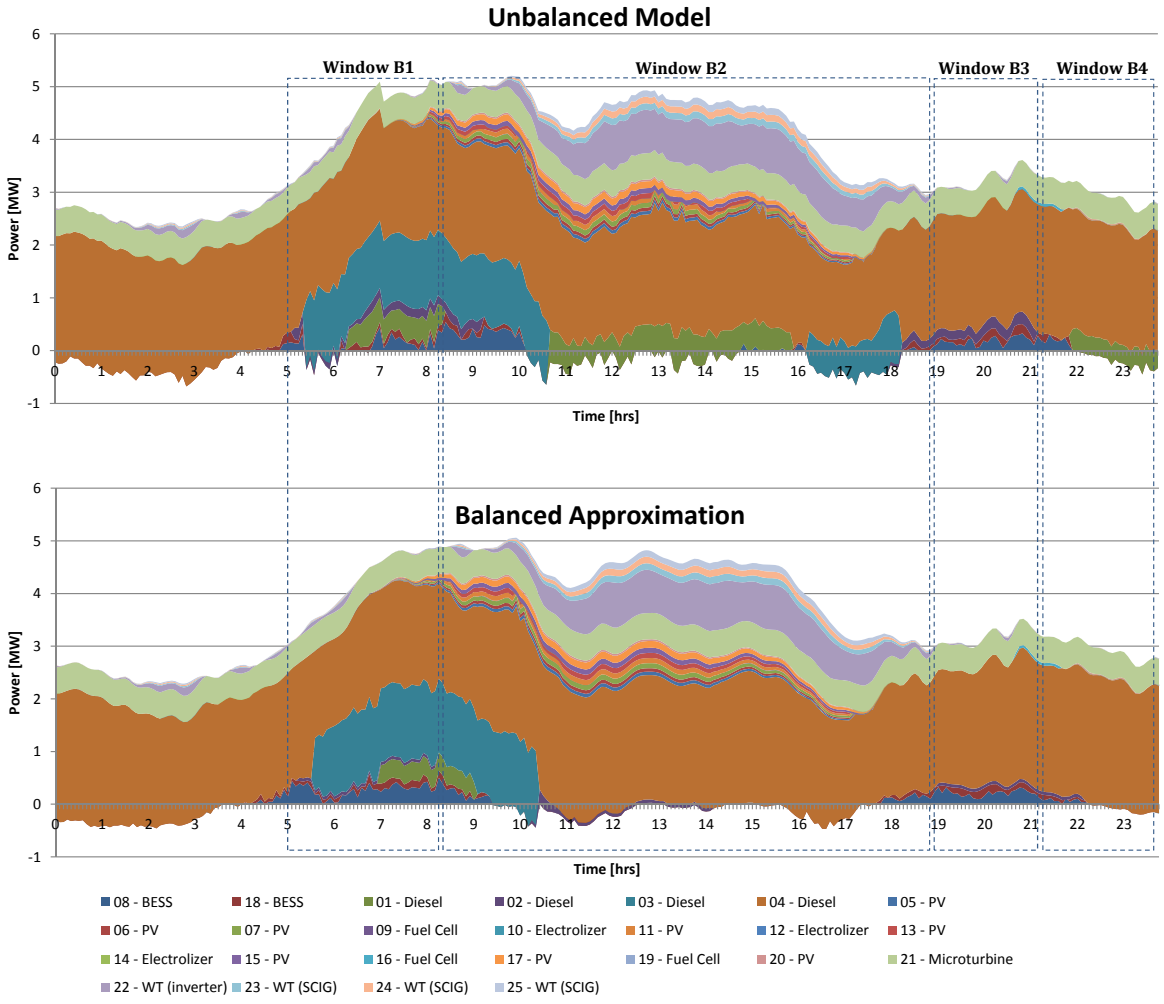

Fig. 4.13: Comparison of dispatch for unbalanced model and balanced approximation with $\lambda = 1.5$.

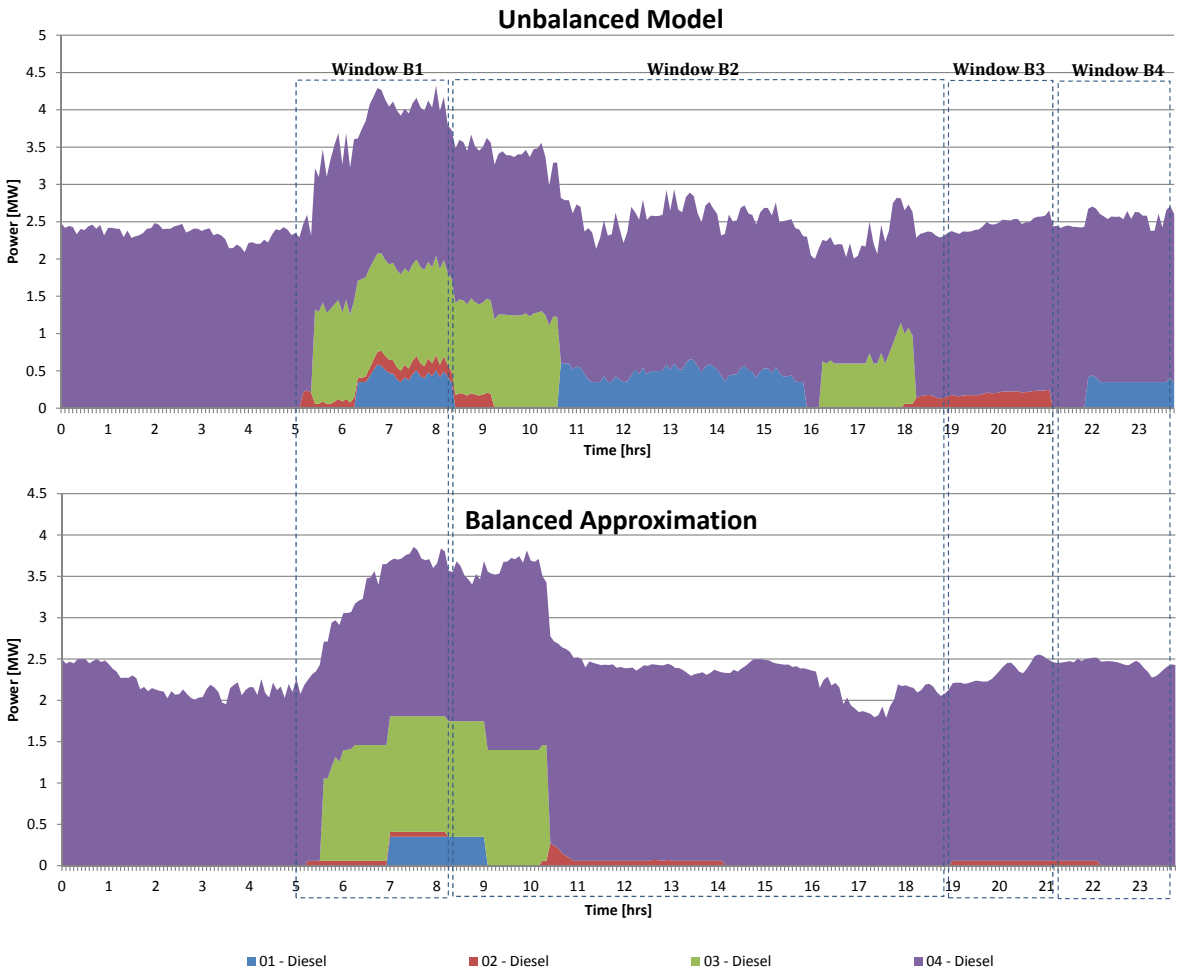

Fig. 4.14: Unbalanced model versus balanced approximation with $\lambda = 1.5$ for diesel generators.

Table 4.3 shows a summary of the simulation results for the case with heavier loading conditions ($\lambda = 1.5$). In this case, 94 warning feedback signals of reactive power deficits are generated by the unbalanced NLP calculations, none of which was detected by the balanced approximation. Also, no emergency start-up or shut-down actions are required, and the peak load is under-estimated by 2.7% by the balanced approximation.

Table 4.3: Summary of Simulation Results ($\lambda = 1.5$)

	Unbalanced Model	Balanced Model
No. of iterations with $u^{emer}_{g,k_t} > 0$	0	0
No. of iterations with $v^{emer}_{g,k_t} > 0$	0	0
No. of iterations with $Q^{aux}_{g,k_t} > 0$	94	0
Peak load	5.2 MW	5.06 MW

4.5 Summary

This chapter presented the architecture and design of a centralized EMS for isolated microgrids using deterministic optimization. The proposed EMS used a formulation of the energy management problem based on a three-phase model of the microgrid, which corresponds to an MINLP problem. A decomposition of the original MINLP formulation into an MILP (UC) problem and an NLP (multi-period OPF) problem was used to reduce computational times and allow the implementation of solutions in the real-time operation of microgrids. The proposed decomposition approach included novel heuristics to account for the effect of reactive power requirements on the UC commitment decisions, introducing auxiliary variables in the NLP formulation to detect reactive power deficits without rendering the problem infeasible. Additional auxiliary variables allowed the use of emergency start-up and shut-down actions.

In the proposed architecture, MILP and NLP formulations were solved sequentially at each time-step of the EMS, with different look-ahead windows, using an MPC approach. Hence, uncertainty associated with load and RE sources was indirectly accounted for by making a close tracking of the optimal dispatch solutions, using the most updated/accurate information available at each time.

The EMS was tested on a realistic MV microgrid test system with a variety of DER units, and the results were compared with a case where a balanced approximation of the mi-

crogrid was used (i.e., loads at each bus were assumed balanced). The comparison showed that neglecting microgrid imbalance might lead to significant deviations in the optimal dispatch of DER units, and most importantly, on the UC decisions. Such deviations were shown to be more significant under heavy loading conditions, where the system imbalance has a higher impact on the active and reactive power requirements of the microgrid.

Chapter 5

Stochastic EMS Approach

Chapter 4 presented an EMS design based on a deterministic formulation of the energy management problem, which considered uncertainty by performing a close tracking of the optimal dispatch solutions with small time steps, using the most current information each time, and including an explicit reserve requirement. Such approach to handle uncertainty is a common trait in most of the EMS designs proposed so far in the technical literature, but it does not offer a direct representation of the uncertainty, and relies on an arbitrary reserve requirement, as discussed in Chapter 1. An alternative to address these limitations is to use SP formulations of the energy management problem, where uncertainty is represented as a finite set of possible realizations that can be readily included in the problem formulation.

This chapter presents modifications to the deterministic EMS design described in Chapter 4, introducing a two-stage SP formulation of the UC problem and necessary changes to the EMS architecture. This approach accounts for uncertainty directly in the problem formulation, and combines the benefits of SP and MPC into a two-stage decision making process. The performance of the proposed stochastic EMS approach under different conditions is investigated in a slightly modified version of the test system used in Chapter 4.

5.1 Reformulation of the UC problem

The UC is re-formulated here as a fixed-recourse, two-stage SP problem, which is referred to as the SUC hereafter. As discussed in Chapter 2, this formulation requires the separation of variables into first and second stage (recourse) variables, where the solution of the

SUC determines the value of first stage variables that minimize the expected cost of the microgrid's dispatch. The uncertainty can be represented as a finite set of discrete scenarios, which enables the formulation of the deterministic equivalent of the SUC as an MILP problem. Thus, the proposed approach features a discrete representation of uncertainty, with scenarios generated using appropriate scenario generation techniques. The variables of the original UC formulation are separated into first- and second-stage variables as follows:

- First-stage variables: UC decision variables $z_{1,t} = [\widehat{w}_t^\intercal \ \widehat{u}_t^\intercal \ \widehat{v}_t^\intercal]^\intercal$, for all DER units at each time-step in the optimization horizon, where $\widehat{w}_t$, $\widehat{u}_t$ and $\widehat{v}_t$ are vectors containing unit commitment variables for all DER units at time t.
- Second-stage variables: Active power dispatch and slack variables, i.e., load shedding and power curtailment, $z_{2,t} = [\widehat{P}_t^\intercal \ P_{shed,t} \ P_{curt,t}]^\intercal$, at each time-step in the optimization horizon, where $\widehat{P}_t$ is the vector of power generation of all DER units, and $P_{shed,t}$ and $P_{curt,t}$ are scalars representing load shedding and power curtailment, at time t.

Power curtailment and load shedding variables are particularly important in the second stage of an SUC formulation, since it might happen that there is no solution of the first-stage variables that produce feasible demand-supply balances for all the possible realizations of the uncertainty.

For simplicity, the uncertainty is assumed to be associated with the RE-based generation only; however, the formulation can be easily adapted to also include uncertainty in load. Each scenario is defined by the pair $\{(\widetilde{P}^{\omega}_{g_{rw}})_t, \pi_\omega\}$, where $(\widetilde{P}^{\omega}_{g_{rw}})_t$ is a sequence of vectors $\widetilde{P}_{g_{rw},t}$ representing the generation of RE-based units at time t for scenario ω, and π_ω is its probability. Since the time-steps of the SUC and multi-period OPF are not necessarily the same, index t is used to represent time-steps in the SUC problem, while k_t is reserved for the multi-period OPF. Thus, the two-stage, fixed-recourse SUC is formulated as follows:

$$\min \quad \sum_{t=1}^{T} \left[c_{uc}^\intercal z_{1,t} + \sum_{\omega \in \Omega} \pi_\omega \Big(d_p^\intercal \widehat{P}_t^\omega - d_c P_{curt,t}^\omega + d_s P_{shed,t}^\omega \Big) \right] \tag{5.1a}$$

$$\text{s.t.} \quad A_1 z_{1,t} \leq 0 \quad \forall t \tag{5.1b}$$

$$\sum_{\bar{t}=t-M_{time}}^{t} A_2^{\bar{t}} z_{1,\bar{t}} \leq a_1 \quad \forall t \tag{5.1c}$$

$$b_1 \widehat{P}_t^\omega + P_{shed,t}^\omega - P_{curt,t}^\omega = b_{2,t} \quad \forall t \quad \forall \omega \tag{5.1d}$$

$$\widehat{P}_{t+1}^\omega - B_2 \widehat{P}_t^\omega \leq b_3 \quad \forall t \quad \forall \omega \tag{5.1e}$$

$$A_3 z_{1,t} + \widehat{P}_t^{\omega} \leq 0 \quad \forall t \quad \forall \omega \tag{5.1f}$$

$$I_{rw} \widehat{P}_t^{\omega} = \widetilde{P}_{g_{rw},t}^{\omega} \quad \forall t \quad \forall \omega \tag{5.1g}$$

The cost function (5.1a) has the following parts: the commitment cost and, for each scenario, the linearized generation cost function for every unit, and penalties for load shedding and power curtailment. The constraint (5.1b) corresponds to restrictions relevant to the binary variables, such as start-up and shut-down logic, and constraint (5.1c) corresponds minimum up-time and minimum down-time limits of generators, where M_{time} represents the maximum of all minimum up- and down-times of all generators. Constraints (5.1d)-(5.1f) correspond to all the restrictions relevant to the dispatch variables that are subject to uncertainties. In particular, (5.1d) represents the power balance constraint, where $b1$ is a row vector of ones used to add up all the generation from the units to perform power balance; (5.1e) represents ramping rates and ESSs energy balance equations; and (5.1f) represents max-min limits of the units. Finally, (5.1g) forces the generation from RE sources to be equal to their expected values, for each scenario, where I_{rw} is a matrix used to extract the RE-based units from $\widehat{P}_t^{\omega}$. The reserve requirement is eliminated from the SUC, as this is inherently considered by the stochastic nature of the formulation. Recourse matrices A_1, A_2^t, A_3, B_1, and B_2 are fixed, i.e., not affected by the outcomes of the random variables.

Formulation (5.1) produces a different solution of the second-stage variables for each possible scenario, where the load shedding and power curtailment can be used to asses the adequacy of the dispatch. The proposed SUC formulation is significantly larger than the deterministic UC, with the size of the instance being determined by the number of scenarios considered. This imposes constraints on the time-step and resolution of the algorithm that need to be considered in the architecture and implementation of the EMS.

5.2 Stochastic-EMS architecture

Similar to the architecture described in Chapter 4, the proposed algorithm features a two-stage decision making process, where the SUC is used to determine the commitment, and the multi-period OPF performs the final dispatch. To accommodate different time resolutions and allow enough time to perform the SUC calculations, different time-step are used for each problem; thus, a 1-hour step (t) is used for the SUC and a 5-minute step (k_t) is used for the multi-period OPF. The architecture of the stochastic EMS is shown in Fig. 5.1, where a forecasting engine provides updated load and RE generation forecasts for multi-step OPF every 5 minutes, and the scenario generation engine provides a number of

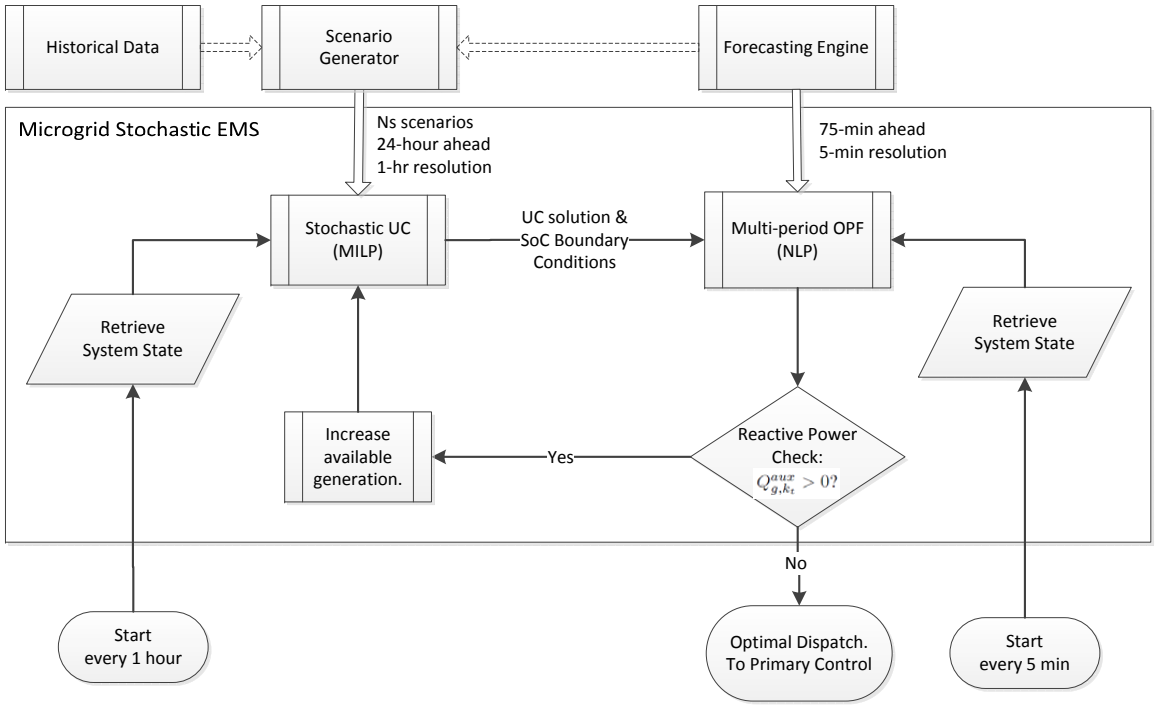

Fig. 5.1: Stochastic EMS internal structure.

possible future scenarios for the SUC routine every 1 hour. As shown in the figure, the scenario generation technique can be based on historical data, or use real-time results of the forecasting engine.

Different look-ahead windows are used for each problem, with a 24-hour window for the SUC, and a 75-minute window for the multi-period OPF. Given its larger look-ahead window, the SUC provides a boundary condition for the SoC of ESSs for the multi-period OPF, in addition to the UC status. The boundary condition for SoC is calculated every 1 hour, and thus it is not updated with every new calculation of the multi-period OPF; therefore, the multi-period OPF considers a shrinking look-ahead window in order to maintain the same boundary conditions, as illustrated in Fig. 5.2. Thus, the operation of the EMS in time can be described as follows:

1. The SUC is solved for time t with a look-ahead window H_{SUC}, in order to obtain the commitment decisions and the SoC of the storage for time $t + T_{SUC}$, which serves as a boundary condition for the multi-period OPF. The solution is issued to the OPF with a lead time of T_{lead} to the corresponding time t.

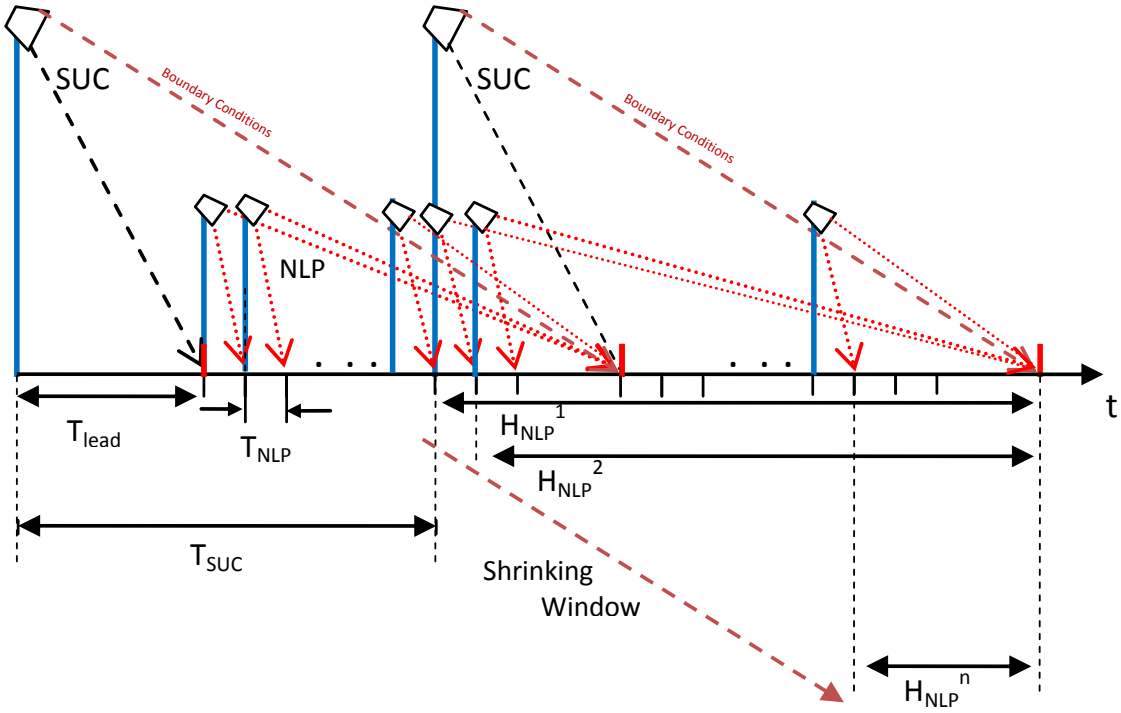

Fig. 5.2: Stochastic EMS operation in time: Time-steps and horizons.

2. Based on the SUC solution, a multi-period OPF is executed a time T_{lead} before the time t, providing sufficient time for calculations and corrections of the SUC if required. Thus, it starts with an initial look-ahead window $H^1_{NLP} = T_{SUC} + T_{lead}$, and this window shrinks by T_{NLP} per time-step in order to maintain the same boundary condition, until it reaches a minimum of $H^n_{NLP} = T_{lead}$, as shown in Fig. 5.2. The multi-period OPF calculates the final dispatch with a time-step T_{NLP}, and requests corrective actions in case reactive power shortages are detected within its look-ahead window, following the same procedure explained in Chapter 4.

Since the SUC calculates a different SoC of the ESSs for each scenario, the following additional constraint needs to be included to make the SoC of each ESS at $t^* = t + T_{SUC}$ equal for all possible scenarios, thus defining a unique boundary condition:

$$SOC^{\omega}_{g_b,t^*} = \overline{SOC}_{g_b,t^*} \quad \forall\omega \tag{5.2}$$

which is equivalent to defining the SoC of ESSs at t^* as a first stage variable. The same condition can be imposed using the ESSs' power injections at time t, as follows:

$$P^{\omega}_{g_b,t} = \overline{P}_{g_b,t} \quad \forall \omega \tag{5.3}$$

5.3 Implementation

The proposed stochastic EMS considers constant time resolutions for the SUC and multi-period OPF formulations, in order to facilitate the coordination of both processes; hence, the multi-period OPF problem uses a 75-minute shrinking horizon with initially 15 steps of 5 minutes, whereas the SUC problem uses a 24-hour horizon in 24 steps of 1 hour. Each solution of the SUC is calculated with a T_{lead} of 15 minutes to the corresponding time t.

In this work, the uncertainty is assumed to be associated with the wind power forecast only, since the load and solar power forecasts have narrow uncertainty bounds, and hence have little impact on the resulting dispatches, which are dominated by the wind uncertainty; thus, scenarios are generated only for wind power profiles. However, the models developed are general and can incorporate several sources of uncertainty simultaneously.

5.3.1 Scenario Generation

The quality of the decision making process from SP is highly dependent on the characterization of the probability space of the uncertainty. In particular, the proposed SUC formulation requires a discrete set of scenarios to be generated at each time-step of the algorithm, for a discrete representation of uncertainty; hence, the generation of scenarios has to be carefully done. In general, some techniques to generate credible RE power scenarios are:

- Moment matching techniques, where a number of discrete scenarios is generated based on predefined statistical properties [110].
- Internal sampling, which corresponds to a form of Monte Carlo scenario generation [111].
- Statistic ensembles, which uses the information from the confidence intervals within a prediction to generate credible scenarios [112].

In particular, the statistic ensembles technique is quite appealing for real-time dispatch applications, since it intrinsically considers the accuracy of the forecasting algorithm, and produces equally probable scenarios respecting the temporal correlation of forecast errors [113]. Furthermore, this technique is not computationally expensive; thus, once a forecast is issued, it can be immediately applied. For these reasons, the statistic ensembles is used here to produce scenarios of wind power generation. The statistic ensembles technique can be summarized as follows:

1. Obtain prediction quantiles and realizations of wind power generation of the last 24 hours.
2. Build an empirical Cumulative Distribution Function (CDF) for each look-ahead time based on the prediction quantiles, and using a linear interpolation.
3. Obtain a measure of the past performance of the forecasting system by assigning the realization wind power generation to its corresponding prediction quantile using the empirical CDF, which yields an uniformly distributed random variable.
4. Apply the Probit Function (inverse of the Gaussian CDF) to the quantiles obtained in step 3 to produce a set of normally distributed random variables representing prediction errors.
5. Calculate the correlation matrix of the set obtained in step 4.
6. Generate N_s sequences of random numbers that follow the correlation matrix calculated in step 5.
7. Obtain N_s sequences of quantiles by applying the Inverse Probit Function to each sequence of random numbers.
8. Obtain N_s sequences of wind power generation (scenarios) by applying the inverse empirical CDF, for each look-ahead time.

In case a forecasting system for RE power is not available, or if it is not possible to produce scenarios, the EMS can be provided with historical data. This approach is a heuristic method that may yield conservative results as demonstrated later in this chapter.

5.4 Simulation Results

The performance of the stochastic EMS is tested for 24 hours of operation, with multi-period OPF calculations every 5 minutes, and SUC calculations every 1 hour. CPLEX and COIN-IPOPT solvers are used for SUC and multi-period OPF, respectively. Simulations are performed in the EMSOL6 server, which features an Intel Xeon CPU L7555 at 1.86 GHz (4 processors), and 64 GB of RAM, running on Windows Server 2008 R2 Enterprise 64-bit.

5.4.1 Test System and Study Cases

The stochastic EMS is tested on a slightly modified version of the test system presented in Appendix B, where the maximum power output from Unit-04 (diesel) is reduced to 2 MW, and Unit-03 (diesel) has been removed; however, the numbering of the units is not changed. These modifications yield a tighter, less flexible, operation of the system, which makes the comparisons of study cases and discussions more meaningful. As an example, observe the optimal operation of the original system using the stochastic EMS approach and a deterministic EMS approach in Figs. 5.3 and 5.4, respectively. In this case, even though the management of ESS units is noticeably different, both approaches yield very similar dispatches for diesel units given the slackness provided by Unit-03 and Unit-04. For example, note that even with a stochastic modelling, Unit-04 provides sufficient reserve levels for adequate operation. A wind power profile with more variability is used here, as illustrated in Fig. 5.5, which represents a more challenging condition for the operation of the stochastic EMS.

A number of study cases are presented here in order to analyse the performance of the proposed stochastic EMS under different system conditions. These study cases address important aspects that may impact the performance of the system, i.e., available storage capacity, scenario generation approach, and length of the optimization window (horizon) of the SUC. Costs of US$5/kWh for load shedding and US$3/kWh for generation curtailment were used in all the study cases.

Base Case

The *Base Case* corresponds to the modified test system described above. For the SUC, 100 scenarios are generated at each time-step (each hour) based on the given 24-hour forecast using the statistic ensembles technique. The scenarios obtained with this technique are

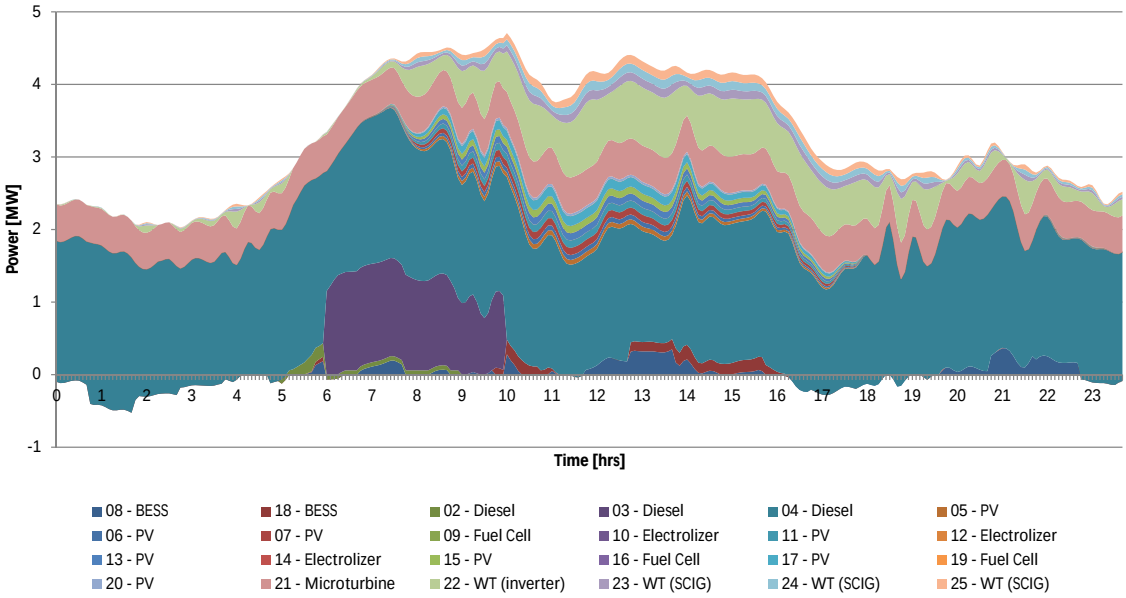

Fig. 5.3: Optimal dispatch of the original test system with a stochastic EMS approach.

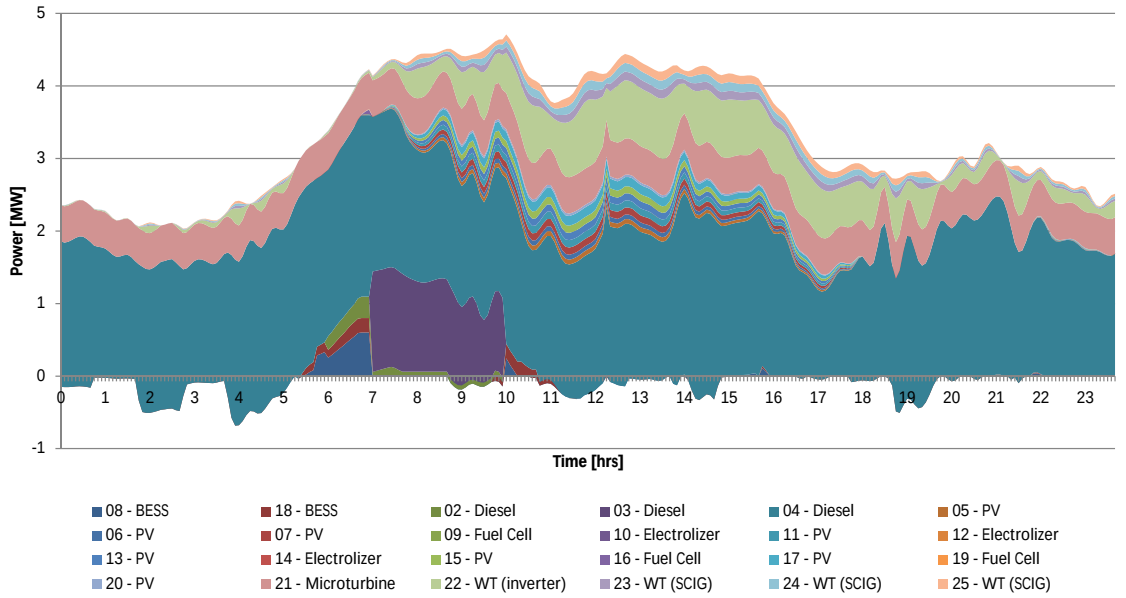

Fig. 5.4: Optimal dispatch of the original test system with a deterministic EMS approach.

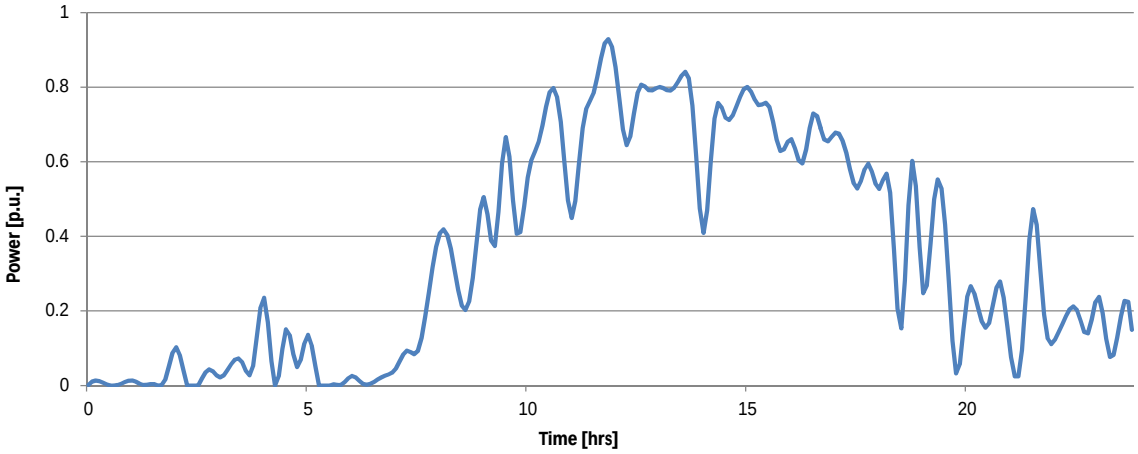

Fig. 5.5: Test system wind power profile.

depicted in Fig. 5.6. The SUC horizon is set to $H_{SUC} = 24$ hours in order to capture complete cycles of the load, solar and wind profiles. The multi-period OPF uses a varying optimization horizon, ranging from 75 minutes to 15 minutes, with 5-minutes time-steps.

Deterministic Approach

The use of a deterministic EMS approach without an explicit reserve requirement would produce a highly unreliable dispatch of the microgrid, which are very likely to produce load shedding and/or power curtailment events. To investigate this characteristic, a study case using a deterministic UC formulation is analysed (*Det.Case*), using the same system and parameters as the *Base Case*. This is accomplished by using only 1 scenario of future wind power generation in the SUC, corresponding to the output of the forecasting system.

Scenarios based on Historical Data

The approach used for generation of scenarios may have an impact on the determination of system reserve and operational cost. Scenarios based on unfiltered historical data (*Hist.Data*) typically corresponds to a pessimistic approach, as they do not take into account the goodness of the forecasting system. In this case, scenarios are given by the realization of wind power generation of the 26 previous days of operation.

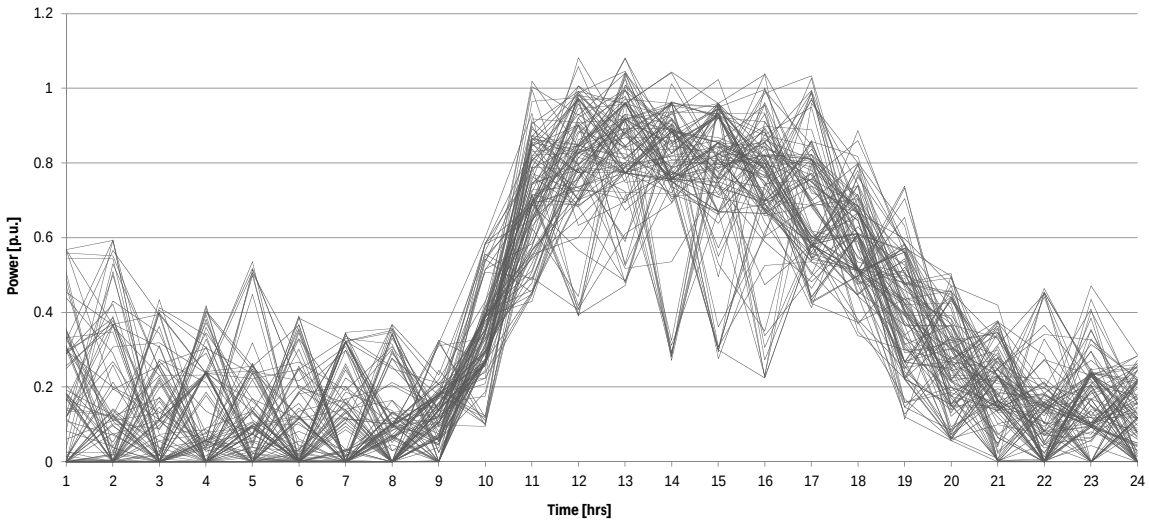

Fig. 5.6: Wind power scenarios for the SUC generated using statistic ensembles.

ESS Capacity

A higher ESS capacity is expected to positively impact the operational costs of the microgrid, due to the higher operational flexibility, and it will also have an effect on the allocation of system reserves. Thus, 2 scenarios with different additional ESS capacities are analyzed: 250 kW–1,250 kWh (*B250*) and 500 kW–2,500 kWh (*B500*), which represent a total battery-ESS capacity of 1050 kW and 1300 kW, respectively. In each case, the additional capacity is included as a single battery-ESS unit located at Bus-1.

SUC Optimization Window

The solution of the SUC using extended optimization horizons can be expensive in terms of computation times. An alternative to reduce the solution times is to reduce the horizon considered in the optimization; however, this alternative may negatively impact the unit commitment decisions and proper management of energy storage resources leading to more expensive solutions. To analyse this effect, 2 study cases with different SUC horizons are presented: $H_{SUC} = 8$ hours (*Var8*), and $H_{SUC} = 12$ hours (*Var12*).

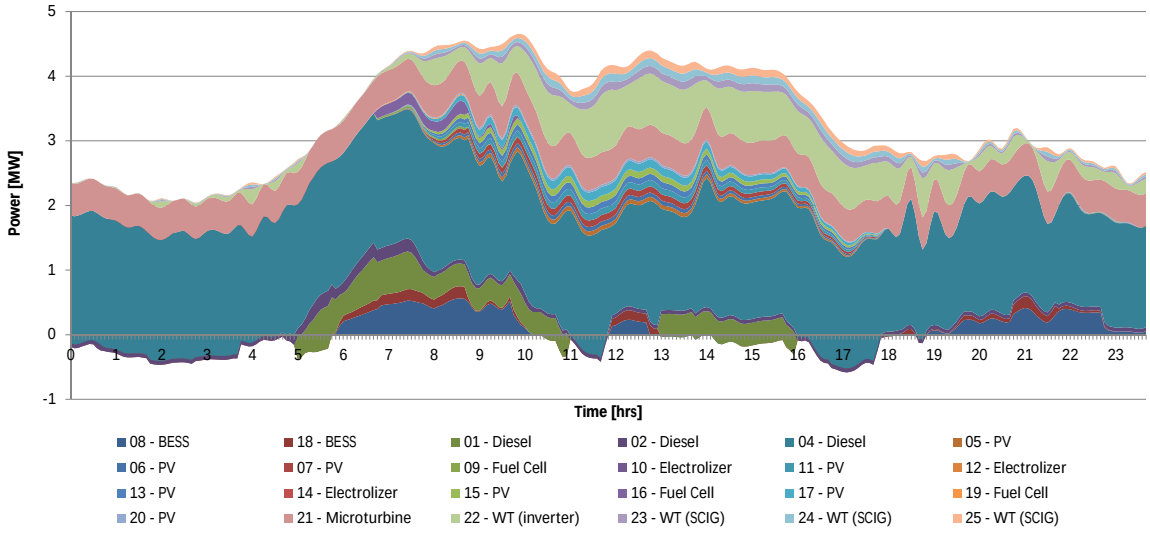

Fig. 5.7: Optimal dispatch obtained by the EMS for *Base Case*.

5.4.2 Steady-state Optimal Conditions

This section presents the steady-state optimal conditions for 3 study cases: *Base Case*, *Det.Case*, and *Hist.Data*. The analysis concentrates on these 3 study cases due to their clear differences in the representation of uncertainty, yielding different levels of conservatism in the dispatch solutions.

Results of the optimal dispatch of all the units for the *Base Case* scenario are shown in Fig. 5.7, and Fig. 5.8 shows the dispatch of a reduced number of units that are more representative of the different dispatch strategies, namely, diesel units (Units 01, 02 and 04), battery-ESSs (Units 08 and 18), and microturbine (Unit-21). Similarly, the optimal dispatch for *Det.Case* is shown in Figs. 5.9 and 5.10, and the optimal dispatch for *Hist.Data* is shown in Figs. 5.11 and 5.12.

It is observed from Fig. 5.8 that in the *Base Case* units 02 and 04 are dispatched during the 24 hours of operation, while Unit-01 is used between hours 5 and 11, and in hours 13 to 16. This represents a more robust dispatch compared to *Det.Case*, where Unit-02 is used only 17 hours, and Unit-01 is used exclusively in peak-load between hours 5 and 9, as can be observed in Figs. 5.9 and 5.10. A more conservative dispatch is produced by *Hist.Data*, with Unit-02 used for 24 hours, and Unit-01 used for 15 hours, as shown in Figs. 5.11 and 5.12.

With respect to the management of storage resources, it is observed that *Det.Case*

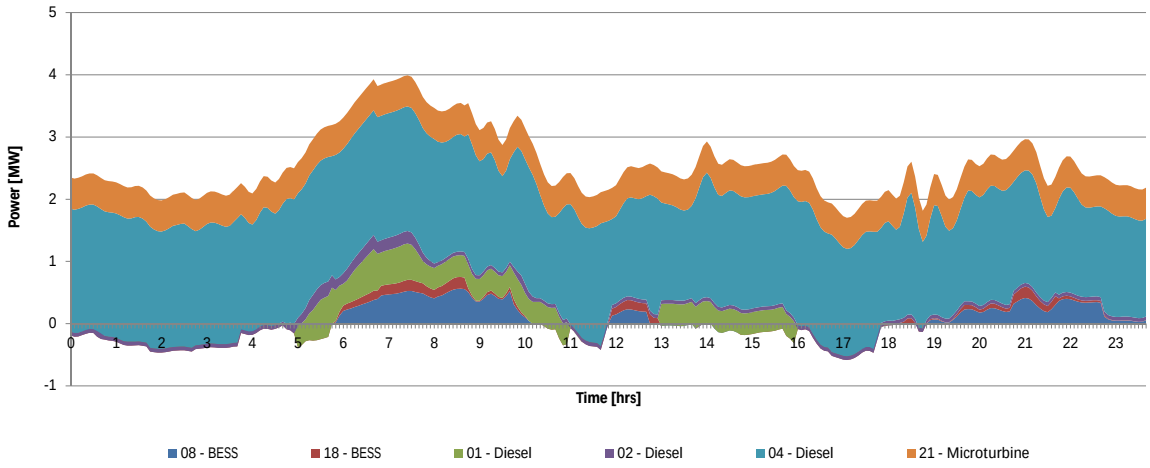

Fig. 5.8: Optimal dispatch of selected units obtained by the EMS for *Base Case*.

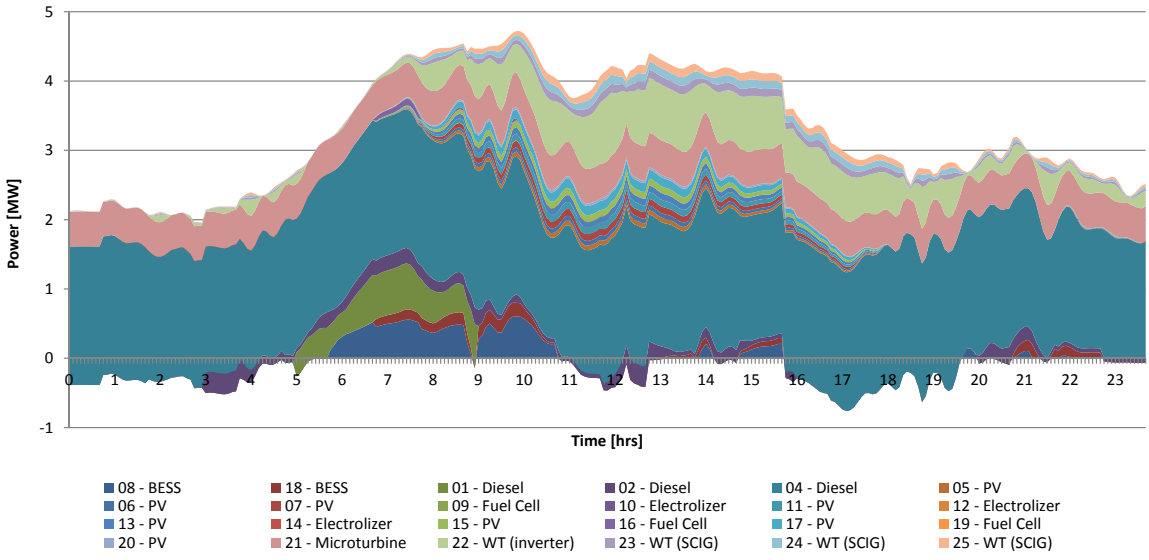

Fig. 5.9: Optimal dispatch obtained by the EMS for *Det.Case*.

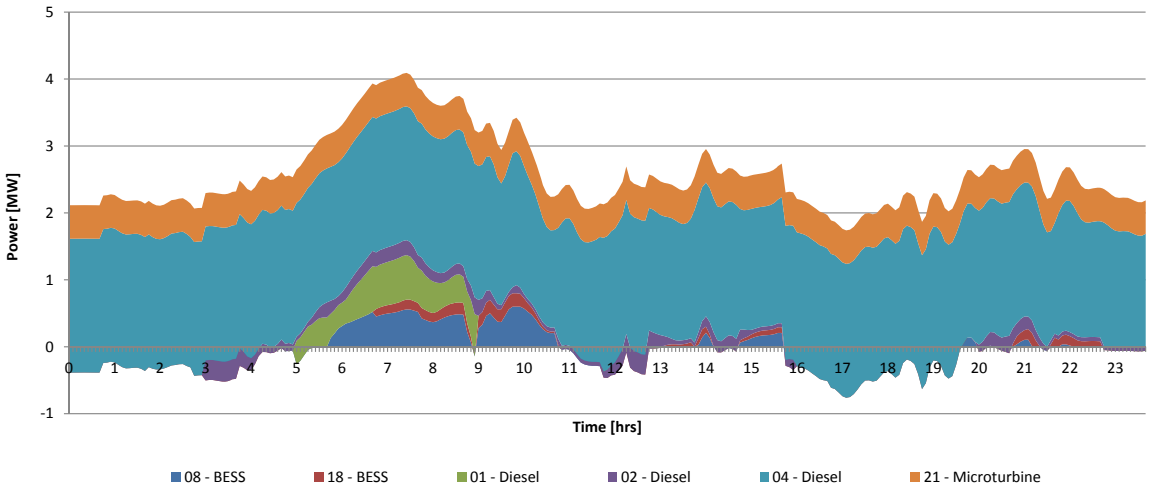

Fig. 5.10: Optimal dispatch of selected units obtained by the EMS for *Det.Case*.

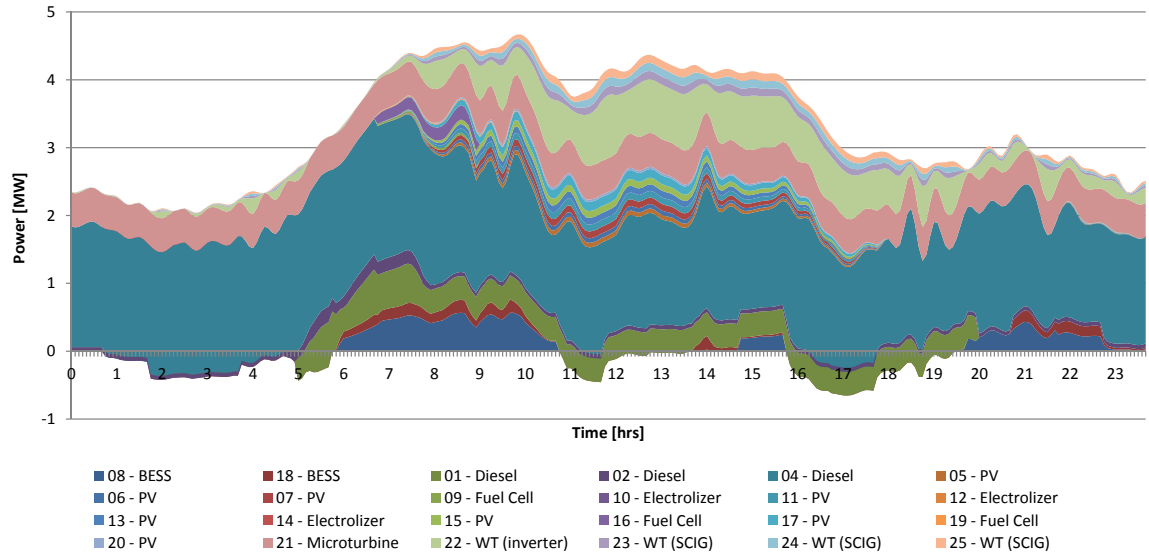

Fig. 5.11: Optimal dispatch obtained by the EMS for *Hist.Data*.

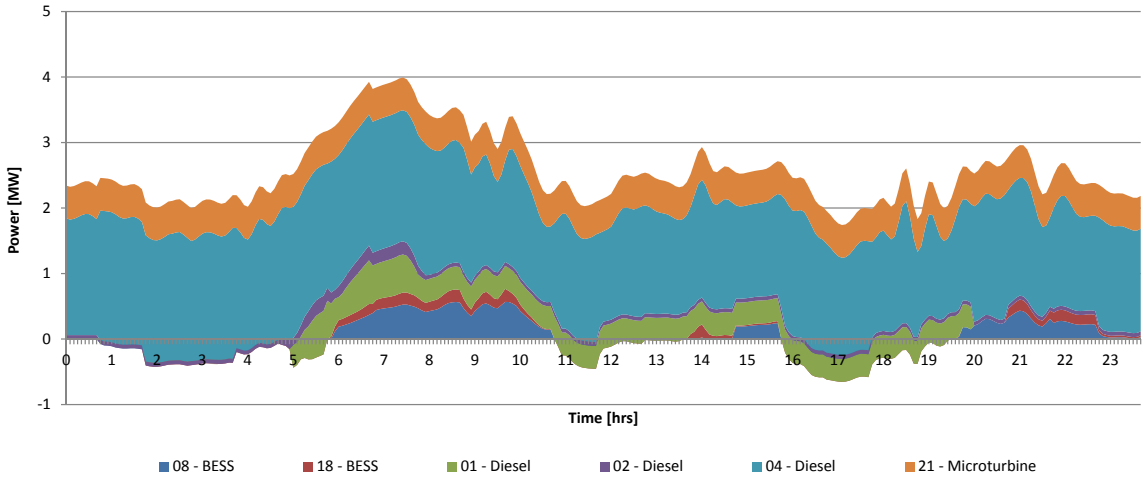

Fig. 5.12: Optimal dispatch of selected units obtained by the EMS for *Hist.Data*.

produces a more dynamic operation of the battery-ESS units due to a changing perception of future system conditions, which is adjusted with every update of the forecasting system. This can be observed near hours 9, 12 and 16, in Fig. 5.10. On the other hand, *Base Case* and *Hist.Data* produce more stable (smooth) charging and discharging patterns, since given the large number of scenarios considered at each iteration of the SUC, the perception of future system conditions is unlikely to change abruptly.

The total simulation time of the stochastic EMS for 24 hours of operation for the *Base Case* was 5,228s. The average computational times were approximately 11s per iteration of the NLP problem (multi-period OPF), and 93s per iteration of the MILP problem (SUC), which are within the proposed dispatch and UC windows, making the algorithm suitable for real-time applications.

5.4.3 Effects of EMS parameters and system configuration

Daily-average reserves, minimum instantaneous reserves, and reserves at peak-load for each study case are shown in Fig. 5.13. Reserve levels have been calculated based on the unused capacity of committed diesel generators and micro-turbine, which corresponds to the classical notion of spinning reserves, without including available ESS capacity. The operational cost of the microgrid for each study case, defined as the total cost of fuel plus the cost of load shedding, is presented in Table 5.1.

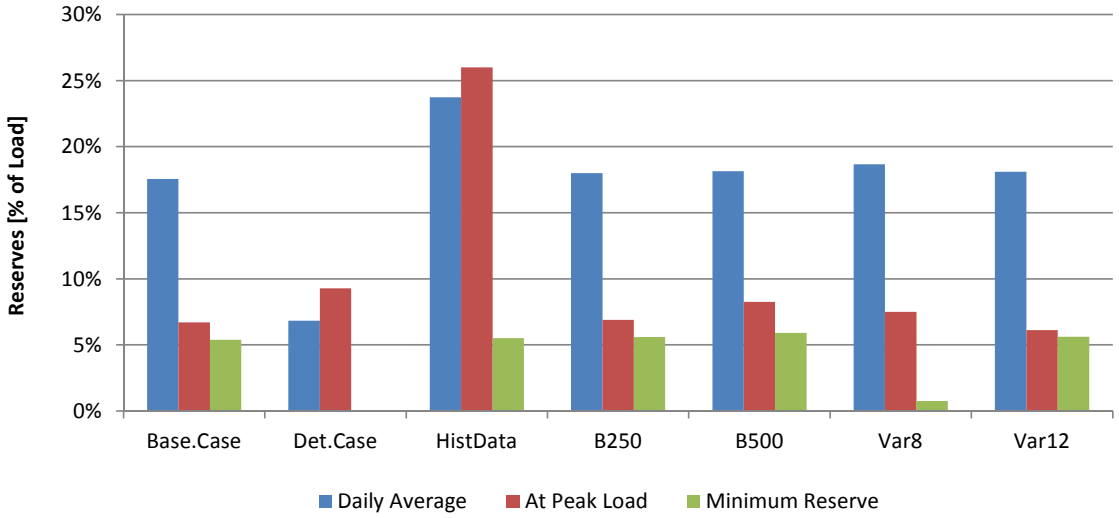

Fig. 5.13: System Reserves for Different Scenarios

It can be observed from Table 5.1 that the proposed stochastic formulation (*Base Case*) outperforms the deterministic case (*Det.Case*) in terms of operation cost, due to the fragile dispatch conditions calculated by the deterministic case without an explicit reserve requirement. From the reserves point of view, *Det.Case* is not able to commit enough reserves to compensate for variations in the instantaneous wind power with respect to the forecast, which results in the need to use expensive load shedding. The *Hist.Data* case shows the effect of a more pessimistic representation of the uncertainty, yielding more conservative results, as can be seen from the high levels of reserve in Fig. 5.13. This also yields higher operation costs as compared to the *Base Case*, although this difference is not significant given the particular cost characteristics of the units in the test system.

Cases with increased ESS capacity (*B250* and *B500*) show a reduction of costs as compared with the *Base Case*, without affecting the levels of reserve, which is attributed to a reduction in the use of more expensive diesel units due to a more flexible operation of the system. Nevertheless, note that the reduction of cost due to increased ESS capacity is not directly proportional, since it depends on several other factors such as the level of penetration of intermittent sources, its correlation with the load profile, the differences in operation costs of units, and the accuracy of the forecasting system. Study cases with reduced SUC look-ahead windows (*Var8* and *Var12*) show poor performance in terms of operation costs; however, they do not yield actual load shedding. The higher costs of these

Table 5.1: Operation Costs

	Diesel Cost	Load Shedding	Total
	US$/day	US$/day	US$/day
Base Case	13,097.1	0.0	13,097.1
Det.Case	13,555.0	1,283.4	14,838.3
Hist.Data	13,176.4	0.0	13,176.4
B250	12,980.3	0.0	12,980.3
B500	12,944.1	0.0	12,944.1
Var8	13,285.4	0.0	13,285.4
Var12	13,232.9	0.0	13,232.9

study cases are associated with their limited ability to foresee future system conditions, which hinders a proper management of energy storage resources and commitment of units.

In order to evaluate the performance of the proposed EMS in terms of robustness, two indices are defined: $eLOLE$ and $eLOEE$. These indices are obtained from the solution of the SUC, and represent estimations of the Loss of Load Expectation (LOLE) and Loss of Energy Expectation (LOEE) [114], respectively. The indices are defined as follows:

- $eLOLE$: Number of hours in all the scenarios for which the SUC produces load shedding at the 1-hour interval $t = 1$, for the whole simulation period of 24 hours, divided by the total number of scenarios.
- $eLOEE$: Total energy shed in all the scenarios at the 1-hour interval $t = 1$, for the whole simulation period of 24 hours, divided by the total number of scenarios.

Note that by using a receding horizon approach in the SUC, each hour of the simulated day corresponds to $t = 1$ of one of the iterations of the SUC; hence, the indices only consider the dispatch commands that are actually implemented in the system at each time-step of the SUC. Also, these indices assume that the uncertainty is properly represented by the scenarios utilized; therefore, the indices are only comparable if they are based on the same scenarios. In this context, indices for study cases *Hist.Data* and *Det.Case* cannot be directly compared with the rest of the study cases, since they use different scenarios.

Indices $eLOLE$ and $eLOEE$ for each scenario, together with the actual loss of load over the 24-hour simulation, are presented in Table 5.2. It is observed from the table that higher levels of ESS capacity yield not only lower operation costs but also lower $eLOLE$

and *eLOEE* indices, improving the adequacy of the system. Also, observe that study cases with reduced look-ahead windows, although more expensive, do not necessarily improve the system adequacy.

Table 5.2: Estimated Adequacy Indices

	eLOLE	*eLOEE*	Loss of Load
	[hours/day]	[kWh/day]	[hours/day]
Base Case	0.93	131.7	0
B250	0.35	9.8	0
B500	0.02	0.5	0
Var8	1.57	272.5	0
Var12	0.84	129.1	0
Hist.Data	N/A	N/A	0
Det.Case	N/A	N/A	1.1

5.5 Summary

This chapter presented the architecture and design of a centralized EMS for isolated microgrids using stochastic optimization. The proposed stochastic EMS was based on the deterministic EMS design presented in Chapter 4, where the original UC (MILP) problem was re-formulated as a two-stage SP problem. Hence, the proposed stochastic approach combined the advantages of SP formulations and close tracking of variations (MPC). The EMS design was adapted to allow more time for the calculation of SUC solutions, and use different time resolutions in each problem (SUC and multi-period OPF), without changing the main structure of the EMS.

The performance of proposed stochastic EMS design was studied using a slightly modified version of the MV microgrid test system for different study cases, including different energy storage capacities, look-ahead windows, and scenario generation techniques. A set of estimated adequacy indices was defined to support the comparison of study cases, and the results demonstrated the advantages of the proposed stochastic approach for dealing with uncertainty and assigning appropriate levels of reserve in the system.

Chapter 6

Conclusions, Contributions and Future Work

6.1 Summary and Conclusions

This thesis has concentrated on the design of a centralized Energy Management System (EMS) for isolated microgrids, considering the uncertainty associated with estimation of load and Renewable Energy (RE)-based generation. A detailed three-phase model of the microgrid was developed based on the principles of distribution system modelling, thus allowing the representation of unbalanced system conditions. The proposed model was then used to formulate the microgrid energy management problem as an Mixed-Integer Nonlinear Programming (MINLP) problem. A decomposition of the MINLP problem into Mixed-Integer Linear Programming (MILP) (UC) and Nonlinear Programming (NLP) (multi-period OPF) problems, together with a heuristic to preserve the interrelation of the problems, were developed to reduce solution times and enable their implementation in the real-time operation of isolated microgrids.

A novel centralized and deterministic EMS design was presented, incorporating the formulation of the energy management problem using an Model Predictive Control (MPC) approach. Hence, uncertainty was indirectly considered by closely tracking the optimal solutions with updated information provided by suitable forecasting systems. The results of the proposed deterministic EMS were compared with a balanced implementation of the EMS, using a realistic isolated microgrid model with multiple Distributed Energy Resources (DERs).

An improvement to the EMS design was proposed with the formulation of the UC problem as a two-stage Stochastic Programming (SP) problem, where uncertainty was directly accounted for in the optimization process by defining a set of possible scenarios using available scenario generation techniques. Finally, the performance of the stochastic approach was tested and evaluated under different conditions based on a proposed set of estimated adequacy indices, utilizing a realistic MV microgrid test system under different conditions, including cases with different energy storage capacities, look-ahead windows, and scenario generation techniques.

The main conclusions of this thesis can be summarized as follows:

- The results showed that neglecting system imbalance leads to deviations in the optimal dispatch commands, and may lead to infeasible UC solutions due to unmet reactive power requirements; such condition was more apparent in heavy loading conditions. Thus, system imbalance needs to be properly considered in the dispatch of isolated microgrids.
- The results demonstrated the advantages of the proposed stochastic approach for dealing with uncertainty and assigning appropriate levels of reserve in the system. This approach yields dispatch with higher adequacy levels, and reduces long-run operation costs by design.
- For both proposed EMS designs, the feasibility of a realistic real-time, autonomous implementation was demonstrated, since the computational times associated with the corresponding implementations were well within the proposed dispatch update rates.

6.2 Contributions

The main contributions of the thesis are the following:

1. A novel, highly detailed formulation of the energy management problem for isolated microgrids has been proposed, featuring a three-phase representation of the system. The formulation includes new steady-state models for Synchronous Generators (SGs) and Squirrel-Cage Induction Generators (SCIGs), which are represented as series elements in the abc frame. The problem has been formulated as a deterministic, multi-period MINLP problem that allows for an appropriate management of energy storage resournces and UC multi-period constraints, while considering power flow constraints and system imbalance.

2. A new deterministic EMS for isolated microgrids has been designed based on the proposed formulation of the energy management problem and using an MPC approach. The proposed EMS design is able to preserve a high level of modelling detail at reduced computational times, using a decomposition approach and novel heuristics to solve the MINLP formulation.

3. A novel stochastic EMS design has been proposed, accounting for the uncertainty associated with RE sources directly in the formulation of the energy management problem by re-formulating the UC as a two-stage SP problem. The treatment of Energy Storage Systems (ESSs) in the SP formulation and the coordination of UC and multi-period OPF solutions are particularly novel.

4. The suitability of the proposed EMS designs for real-time dispatch applications was considered as a criterion in the development of models and calculation algorithms. Thus, by design, the two proposed EMSs are able to produce optimal dispatch solutions in computational times that allow their implementation in the real-time, autonomous operation of isolated microgrid.

Part of the work presented this thesis has been published in a conference proceeding [44], and reported in 2 papers currently under review for publication in IEEE journals [6, 115]. A third journal paper has been prepared and is ready for submission [116], pending authorization by industry research partners.

6.3 Future Work

Based on the work presented in this thesis, further research may be pursued on the following subjects:

- Investigate the performance of the proposed EMS designs under a larger number of conditions, including higher levels of penetration of RE sources and different system topologies, and evaluate the interaction/integration of the EMS with demand response mechanisms.

- Study the performance of the proposed EMS designs in conjunction with state-of-the-art primary controls in an experimental microgrid setup. This testing stage is of up-most importance before the EMS designs can be deemed appropriate for actual implementation in real microgrids. The testing results may reveal important

operational restrictions imposed by primary controllers that should be included as constraints in the proposed mathematical programs.

- Study the implementation of unbalanced optimal dispatch commands as reference values for the primary DER controllers, since the proposed EMS approaches have the ability to determine the three-phase optimal dispatch of inverter-interfaced DER units, which, in principle, can be independent for each phase.

- Investigate the application and performance of alternative optimization formulations to account for uncertainty, such as Robust Optimization and Chance-Constrained Optimization.

- Analyse the impacts of the proposed, and other, energy management strategies on the optimal design and planning of isolated microgrids. In particular, investigate how the warning signals for reactive power problems can be used to determine required investment in reactive power compensation, and how the proposed adequacy indices can used to account for reliability considerations in microgrids' planning.

APPENDICES

Appendix A

MILP Formulation of the Deterministic UC Problem

$$\min \sum_{g,k_t} \Bigg[\Big[\sum_{h} \left(b_g^h P_{g,k_t}^h + c_g^h w_{g,k_t}^h \right) \Big] \Delta t_{k_t} + C_{sup} u_{g,k_t} + C_{sdn} v_{g,k_t} + K_{emer} (u_{g,k_t}^{emer} + v_{g,k_t}^{emer}) \Bigg] \tag{A.1}$$

subject to:

$$\sum_{g} P_{g,k_t} = \sum_{L} \sum_{p} P_{p,L,k_t} + \sum_{n} \sum_{L_n} \sum_{p} \mathrm{Re}\{V_n^{nom2} / Z_{p,L_n,k_t}^{*}\} \quad \forall k_t \tag{A.2}$$

$$\sum_{g_d} w_{g_d} \left[P_{g_d}^{max} - P_{g_d,k_t} \right] = R_{sv} \sum_{g} P_{g,k_t} \quad \forall k_t \tag{A.3}$$

$$\left[\sum_{\widehat{k_t}:\ t_{\widehat{k_t}} = t_{k_t} - M_{up,g}}^{k_t - 1} w_{g,\widehat{k_t}} \Delta t_{\widehat{k_t}} \right] - M_{up,g} \left(v_{g,k_t} - v_{g,k_t}^{emer} \right) \geq 0 \quad \forall g, \forall k_t \tag{A.4}$$

$$M_{dn,g} \left(1 - \left(u_{g,k_t} - u_{g,k_t}^{emer} \right) \right) - \left[\sum_{\widehat{k_t}:\ t_{\widehat{k_t}} = t_{k_t} - M_{dn,g}}^{k_t - 1} w_{g,\widehat{k_t}} \Delta t_{\widehat{k_t}} \right] \geq 0 \quad \forall g, \forall k_t \tag{A.5}$$

$$u_{g,k_t} - v_{g,k_t} = w_{g,k_t} - w_{g,k_t-1} \quad \forall g, \forall k_t \tag{A.6}$$

$$u_{g,k_t} + v_{g,k_t} \leq 1 \quad \forall g, \forall k_t \tag{A.7}$$

$$\sum_h w^h_{g,k_t} \leq 1 \quad \forall g, \forall k_t \tag{A.8}$$

$$w_{g,k_t} = \sum_h w^h_{g,k_t} \quad \forall g, \forall k_t \tag{A.9}$$

$$P_{g,k_t} = \sum_h P^h_{g,k_t} \quad \forall g, \forall k_t \tag{A.10}$$

$$P_{g_b,k_t} = P^{out}_{g_b,k_t} - P^{in}_{g_b,k_t} \quad \forall g_b, \forall k_t \tag{A.11}$$

$$P^{out}_{g_b,k_t},\ P^{in}_{g_b,k_t} \geq 0 \quad \forall g_b, \forall k_t \tag{A.12}$$

$$SOC_{g_b,k_t+1} = SOC_{g_b,k_t} + \left(P^{in}_{g_b,k_t}\eta^{in}_{g_b} - \frac{P^{out}_{g_b,k_t}}{\eta^{out}_{g_b}} \right) \Delta t_{k_t} \quad \forall g_b, \forall k_t \tag{A.13}$$

$$\begin{aligned} SOC_{H_{tank},k_t+1} &= SOC_{H_{tank},k_t} \\ &+ \left(\frac{1}{1+l_c} \frac{\sum_{g_{el} \to H_{tank}} P^{H_{tank}}_{g_{el},k_t}\eta_{g_{el}}}{HHV} - \frac{\sum_{g_{fc} \to H_{tank}} P^{H_{tank}}_{g_{fc},k_t}}{HHV\eta_{g_{fc}}} \right) \Delta t_{k_t} \quad \forall H_{tank}, \forall k_t \end{aligned} \tag{A.14}$$

$$P_{g,k_t+1} - P_{g,k_t} - u_{g,k_t+1}P^{max}_g \leq R_{up,g}\Delta t_{kt} \quad \forall g, \forall k_t \tag{A.15}$$

$$P_{g,k_t} - P_{g,k_t+1} - v_{g,k_t+1}P^{max}_g \leq R_{dn,g}\Delta t_{kt} \quad \forall g, \forall k_t \tag{A.16}$$

$$P_g^{min,h} w_{g,k_t}^h \leq P_{g,k_t}^h \leq P_g^{max,h} w_{g,k_t}^h \quad \forall g, \forall k_t \tag{A.17}$$

$$P_{g,k_t}^{min} w_{g,k_t} \leq P_{g,k_t} \leq P_{g,k_t}^{max} w_{g,k_t} \quad \forall g, \forall k_t \tag{A.18}$$

$$P_{g,k_t}^{max} = \widetilde{P}_{g,k_t} \quad \forall g_{rw}, \forall k_t \tag{A.19}$$

$$SOC_{g_b}^{min} \leq SOC_{g_b,k_t} \leq SOC_{g_b}^{max} \quad \forall g_b, \forall k_t \tag{A.20}$$

$$SOC_{H_{tank}}^{max} \leq SOC_{H_{tank},k_t} \leq SOC_{H_{tank}}^{max} \quad \forall H_{tank}, \forall k_t \tag{A.21}$$

$$u_{g,k_t},\ v_{g,k_t},\ w_{g,k_t},\ w_{g,k_t}^h \in \{0,1\} \quad \forall g, \forall k_t, \forall h \tag{A.22}$$

Appendix B

Modified CIGRE Medium-Voltage Test System Data

The test system data presented in Tables B.2 and B.3 correspond to the CIGRE MV benchmark system presented in [107]. Table B.1 contains additional data associated with transformers interfacing additional generators included in the particular test system used in for this work. Tables B.4, B.5 and B.6 contain technical parameters of DERs based on synchronous generators, inverter-interfaced, and squirrel-cage induction generators, respectively, obtained from multiple sources. Table B.7 contains minimum up-time, minimum down-time and ramping limits for all the generating units. Finally, Table B.8 contains data associated with operating costs of fuel-driven DGs.

Table B.1: Transformers Parameters

TF No	Node from-to	X [pu]	*Type*	V from [kV]	V to [kV]	S_{rated} [kVA]
1	14-1	0.05	$\Delta - Y_g$	0.48	12.47	5,000
2	15-9	0.05	$\Delta - Y_g$	0.48	12.47	500
3	16-7	0.05	$\Delta - Y_g$	0.48	12.47	700

Table B.2: Line Parameters

Line No	Node from-to	R_{ph} [Ω]	X_{ph} [Ω]	B_{ph} [μS]	R_0 [Ω]	X_0 [Ω]	B_0 [μS]
1	1-2	0.208	0.518	4.596	0.421	2.160	1.884
2	2-3	0.173	0.432	3.830	0.351	1.800	1.570
3	3-4	0.106	0.264	2.336	0.214	1.098	0.958
4	4-5	0.097	0.242	2.145	0.197	1.008	0.879
5	5-6	0.266	0.665	5.898	0.541	2.772	2.418
6	6-7	0.042	0.104	0.919	0.084	0.432	0.377
7	7-8	0.289	0.721	6.396	0.586	3.006	2.622
8	8-9	0.055	0.138	1.226	0.112	0.576	0.502
9	9-10	0.133	0.333	2.949	0.270	1.386	1.209
10	10-11	0.057	0.143	1.264	0.116	0.594	0.518
11	11-4	0.085	0.212	1.877	0.172	0.882	0.769
12	3-8	0.225	0.562	4.979	0.456	2.340	2.041
13	1-12	0.846	2.112	18.729	1.716	8.802	7.677
14	12-13	0.517	1.292	11.452	1.049	5.382	4.694
15	13-8	0.346	0.864	7.660	0.702	3.600	3.140

Table B.3: Load Parameters

Node	Apparent Power [kVA]						Power Factor	
	Phase A		Phase B		Phase C			
	Res	Com	Res	Com	Res	Com	Res	Com
1	344.00	80.00	172.00	180.00	200.00	180.00	0.90	0.80
2	100.00	200.00	50.00	200.00	0.00	200.00	0.95	0.85
3	0.00	80.00	200.00	80.00	50.00	80.00	0.90	0.80
4	200.00	0.00	100.00	0.00	100.00	0.00	0.90	1.00
5	200.00	50.00	172.00	200.00	0.00	50.00	0.95	0.85
6	50.00	0.00	100.00	0.00	172.00	0.00	0.95	1.00
7	0.00	100.00	100.00	100.00	0.00	100.00	0.95	0.95
8	100.00	0.00	150.00	0.00	0.00	200.00	0.90	0.90
9	100.00	0.00	150.00	0.00	100.00	0.00	0.95	1.00
10	150.00	0.00	100.00	0.00	250.00	0.00	0.90	1.00
11	50.00	150.00	50.00	150.00	0.00	150.00	0.95	0.85
12	0.00	145.00	0.00	145.00	0.00	145.00	0.95	0.85
13	0.00	90.00	0.00	90.00	172.00	90.00	0.90	0.90

Table B.4: Directly-Connected Synchronous Generators Parameters

Unit No.	S_{base} [kVA]	V_{base} [kV]	P_{max} [kW]	P_{min} [kW]	x_d [pu]	x''_d [pu]	x''_q [pu]	x_0 [pu]
1	1000	0.48	800	350	3.05	0.134	0.153	0.051
2	390	0.48	310	60	3.5	0.142	0.166	0.038
3	1750	0.48	1400	600	3.05	0.134	0.153	0.051
4	3125	0.48	2500	1000	3.05	0.134	0.153	0.051

Table B.5: Inverter-interfaced DERs Parameters

	DER				Inverter		
Unit No.	P_{max} [kW]	P_{min} [kW]	Eff_{in} [%]	Eff_{out} [%]	S_{max} [kVA]	$Eff\|_{P_{max}}$ [%]	$Eff\|_{20\%P_{max}}$ [%]
5	20	0	-	-	250	91%	95%
6	20	0	-	-	250	91%	95%
7	30	0	-	-	375	91%	95%
8	600	0	95%	95%	750	91%	95%
9	33	6	-	60%	42	91%	95%
10	30	6	60%	-	38	91%	95%
11	30	0	-	-	38	91%	95%
12	50	10	60%	-	63	91%	95%
13	30	0	-	-	38	91%	95%
14	200	40	60%	-	250	91%	95%
15	30	0	-	-	38	91%	95%
16	212	50	-	60%	265	91%	95%
17	40	0	-	-	50	91%	95%
18	200	0	95%	95%	250	91%	95%
19	14	0	-	60%	18	91%	95%
20	10	0	-	-	13	91%	95%
21	500	100	-	-	625	91%	95%
22	1000	0	-	-	1250	91%	95%

Table B.6: Directly-connected SCIG Parameters

Unit	S_{base}	V_{base}	P_{max}	P_{min}	r_s	x_s	r'_r	x'_r	x_m
No.	[kVA]	[kV]	[kW]	[kW]	[pu]	[pu]	[pu]	[pu]	[pu]
23	190	0.48	150	0	0.007	0.15	0.0072	0.15	2.95
24	190	0.48	150	0	0.007	0.15	0.0072	0.15	2.95
25	190	0.48	150	0	0.007	0.15	0.0072	0.15	2.95

Table B.7: Minimum Up-time, Down-time and Ramping Limits

Unit	R_{up}	R_{dn}	M_{up}	M_{dn}
No.	[kW/min]	[kW/min]	[hr]	[hr]
1	16	16	2	1
2	6.2	6.2	3	2
3	28	28	2	1
4	50	50	3	2
5	4	4	0	0
6	4	4	0	0
7	6	6	0	0
8	120	120	0	0
9	6.6	6.6	1	1
10	6	6	1	1
11	6	6	0	0
12	10	10	1	1
13	6	6	0	0
14	40	40	1	1
15	6	6	0	0
16	42.4	42.4	1	1
17	8	8	0	0
18	40	40	0	0
19	2.8	2.8	1	1
20	2	2	0	0
21	10	10	2	2
22	200	200	0	0
23	30	30	0	0
24	30	30	0	0
25	30	30	0	0

Table B.8: Cost Functions, Start-up and Shut-down Costs of Generators

Unit	a	b	c	C_{Sup}	C_{Sdn}
No.	$[US\$/kWh^2]$	$[US\$/kWh]$	$[US\$]$	$[US\$]$	$[US\$]$
1	0	0.2881	7.5	15	5.3
2	0	0.2876	0	7.35	1.44
3	0	0.2571	25.5	45	8.3
4	0.00001	0.224	45.5	95	15.3
21	0	0.053	3.1	3	0.5

*Cost functions are based on a diesel price of US$3.78/gal and a gas price of US$5/MBTu

Appendix C

Forecasting System Characteristics

Time series for load, wind power, and solar power forecasting systems used in this thesis have been obtained from a real forecasting system implemented in a remote microgrid in Huatacondo, Chile [11]. These forecasting systems are based on fuzzy confidence interval models [117], where Takagi & Sugeno fuzzy models are defined for the expected values, and the upper and lower bounds of confidence intervals of each variable (load, wind power and solar power). Thus, output values of the forecasting systems at each time-step are defined by a linear combination of a number of linear autoregressive models representing different operating points of the system, with different degrees of activation (weights). Forecasting systems for load, wind power and solar power were applied to the particular conditions of Huatacondo, producing the performance indices shown in Table C.1.

Table C.1: Forecasting errors

		15-min ahead	24-hour ahead
Wind Power	RMSE [p.u.]	0.1221	0.1429
	σ [p.u.]	0.0224	0.0703
Solar Power	RMSE [p.u.]	0.0810	0.0960
	σ [p.u.]	0.0074	0.0110
Load	RMSE [p.u.]	0.0740	0.0875
	σ [p.u.]	0.0070	0.0088

References

[1] R. E. P. N. for the 21st Century, "Renewables 2013 global status report," REN21, Tech. Rep., 2013.

[2] M. Moner-Girona and M. Solano-Peralta, "Adapted feed-in tariff for the promotion of renewable energies for off-grid areas," in *Expert Group Meeting - Potential of renewable energy options in off-grid areas in Africa: importance of mini-grid energy systems*, Apr. 3-5, 2012.

[3] M. Fulton, B. Kahn, N. Mellquist, E. Soong, J. Baker, and L. Cotter, "Get fit program," DB Climate Change Advisors - Deutsche Bank Group, Tech. Rep., April 2010.

[4] I. E. Agency, "Energy poverty - how to make modern energy access universal?" OECD/IEA, Tech. Rep., 2010.

[5] N. Hatziargyriou, H. Asona, R. Iravani, and C. Marnay, "Microgrids," *IEEE Power and Energy Magazine*, vol. 5, no. 4, pp. 78–94, Jul./Aug. 2007.

[6] D. E. Olivares, A. Mehrizi-Sani, A. H. Etemadi, C. A. Cañizares, R. Iravani, M. Kazerani, A. H. Hajimiragha, O. Gomis-Bellmunt, M. Saeedifard, R. Palma-Behnke, G. A. Jimenez-Estevez, and N. Hatziargyriou, "Trends in microgrid control," *IEEE Trans. Smart Grid*, submitted June 2013, 15 pages.

[7] R. Firestone and C. Marnay, "Energy manager design for microgrids," Consortium for Electric Reliability Technology Solutions (CERTS), Tech. Rep., 2005.

[8] A. Hajimiragha and M. R. D. Zadeh, "Research and development of a microgrid control and monitoring system for the remote community of Bella Coola: challenges, solutions achievements and lessons learned," in *Proc. IEEE International Conference on Smart Energy Grid Engineering (SEGE'13)*, Aug. 2013.

[9] C. Hernandez-Aramburo, T. Green, and N. Mugniot, "Fuel consumption minimization of a microgrid," *IEEE Trans. Ind. Applications*, vol. 41, no. 3, pp. 673 – 681, May-June 2005.

[10] F. Pilo, G. Pisano, and G. Soma, "Neural implementation of microgrid central controllers," in *Proc. IEEE 5th International Conference on Industrial Informatics*, vol. 2, June 2007, pp. 1177 –1182.

[11] R. Palma-Behnke, C. Benavides, F. Lanas, B. Severino, L. Reyes, J. Llanos, and D. Sáez, "A microgrid energy management system based on the rolling horizon strategy," *IEEE Trans. Smart Grid*, vol. 4, no. 2, pp. 996–1006, 2013.

[12] Y. Levron, J. Guerrero, and Y. Beck, "Optimal power flow in microgrids with energy storage," *IEEE Trans. Power Systems*, vol. 28, no. 3, pp. 3226–3234, 2013.

[13] S. Conti, R. Nicolosi, and S. Rizzo, "Optimal dispatching of distributed generators in an MV autonomous micro-grid to minimize operating costs and emissions," in *Proc. IEEE International Symposium on Industrial Electronics (ISIE)*, July 2010, pp. 2542 –2547.

[14] N. Hatziargyriou, G. Contaxis, M. Matos, J. Lopes, G. Kariniotakis, D. Mayer, J. Halliday, G. Dutton, P. Dokopoulos, A. Bakirtzis, J. Stefanakis, A. Gigantidou, P. O'Donnell, D. McCoy, M. Fernandes, J. Cotrim, and A. Figueira, "Energy management and control of island power systems with increased penetration from renewable sources," in *Proc. IEEE-PES Winter Meeting*, vol. 1, 2002, pp. 335 – 339.

[15] C. Colson, M. Nehrir, and S. Pourmousavi, "Towards real-time microgrid power management using computational intelligence methods," in *Proc. IEEE-PES General Meeting, 2010*, July 2010, pp. 1 –8.

[16] C. Colson, M. Nehrir, and C. Wang, "Ant colony optimization for microgrid multiobjective power management," in *Proc. IEEE Power Systems Conference and Exposition (PSCE '09)*, March 2009, pp. 1 –7.

[17] A. Chaouachi, R. Kamel, R. Andoulsi, and K. Nagasaka, "Multiobjective intelligent energy management for a microgrid," *IEEE Trans. Industrial Electronics*, vol. 60, no. 4, pp. 1688–1699, 2013.

[18] C. Chen, S. Duan, T. Cai, B. Liu, and G. Hu, "Smart energy management system for optimal microgrid economic operation," *Renewable Power Generation, IET*, vol. 5, no. 3, pp. 258–267, 2011.

[19] E. Barklund, N. Pogaku, M. Prodanovic, C. Hernandez-Aramburo, and T. Green, "Energy management in autonomous microgrid using stability-constrained droop control of inverters," *IEEE Trans. Power Electronics*, vol. 23, no. 5, pp. 2346–2352, 2008.

[20] Q. Jiang, M. Xue, and G. Geng, "Energy management of microgrid in grid-connected and stand-alone modes," *IEEE Trans. Power Systems*, vol. 28, no. 3, pp. 3380–3389, 2013.

[21] C. Schwaegerl, L. Tao, P. Mancarella, and G. Strbac, "A multi-objective optimization approach for assessment of technical, commercial and environmental performance of microgrids," *European Transactions on Electrical Power*, vol. 21, no. 2, pp. 1269–1288, 2011. [Online]. Available: http://dx.doi.org/10.1002/etep.472

[22] E. Alvarez, A. Lopez, J. Gomez-Aleixandre, and N. de Abajo, "On-line minimization of running costs, greenhouse gas emissions and the impact of distributed generation using microgrids on the electrical system," in *Proc. IEEE Conference on Sustainable Alternative Energy (SAE)*, Sept. 2009, pp. 1 –10.

[23] H. Kanchev, D. Lu, B. Francois, and V. Lazarov, "Smart monitoring of a microgrid including gas turbines and a dispatched PV-based active generator for energy management and emissions reduction," in *Proc. IEEE Innovative Smart Grid Technologies Conference Europe (ISGT Europe)*, Oct. 2010, pp. 1 –8.

[24] S. Conti, R. Nicolosi, S. A. Rizzo, and H. Zeineldin, "Optimal dispatching of distributed generators and storage systems for MV islanded microgrids," *IEEE Trans. Power Delivery*, vol. 27, no. 3, pp. 1243–1251, 2012.

[25] F. Katiraei, R. Iravani, N. Hatziargyriou, and A. Dimeas, "Microgrids management: Controls and operation aspects of microgrids," *IEEE Power and Energy Magazine*, vol. 6, no. 3, pp. 54–65, May/Jun. 2008.

[26] A. Borghetti, M. Bosetti, C. Bossi, S. Massucco, E. Micolano, A. Morini, C. Nucci, M. Paolone, and F. Silvestro, "An energy resource scheduler implemented in the automatic management system of a microgrid test facility," in *Proc. IEEE International Conference on Clean Electrical Power (ICCEP '07)*, May 2007, pp. 94 –100.

[27] M. Korpas and A. Holen, "Operation planning of hydrogen storage connected to wind power operating in a power market," *IEEE Trans. Energy Conversion*, vol. 21, no. 3, pp. 742 –749, Sept. 2006.

[28] T. Logenthiran and D. Srinivasan, "Short term generation scheduling of a microgrid," in *Proc. IEEE Region 10 Conference (TENCON'09)*, Jan. 2009, pp. 1 –6.

[29] T.-M. Tveit, T. Savola, A. Gebremedhin, and C.-J. Fogelholm, "Multi-period MINLP model for optimising operation and structural changes to CHP plants in district heating networks with long-term thermal storage," *Energy Conversion and Management*, vol. 50, no. 3, pp. 639 – 647, 2009. [Online]. Available: http://www.sciencedirect.com/science/article/pii/S0196890408004159

[30] S. Chakraborty, M. Weiss, and M. Simoes, "Distributed intelligent energy management system for a single-phase high-frequency ac microgrid," *IEEE Trans. Industrial Electronics*, vol. 54, no. 1, pp. 97–109, 2007.

[31] L. Xiaoping, D. Ming, H. Jianghong, H. Pingping, and P. Yali, "Dynamic economic dispatch for microgrids including battery energy storage," in *Proc. IEEE 2nd International Symposium on Power Electronics for Distributed Generation Systems (PEDG'10)*, June 2010, pp. 914 –917.

[32] A. Hajimiragha and M. R. D. Zadeh, "Practical aspects of storage modeling in the framework of microgrid real-time optimal control," in *Proc. IET Conference on Renewable Power Generation (RPG)*, Sept. 2011, pp. 93–98.

[33] J. Takayuki, S. Birge, "Stochastic unit commitment problem," *Int. Trans. in Operational Research*, vol. 11, no. 1, pp. 19–32, 2004.

[34] A. Papavasiliou, S. Oren, and R. O'Neill, "Reserve requirements for wind power integration: A scenario-based stochastic programming framework," *IEEE Trans. Power Systems*, vol. 26, no. 4, pp. 2197–2206, 2011.

[35] F. Bouffard and F. Galiana, "Stochastic security for operations planning with significant wind power generation," *IEEE Trans. Power Systems*, vol. 23, no. 2, pp. 306–316, 2008.

[36] L. Wu, M. Shahidehpour, and T. Li, "Stochastic security-constrained unit commitment," *IEEE Trans. Power Systems*, vol. 22, no. 2, pp. 800–811, 2007.

[37] S. Russell and P. Norvig, *Artificial Intelligence: A Modern Approach*, 2nd ed. Upper Saddle River, NJ: Prentice Hall, 2003.

[38] A. L. Dimeas and N. D. Hatziargyriou, "Operation of a multiagent system for microgrid control," *IEEE Trans. Power Systems*, vol. 20, no. 3, pp. 1447–1455, Aug. 2005.

[39] T. Logenthiran, D. Srinivasan, and D. Wong, "Multi-agent coordination for DER in microgrid," in *Proc. IEEE International Conference on Sustainable Energy Technologies (ICSET'08)*, Nov. 2008, pp. 77–82.

[40] J. Oyarzabal, J. Jimeno, J. Ruela, A. Engler, and C. Hardt, "Agent based micro grid management system," in *Proc. IEEE International Conference on Future Power Systems*, Nov. 2005, pp. 6–11.

[41] K. De Brabandere, K. Vanthournout, J. Driesen, G. Deconinck, and R. Belmans, "Control of microgrids," in *Proc. IEEE Power Engineering Society General Meeting*, June 2007, pp. 1 –7.

[42] W.-D. Zheng and J.-D. Cai, "A multi-agent system for distributed energy resources control in microgrid," in *Proc. IEEE 5th International Conference on Critical Infrastructure (CRIS)*, Sept. 2010, pp. 1 –5.

[43] T. Logenthiran, D. Srinivasan, A. Khambadkone, and H. Aung, "Multi-agent system (MAS) for short-term generation scheduling of a microgrid," in *Proc. IEEE International Conference on Sustainable Energy Technologies (ICSET)*, Dec. 2010, pp. 1 –6.

[44] D. Olivares, C. Canizares, and M. Kazerani, "A centralized optimal energy management system for microgrids," in *Proc. IEEE PES General Meeting, 2011*, July 2011, pp. 1–6.

[45] B. Lasseter, "Microgrids [distributed power generation]," in *Proc. IEEE-PES Winter Meeting*, vol. 1, Jan. 2001, pp. 146 –149.

[46] R. Lasseter, "Microgrids," in *Proc. IEEE Power Engineering Society Winter Meeting*, vol. 1, Jan. 2002, pp. 305 – 308.

[47] (2013) CERTS microgrid concept website. [Online]. Available: http://certs.lbl.gov/certs-der-micro.html

[48] (2013) Microgrids and more microgrids projects' website. [Online]. Available: http://www.microgrids.eu/default.php

[49] H. Karimi, H. Nikkhajoei, and M. R. Iravani, "Control of an electronically-coupled distributed resource unit subsequent to an islanding event," *IEEE Trans. Power Delivery*, vol. 23, no. 1, pp. 493–501, Jan. 2008.

[50] F. Katiraei, M. R. Iravani, and P. W. Lehn, "Micro-grid autonomous operation during and subsequent to islanding process," *IEEE Trans. Power Delivery*, vol. 20, no. 1, pp. 248–257, Jan. 2005.

[51] C. Wang and M. Nehrir, "Power management of a stand-alone wind/photovoltaic/fuel cell energy system," *IEEE Trans. Energy Conversion*, vol. 23, no. 3, pp. 957 –967, Sept. 2008.

[52] C. Alvial-Palavicino, N. Garrido-Echeverría, G. Jiménez-Estévez, L. Reyes, and R. Palma-Behnke, "A methodology for community engagement in the introduction of renewable based smart microgrid," *Energy for Sustainable Development*, vol. 15, no. 3, pp. 314 – 323, 2011. [Online]. Available: http://www.sciencedirect.com/science/article/pii/S0973082611000469

[53] J. A. P. Lopes, C. L. Moreira, and A. G. Madureira, "Defining control strategies for microgrids islanded operation," *IEEE Trans. Power Systems*, vol. 21, no. 2, pp. 916–924, May 2006.

[54] F. Katiraei, "Dynamic analysis and control of distributed energy resources in a micro-grid," Ph.D. Dissertation, Univ. Toronto, Dept. Electr. Comput. Eng., July 2005.

[55] M. Barnes, J. Kondoh, H. Asano, J. Oyarzabal, G. Ventakaramanan, R. Lasseter, N. Hatziargyriou, and T. Green, "Real-world microgrids-an overview," in *Proc. IEEE International Conference on System of Systems Engineering (SoSE)*, April 2007, pp. 1 –8.

[56] A. F. Burke, "Batteries and ultracapacitors for electric, hybrid, and fuel cell vehicles," *Proc. IEEE*, vol. 95, no. 4, pp. 806–820, Apr. 2007.

[57] "Bottling electricity: Storage as a strategic tool for managing variability and capacity concerns in the modern grid," White Paper, DOE Electricity Advisory Committee, Dec. 2008. [Online]. Available: http://www.oe.energy.gov/final-energy-storage_12-16-08.pdf

[58] J. M. Guerrero, J. C. Vasquez, J. Matas, L. G. de Vicuña, and M. Castilla, "Hierarchical control of droop-controlled AC and DC microgrids—A general approach towards standardization," *IEEE Trans. Industrial Electronics*, vol. 58, no. 1, pp. 158–172, Jan. 2011.

[59] Y. A.-R. I. Mohamed and A. A. Radwan, "Hierarchical control system for robust microgrid operation and seamless mode transfer in active distribution systems," *IEEE Trans. Smart Grid*, vol. 2, no. 2, pp. 352–362, Jun. 2011.

[60] A. Mehrizi-Sani and R. Iravani, "Potential-function based control of a microgrid in islanded and grid-connected modes," *IEEE Trans. Power Systems*, vol. 25, no. 4, pp. 1883–1891, Nov. 2010.

[61] "Advanced architectures and control concepts for more microgrids: Definition of ancillary services and short-term energy markets," Deliverable DD4, MORE MICROGRIDS, Dec. 2009. [Online]. Available: http://www.microgrids.eu/documents/686.pdf

[62] H. Karimi, A. Yazdani, and M. R. Iravani, "Negative-sequence current injection for fast islanding detection of a distributed resource unit," *IEEE Trans. Power Electronics*, vol. 23, no. 1, pp. 298–307, Jan. 2008.

[63] F. Blaabjerg, R. Teodorescu, M. Liserre, and A. V. Timbus, "Overview of control and grid synchronization for distributed power generation systems," *IEEE Trans. Industrial Electronics*, vol. 53, no. 5, pp. 1398–1409, Oct. 2006.

[64] F. Gao and M. R. Iravani, "A control strategy for a distributed generation unit in grid-connected and autonomous modes of operation," *IEEE Trans. Power Delivery*, vol. 23, no. 2, pp. 850–859, Apr. 2008.

[65] M. C. Chandorkar, D. M. Divan, and R. Adapa, "Control of parallel connected inverters in standalone ac supply systems," *IEEE Trans. Industry Applications*, vol. 29, no. 1, pp. 136–143, Jan./Feb. 1993.

[66] M. Prodanović and T. C. Green, "High-quality power generation through distributed control of a power park microgrid," *IEEE Trans. Industrial Electronics*, vol. 53, no. 5, pp. 1471–1482, Oct. 2006.

[67] "Master controller requirements specification for perfect power systems (as outlined in the Galvin electricity initiative)," White paper, EPRI, Palo Alto, CA and The Galvin Project, Inc., Chicago, IL, Feb. 2007.

[68] S. Paudyal, C. Canizares, and K. Bhattacharya, "Optimal operation of distribution feeders in smart grids," *IEEE Trans. Industrial Electronics*, vol. 58, no. 10, pp. 4495–4503, 2011.

[69] W. H. Kersting, *Distribution System Modeling and Analysis, Second Edition*, 2nd ed. Bosa Roca, FL, USA: CRC Press, 2006.

[70] R. R. Negenborn, Z. Lukszo, and H. Hellendoorn, *Intelligent Infrastructures*, 1st ed. Netherlands: Springer, 2010.

[71] F. Oldewurtel, "Stochastic model predictive control for energy efficient building climate control," Ph.D. dissertation, ETH Zurich, 2011.

[72] R. Findeisen, "Nonlinear model predictive control: A sampled–data feedback perspective," Ph.D. dissertation, Univ. Stuttgart, 2004.

[73] H. Dommel and W. Tinney, "Optimal power flow solutions," *IEEE Trans. Power Apparatus and Systems*, vol. PAS-87, no. 10, pp. 1866–1876, 1968.

[74] O. Alsac and B. Stott, "Optimal load flow with steady-state security," *IEEE Trans. Power Apparatus and Systems*, vol. PAS-93, no. 3, pp. 745–751, 1974.

[75] R. Zarate, "Optimal power flow with stability constraints," Ph.D. dissertation, Univ. Castilla-La Mancha, 2010.

[76] A. J. Wood and B. F. Wollenberg, *Power Generation, Operation and Control*, 2nd ed. New York, NY, USA: John Wiley & Sons, 1996.

[77] J. Momoh, R. Adapa, and M. El-Hawary, "A review of selected optimal power flow literature to 1993. I. Nonlinear and quadratic programming approaches," *IEEE Trans. Power Systems*, vol. 14, no. 1, pp. 96–104, 1999.

[78] J. Momoh, M. El-Hawary, and R. Adapa, "A review of selected optimal power flow literature to 1993. II. Newton, linear programming and interior point methods," *IEEE Trans. Power Systems*, vol. 14, no. 1, pp. 105–111, 1999.

[79] K. Pandya and S. Joshi, "A survey of optimal power flow methods," *Journal of Theoretical and Applied Information Technology*, May 2008.

[80] N. Padhy, "Unit commitment – a bibiliographical survey," *IEEE Trans. Power Systems*, vol. 19, no. 2, pp. 1196–1205, 2004.

[81] P. G. Lowery, "Generating unit commitment by dynamic programming," *IEEE Trans. Power Apparatus and Systems*, vol. PAS-85, no. 5, pp. 422–426, 1966.

[82] W. Snyder, H. Powell, and J. Rayburn, "Dynamic programming approach to unit commitment," *IEEE Trans. Power Systems*, vol. 2, no. 2, pp. 339–348, 1987.

[83] G. Lauer, N. Sandell, D. Bertsekas, and T. Posbergh, "Solution of large-scale optimal unit commitment problems," *IEEE Trans. Power Apparatus and Systems*, vol. PAS-101, no. 1, pp. 79–86, 1982.

[84] A. I. Cohen and M. Yoshimura, "A branch-and-bound algorithm for unit commitment," *IEEE Trans. Power Apparatus and Systems*, vol. PAS-102, no. 2, pp. 444–451, 1983.

[85] M. Madrigal and V. Quintana, "An interior-point/cutting-plane method to solve unit commitment problems," *IEEE Trans. Power Systems*, vol. 15, no. 3, pp. 1022–1027, 2000.

[86] N. Redondo and A. Conejo, "Short-term hydro-thermal coordination by lagrangian relaxation: solution of the dual problem," *IEEE Trans. Power Systems*, vol. 14, no. 1, pp. 89–95, 1999.

[87] S. Virmani, E. C. Adrian, K. Imhof, and S. Mukherjee, "Implementation of a lagrangian relaxation based unit commitment problem," *IEEE Trans. Power Systems*, vol. 4, no. 4, pp. 1373–1380, 1989.

[88] A. H. Mantawy, Y. Abdel-Magid, and S. Selim, "Integrating genetic algorithms, tabu search, and simulated annealing for the unit commitment problem," *IEEE Trans. Power Systems*, vol. 14, no. 3, pp. 829–836, 1999.

[89] ——, "A simulated annealing algorithm for unit commitment," *IEEE Trans. Power Systems*, vol. 13, no. 1, pp. 197–204, 1998.

[90] Z. Ouyang and S. M. Shahidehpour, "A hybrid artificial neural network-dynamic programming approach to unit commitment," *IEEE Trans. Power Systems*, vol. 7, no. 1, pp. 236–242, 1992.

[91] P. Kall and J. Mayer, *Stochastic Linear Programming: Models, Theory, and Computation*, 2nd ed. New York, NY, USA: Springer, 2011.

[92] J. Birge, "Stochastic programming computation and applications," *INFORMS Journal on Computing*, vol. 9, no. 2, pp. 111–133, 1997.

[93] J. Tamura, I. Takeda, M. Kimura, M. Ueno, and S. Yonaga, "A synchronous machine model for unbalanced analyses," *Elect. Eng. Jpn.*, vol. 119, pp. 46–59, 1997.

[94] M. Muljadi, M. Singh, and V. Gevorgian, "Fixed-speed and variable-slip wind turbines providing spinning reserves to the grid," National Renewable Energy Laboratory (NREL), Tech. Rep., July 2013.

[95] M. Kamh and R. Iravani, "Unbalanced model and power-flow analysis of microgrids and active distribution systems," *IEEE Trans. Power Delivery*, vol. 25, no. 4, pp. 2851–2858, 2010.

[96] M. Liserre, F. Blaabjerg, and S. Hansen, "Design and control of an lcl-filter-based three-phase active rectifier," *IEEE Trans. Industry Applications*, vol. 41, no. 5, pp. 1281–1291, 2005.

[97] H. Bergveld, "Battery management systems: Design by modelling," Ph.D. dissertation, Universiteit Twente, 2001.

[98] K. W. Harrison, R. Remick, G. D. Martin, A. Hoskin, T. Grube, and D. Stolten, "Hydrogen production: Fundamentals and case study summaries," in *Proc. 18th World Hydrogen Energy Conference 2010*, Essen, Germay, May 2010. [Online]. Available: http://juser.fz-juelich.de/record/135438

[99] F. He, Z. Zhao, and L. Yuan, "Impact of inverter configuration on energy cost of grid-connected photovoltaic systems," *Renewable Energy*, vol. 41, pp. 328–335, 2012. [Online]. Available: http://www.sciencedirect.com/science/article/pii/S096014811100632X

[100] O. Elma and U. S. Selamogullari, "A comparative sizing analysis of a renewable energy supplied stand-alone house considering both demand side and source side dynamics," *Applied Energy*, vol. 96, pp. 400–408, 2012. [Online]. Available: http://www.sciencedirect.com/science/article/pii/S0306261912001821

[101] J. Arroyo and A. Conejo, "Optimal response of a thermal unit to an electricity spot market," *IEEE Trans. Power Systems*, vol. 15, no. 3, pp. 1098–1104, 2000.

[102] R. E. Rosenthal, *GAMS – A User's Guide*, GAMS Development Corporation, Washington, DC, USA, December 2012.

[103] M. Arriaga, C. Canizares, and M. Kazerani, "Renewable energy alternatives for remote communities in northern ontario, canada," *IEEE Trans. Sustainable Energy*, vol. 4, no. 3, pp. 661–670, 2013.

[104] S. Soman, H. Zareipour, O. Malik, and P. Mandal, "A review of wind power and wind speed forecasting methods with different time horizons," in *Proc. North American Power Symposium (NAPS), 2010*, 2010, pp. 1–8.

[105] CPLEX 12, Solver Manual. [Online]. Available: http://www.gams.com/dd/docs/solvers/cplex.pdf

[106] A. Wchter and L. T. Biegler, "On the implementation of an interior-point filter line-search algorithm for large-scale nonlinear programming," *Mathematical Programming*, vol. 106, pp. 25–57, 2006. [Online]. Available: http://dx.doi.org/10.1007/s10107-004-0559-y

[107] K. Rudion, A. Orths, Z. Styczynski, and K. Strunz, "Design of benchmark of medium voltage distribution network for investigation of dg integration," in *Proc. IEEE PES General Meeting, 2006*, 2006, pp. 1–6.

[108] "Continuous 1650 ekW, 2063 kVA diesel genset datasheet," Caterpillar, 2012. [Online]. Available: http://www.cat.com/en_US/products/new/power-systems/electric-power-generation/diesel-generator-sets/

[109] "Prime 513 kVA diesel genset model DFEJ 60 Hz datasheet," Cummins Power Generation, 2004-2006. [Online]. Available: https://www.cumminsgeneratortechnologies.com/en/download/datasheets/displayDownloadDatasheets.do

[110] K. Høyland and S. W. Wallace, "Generating scenario trees for multistage decision problems," *Management Science*, vol. 47, no. 2, pp. 295–307, 2001.

[111] J. L. Higle and S. Sen, "Stochastic decomposition: An algorithm for two-stage linear programs with recourse," *Mathematics of Operations Research*, vol. 16, no. 3, pp. 650–669, 1991.

[112] P. Pinson, H. Madsen, H. A. Nielsen, G. Papaefthymiou, and B. Klöckl, "From probabilistic forecasts to statistical scenarios of short-term wind power production," *Wind Energy*, vol. 12, no. 1, pp. 51–62, 2009.

[113] P. Pinson, "Wind energy: Forecasting challenges for its operational management," *Preprint Statistical Science*, 2013. [Online]. Available: http://http://pierrepinson.com/docs/pinson13_windstat.pdf

[114] PSE-Committee, "Reliability indices for use in bulk power supply adequacy evaluation," *IEEE Trans. PAS*, vol. 97, no. 4, pp. 1097–1103, 1978.

[115] D. E. Olivares, C. Cañizares, and M. Kazerani, "A centralized energy management system for isolated microgrids," *IEEE Trans. Smart Grid*, submitted May 2013, revised and resubmitted October 2013, 12 pages.

[116] D. E. Olivares, J. Lara, C. Cañizares, and M. Kazerani, "Stochastic-predictive energy management system for isolated microgrids," *IEEE Trans. Smart Grid*, to be submitted.

[117] T. Takagi and M. Sugeno, "Fuzzy identification of systems and its applications to modeling and control," *IEEE Trans. Systems, Man and Cybernetics*, vol. 15, no. 1, pp. 116–132, 1985.